Reservoir Geological Uncertainty Reduction and Its Applications in Reservoir Development Optimization

by

Shahed Rahim

A thesis submitted in partial fulfillment of the requirements for the degree of

Master of Science
in
Chemical Engineering

Department of Chemical and Materials Engineering
University of Alberta

Abstract

Three different studies related to geological uncertainty reduction in reservoir applications are performed in this thesis. The first study proposes an optimal realization reduction framework for quantifying geological uncertainty. The second study applies the optimal realization reduction framework to incorporate geological uncertainty into an application of vertical well placement optimization. The third study proposes a two stage Steam Assisted Gravity Drainage (SAGD) well drainage area (DA) arrangement optimization method and incorporates geological uncertainty to the SAGD arrangement optimization by using the optimal realization reduction framework.

Geological uncertainty is reduced by generating and incorporating multiple realizations in the application of reservoir development or controls optimization. However, only few realizations are selected from a large superset for the reservoir application due to intensive computational efforts. The proposed optimal realization reduction method is a mixed integer linear optimization model which minimizes the probability distance between the discrete distribution represented by the superset of realizations and the reduced discrete distribution represented by the selected realizations. The results of applying the realization reduction method to various case studies show that the proposed method can effectively select realizations and assign probabilities such that the extreme and expected reservoir performances are recovered better than any of the other realization reduction methods. The optimal realization reduction method is then used to select a subset of realizations and incorporate them into a framework of robust vertical well placement optimization under geological uncertainty. Applying the well placement optimization framework to reservoirs demonstrate the similarity between the expected reservoir performance results from

well placement optimization using the realization reduction method and well placement optimization using all the realizations in the superset.

SAGD is an increasingly popular in-situ method for extraction of bitumen from Alberta's oil sands. The first stage of the model determines the optimal arrangement of the compact set of all the DAs that maximize the available bitumen. The second stage of the model selects a smaller set of DA and surface pad (SP) from the compact arrangement that maximize the available bitumen and minimizes the distance between the selected SPs. Results of applying the SAGD well arrangement optimization method to a reservoir lease area showed a compact DA arrangement with DAs containing higher bitumen content and SPs in close proximity to each other being selected. Geological uncertainty is incorporated to the optimization method by using selected realizations obtained from the optimal realization reduction framework. Results showed DA arrangement plan with higher expected bitumen and greater number of DAs within the compact arrangement.

Preface

A significant amount of research contributions of the thesis are a part of a journal paper which is in publication at the time of submission of the thesis document. I am the first author and the principal collaborator for the journal paper.

Chapter 2 of the thesis is adapted from the journal paper by Rahim S, Li Z, Trivedi J, (2015) with the title of "Reservoir Geological Uncertainty Reduction: an Optimization Based Method using Multiple Static Measures" and is in publication at *Math Geosci* with doi:10.1007/s11004-014-9575-5.

I would like to dedicate this thesis to my parents who provided constant guidance and support throughout my graduate studies.

Acknowledgement

I would like to thank you very much, Dr. Zukui Li, for accepting me in your research group and mentoring me as my supervisor for the Master's program. From the bottom of my heart, I would like to thank you for believing in me and giving me the opportunity to be involved in research projects based on my interests. You have constantly provided support and guided me through my graduate studies at University of Alberta. I am very fortunate to have a friendly and understanding supervisor like you. I can confidently say that you have made a positive impact in my career.

I would like to express my gratitude to all the members of my examination committee for taking their valuable time to read my thesis and providing recommendations for improvement.

I would also like to thank the staff, professors and graduate students at the department of Chemical Engineering at University of Alberta for providing an excellent learning opportunity and for constantly assisting me throughout my program.

I would like to acknowledge my parents; Khawja M. Sebgatullah and Aziza Khatun, for providing me encouragement and moral support during my graduate program. My parents motivated me to work harder with passion and dedication. I am very fortunate to have their blessings and prayers. I would also like to thank all my brothers and specifically my elder brother for being a true friend and always having my back.

Table of Contents

List of Tables

List of Figures

List of Symbols

COP	Cumulative oil production
NPV	Net Present Value
MRST	Matlab Reservoir Simulation Toolbox
SAGD	Steam Assisted Gravity Drainage
MILP	Mixed Integer linear Programming
DA	Drainage Area
SP	Surface Pad
CHV	Connected Hydrocarbon Volume
CDF	Cumulative Distribution Function
MADS	Mesh Adaptive Direct Search
BCB	Bottom Continuous Bitumen
TCB	Top Continuous Bitumen
NCB	Net Continuous Bitumen
$COP_{Expected}$	Expected Cumulative oil production
$NPV_{Expected}$	Expected Net Present Value
$R_{Expected}$	Expected total available bitumen
D_{kan}	Kantorovich Distance
I_c^{net}	Net indicator parameter for cell *c*
S_c	Irreducible water saturation of grid cell *c*
ϕ_c	Porosity of grid cell *c*

k_c	Permeability of grid cell *c*
ϕ_0	Threshold porosity
k_0	Threshold permeability
K_{net}	Average net permeability
ϕ_{net}	Average net porosity
S_{net}	Average net irreducible water saturation
F_{net}	Fraction of net cells
I_c^{LC}	Locally connected indicator parameter for cell *c*
F_{LC}	Fraction of locally connected cells
V_c	Volume of grid cell *c*
PV_{net}	Net pore volume
$OOIP$	Original oil-in-place
OIP_{net}	Net oil-in-place
CHV_{local}	Locally connected hydrocarbon volume
τ	Tortuosity
A_v	Surface area

Chapter 1

Introduction

1.1 Background

Reservoir geological properties are important parameters used in the design and optimization of oil extraction processes from reservoirs. These parameters dictate the ease with which oil can be extracted and also the quantity of oil that can be extracted. Optimal location of wells and the well controls depend on the geological properties of the reservoir. Geological uncertainty exists because it is not possible to know the exact geological properties of every section of a realistic reservoir. Techniques such as well exploration and core holes can give an idea of the geological properties of particular areas of the reservoir. However, the geological parameters of the areas between the exploration wells or core holes will still be unknown. As a result, geological uncertainty will always exist for a reservoir. Geological uncertainty is quantified by generating a large number of geological realizations of a given reservoir and then selecting a smaller subset of those realizations for determination of the performance parameter of interest such as Cumulative Oil Production (COP) or Net Present Value (NPV). Therefore, a realization reduction method which selects a smaller number of realizations from a larger superset of realizations is crucial for geological uncertainty reduction.

An optimal realization reduction method is proposed in this thesis which selects a smaller subset of realizations from a larger set of realization. The realization reduction method is computed efficiently with minimal computational time and generates a smaller subset of realizations which is a good statistical representation of the larger superset of realizations.

Well placement optimization determines the optimal positions of wells which maximize the production of the underground resources such as oil, gas or bitumen. On the other hand, well control optimization determines the optimal settings for a well, such as bottomhole pressure or injector flow rate, which results in either the maximum production of oil or maximum

profitability. It is important to incorporate geological uncertainty for both well placement optimization and well control optimization.

In this thesis, a robust vertical producer well placement optimization under geological uncertainty is performed by incorporating a subset of realizations from the optimal realization reduction method. Steam Assisted Gravity Drainage (SAGD) wells are divided into Drainage Area (DA) and Surface Pad (SP). DA are sets of horizontal producer and injector wells in parallel under the ground. SP are the surface facilities from which the horizontal sets of injector and producer wells are drilled. A two-stage SAGD DA and SP arrangement optimization is proposed in this thesis. In addition, geological uncertainty is incorporated to the SAGD arrangement optimization by developing a robust optimization step using a subset of realizations obtained from the optimal realization reduction method.

1.2 Motivation

The motivation for the work proposed in this thesis stems from the lack of distance based realization reduction method using simple and easily computable measures for large and complex reservoir grids. The realization reduction method requires minimal computational effort for reservoir grids and also ensures that the selected subset of realizations is a good representation of the superset of realizations. As a result, geological uncertainty can be included for computationally expensive applications such as well placement or well control optimizations.

The motivation for developing a SAGD DA arrangement optimization method is due to the increasing commercial use of SAGD method in the extraction of bitumen from the oil sands and the absence of structured framework for SAGD well placement in literature which incorporates geological uncertainty, by selecting a subset of realizations, to the developed SAGD DA arrangement optimization process.

1.3 Objective of Thesis

The principle objective of the thesis is to propose an optimal realization reduction method and use the proposed method in various applications to show that the smaller subset of realizations selected from the proposed realization reduction method is a very good representation of the larger superset of all the realization.

The specific goals of this thesis are broadly divided into three different parts as given:

1. Propose an optimal realization reduction method which selects a smaller subset of realizations from a larger superset of realizations in order to quantify geological uncertainty associated with reservoir studies. Compare the performance of the optimal realization reduction method with respect to the performance of the full set of realizations in the superset.

2. Apply the proposed optimal realization reduction method in an application of robust vertical well placement optimization to determine the optimal producer well locations. Compare the well placement plan using the realizations from the proposed optimal realization reduction method to the well placement plan using all the realizations in the larger superset of realizations.

3. Propose a two stage SAGD well arrangement optimization method for selecting a compact set of DAs and SPs and then incorporate geological uncertainty to the proposed SAGD DA arrangement optimization method. A subset of realization obtained from the optimal realization reduction method is used in the proposed SAGD DA arrangement optimization.

1.4 Thesis Outline

The three different sub-objectives of the thesis are given in chapters 2, 3 and 4. The thesis is structured as follows. Chapter 2 provides a detailed description of the optimal realization

reduction method along with various case studies to illustrate the performance of the proposed method. Vertical well placement optimization under geological uncertainty is explained and applied to two different case studies in chapter 3. Chapter 4 proposes the two-stage SAGD DA arrangement optimization method, followed by an application of the proposed two-stage optimization method to a realistic reservoir lease area. Chapter 4 also provides a case study in which the optimal realization reduction method is used to incorporate geological uncertainty in the proposed SAGD DA arrangement optimization method. The thesis is concluded in Chapter 5.

Chapter 2 provides the optimal realization reduction method. The background and summary of different realization reduction methods used in the literature are given in section 2.1. The problem statement for the optimal realization reduction method is given in section 2.2. Static measures are used in the proposed optimal realization reduction method and therefore section 2.3 provides a detailed list of all the different static measures used. The algorithm of the proposed realization reduction method is given in section 2.4. The realization reduction method is applied to different case studies with increasing reservoir complexity and is given in section 2.5. The chapter is concluded in section 2.6.

Vertical well placement optimization under geological uncertainty is given in chapter 3. Sections 3.1 and 3.2 introduce the well placement optimization problem by providing a summary of literature review and the problem statement. The objective function and the methodology used in the vertical well placement optimization under geological uncertainty are given in section 3.3. The quantification of the geological uncertainty in the well placement optimization problem is explained in section 3.4. Section 3.5 provides the result and discussion of applying the vertical well placement optimization under uncertainty to two different case studies representing a two-dimensional and a three-dimensional reservoir grid. The chapter is concluded in section 3.6.

The two-stage SAGD DA arrangement optimization is proposed in chapter 4. The background associated with SAGD wells and the problem statement of the SAGD DA arrangement optimization is given in sections 4.1 and 4.2 respectively. Section 4.3 explains how the reservoir quality in terms of available bitumen is determined for the SAGD well arrangement optimization. The workflow for the SAGD DA arrangement optimization model and the description of the subsequent stages of the optimization model are provided in section 4.4. Section 4.5 provides a realistic case study where both the stages of the SAGD DA arrangement

optimization method were applied. The SAGD DA arrangement optimization problem under geological uncertainty is investigated in section 4.6. The results of a case study using the SAGD DA arrangement optimization under geological uncertainty by incorporating selected realizations obtained from the optimal realization reduction method are also given in section 4.6. Chapter 4 is concluded in section 4.7. Conclusion of the thesis and future work is given in Chapter 5.

Chapter 2

Reservoir Geological Uncertainty Reduction[1]

2.1 Background and Literature Review

Reservoir performance can be quantified by flow simulation which provides production parameters of interest such as the cumulative oil production (COP) rate and the net present value (NPV). All of the production parameters depend on the geological properties of the reservoir. It is very important to incorporate geological uncertainty in a reservoir model. Otherwise, the model may give an incorrect prediction of production parameters. To represent the geological uncertainty, multiple geological realizations are usually generated using geostatistical tools so as to obtain a broad range of possible geological properties for a reservoir. However, reservoir flow simulations cannot be run for all of the possible realizations due to the significant computer processing time. Therefore, in practice, only a small number of geological realizations are chosen to perform reservoir simulations to obtain a reservoir performance model which incorporates geological uncertainty. It is important to generate a large set of realizations so that the geological uncertainty space of the reservoir is adequately represented. A large set of realizations will result in a wide range of geological property of the reservoir. As a result, the subset of realizations selected from the large set of realization will be able to represent the geological uncertainty of the reservoir very well. Various methods for selecting geological realizations exist in the literature and can be broadly classified as follows: random selection method, static measure based ranking method, distance based kernel clustering technique and probability distance based realization reduction method.

Random selection of a subset of realizations is the easiest method for implementation, but it may result in the wrong measure of geological uncertainty especially when the number of selected realizations is small. Many studies in the literature use the single static measure based ranking

[1] The content of this chapter is adapted from the following journal paper. Rahim S, Li Z, Trivedi J (2015), Reservoir Geological Uncertainty Reduction: an Optimization Based Method using Multiple Static Measures. *Math Geosci* doi:10.1007/s11004-014-9575-5

method to select geological realizations and to quantify the uncertainty in reservoir performance. The ranking method was introduced by Ballin et al. (1992). Ranking based reduction arranges realizations of an easily computable measure in an ascending/descending order and then selects the realizations that have low, medium and high measure values. The selected realizations are then used as input for flow simulations to obtain the reservoir production response. Deutsch (1998, 1999) developed software tools to rank realizations based on the number of connected cells, connectivity to a well location or connectivity between multiple wells. Deutsch and Begg (2001) proposed that ranking all of the realizations based on a measure and then choosing a subset of equally spaced realizations result in a better representation of uncertainty than choosing the low, medium and high performance realizations. A ranking based method for the Steam Assisted Gravity Drainage (SAGD) process using a measure known as connected contained bitumen was used by McLennan and Deutsch (2004). The connected contained bitumen was calculated using net cells connected to the SAGD producer well. The realizations with low, medium and high ranking measures were selected from the superset of realizations. In another study, McLennan and Deutsch (2005) used several measures based on statistical, volumetric, global and local connectivity metrics to select a subset of realizations. Fenik et al. (2009) used a ranking method based on connected hydrocarbon volume (CHV) to select a subset of realizations for a SAGD application. Li et al. (2012) adopted a static quality measure, which was a modification to the CHV measure, to rank geological realizations. Rankings based on the static quality measure showed improved performance over rankings based on CHV. While efforts have been made to improve static measures for ranking, the limitation of existing ranking methods for selecting realizations is that they rely greatly on the measure used. If the measure has poor correlation to the production performance parameter of the reservoir, then the selected realizations will not be a good representation of the superset of realizations. Furthermore, all of the selected realizations based on the ranking method have equal probability in the reduced distribution.

The distance based kernel clustering method has also received lots of attention in the past. Scheidt and Caers (2009) used simplified streamline simulation results to compute the distance between realizations and to form a distance matrix. The uncertainty associated with the distance matrix is modelled using multidimensional scaling and kernel techniques. The superset of realizations is grouped into clusters using kernel k-means clustering, and a subset of selected

realizations can be extracted from the clusters. Scheidt and Caers (2010) compared the statistics associated with the traditional ranking method, the kernel k-means clustering method and the random selection method. They used the bootstrap technique to compute the confidence intervals of the P10, P50 and P90 quantiles of the reduced subset of realizations and showed that the distance based kernel clustering method provides the most robust results (Scheidt and Caers, 2010; Park and Caers, 2011). Singh et al. (2014) used the kernel k-means clustering method to quantify uncertainty associated with various history matched geological models and to forecast production information. The distance matrix in the clustering method uses oil recovery factors between realizations. These clustering methods generally rely on streamline simulations to calculate distance between realizations, which is still computationally demanding for large reservoir models, and the problem has to be reformulated if the number of wells or well location changes. Additionally, simplified fluid flow assumptions are used for streamline simulations, which may undermine the geological heterogeneity of the reservoir, resulting in a poor representation of geological uncertainty (Gilman et al., 2002). There is a need for a realization reduction method that is computationally less expensive and provides a better representation of the original distribution than the current ranking methods.

Apart from the ranking method and the clustering method, a probability distance based realization reduction/selection method associated with a scenario reduction technique for optimization under uncertainty (Dupacova et al., 2003; Li and Floudas, 2014) has been investigated recently. Following this direction, Armstrong et al. (2013) proposed a realization reduction method based on minimizing the Kantorovich distance between distributions and applied the method to metal mining. The method iteratively generates a random subset of realizations without replacements from the superset of realizations until the Kantorovich distance between the distributions is minimized. While their method relies on heuristic random searches to minimize the Kantorovich distance, a novel method is proposed in this work for geological realization reduction following the concept of probability distance minimization.

2.2 Problem Statement

Static measures and geological data are used to develop a realization reduction method which can be easily computable for a large number of realizations and ensure that the selected realizations have a similar statistical distribution to the superset of all the realizations. An optimal realization reduction method is proposed in this thesis. The realization reduction method considers multiple static measures and geological properties to select geological realizations. Specifically, an optimal realization reduction model is developed based on the mixed integer linear optimization (MILP) technique. The proposed algorithm uses reservoir geological properties and static measures to quantify the dissimilarity between realizations and uses the Kantorovich distance to quantify the probability distance between the superset and the subset of realizations. The objective is to find a reduced optimal subset that has similar statistical distribution to the superset of all the realizations in terms of the reservoir production performance.

2.3 Static Measures

Static measures are simplified metrics designed to achieve a good correlation with the reservoir production performance variable of interest. Static measures are computationally much easier for evaluation when compared to reservoir flow simulation. It can be easily computed for a large set of realizations. Static measures can be classified into the following categories (Deutsch and Srinivasan, 1996; McLennan and Deutsch, 2005): (i) statistical static measures which quantify the statistical average of geological parameters, (ii) fractional static measures that determine the active fraction of the reservoir, and (iii) volumetric static measures which calculate the volume of a reservoir capable of oil transport. Details on the different static measures are given in the following subsections.

2.3.1 Statistical static measures

Statistical static measures considered in this paper are calculated for net cells in the reservoir. Any cell which has a porosity and permeability above a threshold value is defined as a net cell. A

binary indicator parameter I_c^{net} is used to denote whether a cell c in the reservoir grid is net ($I_c^{net} = 1$) or not ($I_c^{net} = 0$). The idea of a net cell stems from the fact that if a section of the reservoir rock has very low porosity and permeability value, then that section of the rock will be unable to carry any oil through it. As a result, that non-net section of the rock plays no role in oil recovery from the reservoirs. Mathematically I_c^{net} is defined as

$$I_c^{net} = \begin{cases} 1, & \text{if } \phi_c \geq \phi_0 \text{ and } k_c \geq k_0 \\ 0, & \text{otherwise} \end{cases} \tag{2.1}$$

In Eq. (2.1), ϕ_c and k_c denote the porosity and the permeability of cell c, respectively, whereas ϕ_0 and k_0 denote the threshold values.

Statistical static measures are the simplest measures for ranking realizations. The average net permeability (K_{net}) for each realization is given by Eq. (2.2)

$$K_{net} = \frac{\sum_c k_c I_c^{net}}{\sum_c I_c^{net}} \tag{2.2}$$

Indicator I_c^{net} is used in Eq. (2.2) to ensure that the average permeability is only calculated for the net cells. Using a similar idea, the average net porosity (ϕ_{net}) for each realization is given by Eq. (2.3)

$$\phi_{net} = \frac{\sum_c \phi_c I_c^{net}}{\sum_c I_c^{net}} \tag{2.3}$$

The average net irreducible water saturation (S_{net}) for each realization is given by Eq. (2.4)

$$S_{net} = \frac{\sum_c S_c I_c^{net}}{\sum_c I_c^{net}} \tag{2.4}$$

where S_c is the irreducible water saturation of cell *c*. Similar to average permeability and porosity, average irreducible water saturation is only calculated for the net cells.

2.3.2 Fractional static measures

Fractional static measures use indicator parameters to calculate the fraction of cells that are either net or locally connected to a well. These static measures provide a good basis for understanding the quality of a reservoir and the amount of oil that can be extracted from a reservoir.

The fraction of net cells (F_{net}) of a reservoir is also known as the net to gross ratio. It is calculated by the summation of I_c^{net} values of each cell and divided by the total number of cells *N* as given in Eq. (2.5) below

$$F_{net} = \frac{1}{N}\sum_c I_c^{net} \tag{2.5}$$

As the number of net cells in a reservoir increases, the net to gross ratio increases as well. Therefore a higher net to gross ratio implies that the reservoir will have better oil production.

The fraction of locally connected cells (F_{LC}) is the fraction of cells that are net and are connected to a producer well. A cell *c* is defined as locally connected if $I_c^{net} = 1$ and there is a path of net cells from cell *c* to a producer well. Therefore, all locally connected cells are net cells, but net cells are not necessarily locally connected cells. Mathematically I_c^{LC} is denoted by Eq. (2.6)

$$I_c^{LC} = \begin{cases} 1, & \text{if } I_c^{net} = 1 \text{ and connected to producer well} \\ 0, & \text{if } I_c^{net} = 0 \text{ or not connected to producer well} \end{cases} \tag{2.6}$$

The fraction of locally connected cells is calculated using the binary variables I_c^{net} and I_c^{LC} as given by Eq. (2.7)

$$F_{LC} = \frac{1}{N}\sum_c I_c^{net} I_c^{LC} \tag{2.7}$$

Since the local connectivity calculation considers only active cells connected to a well, it is shown to be a good indication of production parameters such as COP or NPV.

2.3.3 Volumetric static measures

Volumetric static measures incorporate the volume of each cell in its calculation and therefore provide a good basis for determining the volume of oil each cell in the reservoir can produce.

Net pore volume (PV_{net}) is the simplest volumetric static measure that utilizes the volume of each cell and the corresponding porosity of that cell. The calculation of net pore volume is only for net cells since these are the only cells that have the ability to produce or transport oil. The net pore volume is given by Eq. (2.8) below

$$PV_{net} = \sum_c V_c \phi_c I_c^{net} \tag{2.8}$$

where V_c is the volume of cell *c*.

Original oil-in-place (*OOIP*) is calculated for all cells in the reservoir and is calculated by the summation of the product of volume (V_c), porosity (ϕ_c) and the oil saturation $(1-S_c)$ of cell *c*. *OOIP* is given by Eq. (2.9) below

$$OOIP = \sum_c V_c \phi_c (1 - S_c) \tag{2.9}$$

where S_c is the irreducible water saturation of cell *c*.

Net oil-in-place (OIP_{net}), which is also known as net hydrocarbon volume, is simply the *OOIP* for the net cells of the reservoir. Therefore, in principle, OIP_{net} is expected to be a better static measure than *OOIP*. OIP_{net} is given by Eq. (2.10) below

$$OIP_{net} = \sum_c V_c \phi_c (1 - S_c) I_c^{net} \tag{2.10}$$

Locally connected hydrocarbon volume (CHV_{local}) is the *OOIP* calculated for net cells connected to the producer well (Deutsch, 1998). A cell is considered to be locally connected when an active cell pathway can be formed from the cell to a producer well so that the oil can be transported (McLennan and Deutsch, 2004). Locally connected hydrocarbon volume is given by Eq. (2.11)

$$CHV_{local} = \sum_{c} V_c \phi_c (1 - S_c) I_c^{net} I_c^{LC} \tag{2.11}$$

2.4 Proposed Realization Reduction Algorithm

2.4.1 Dissimilarity between realizations

Considering two geological realizations i and i', a dissimilarity measure is used to quantify the difference between them. In this work, the dissimilarity between realizations is computed using the geological properties and the static measures introduced in the previous section. Specifically, the dissimilarity between two realizations i and i' is evaluated by Eq. (2.12)

$$c_{i,i'} = \sum_{k} \left| m_{ik} - m_{i'k} \right| + \sum_{c,t} \gamma \left| \theta_{ict} - \theta_{i'ct} \right| \qquad \forall i, i' \tag{2.12}$$

where m_{ik} is the value of the k type of static measure for realization i, θ_{ict} is the t type of geological property value of cell c in the reservoir grid for realization i and γ is a weight parameter which reflects the contribution of geological property data in the dissimilarity calculation. The geological property t considered in this work is the porosity and permeability of all the cells in the reservoir. The static measure parameters are given a larger weight here to emphasize its importance in the dissimilarity evaluation (γ is set as 0.01 in this work). Since static measures are easily computable for any given realization, the dissimilarity values between any two geological realizations can be calculated very efficiently.

2.4.2 Kantorovich distance in realization reduction

All of the geological realizations generated from geostatistical tools form a superset from which a subset containing a small number of realizations is to be selected for further investigation (e.g.,

flow simulation). The objective of realization reduction is that the selected subset of realizations can represent the superset of realizations very well in terms of reservoir production performance.

In this work, the aforementioned superset and subset are considered as two discrete probability distributions. The first distribution (also called the original distribution) consists of the superset of realizations, and each realization i has probability p_i^{orig}. Notice that this probability value p_i^{orig} is normally set as equal to $1/|I|$, where I is the superset of realizations and $|I|$ is the set cardinality (i.e., total number of realizations). The second distribution (also called the reduced distribution) consists of a subset of selected realizations in which each realization i has probability p_i^{new}. The reduced distribution can be viewed as an updated version of the original distribution with probabilities on each realization adjusted. All of the removed realizations have zero probability in the reduced distribution.

The Kantorovich distance is a type of probability metric to quantify the dissimilarity between two probability distributions. It is defined by a transportation problem which minimizes the transportation cost associated with moving the probability mass from one distribution to the other distribution. The theory of optimal transportation was first introduced by Monge (1781) and rediscovered by Kantorovich (1942). For the realization reduction problem, the Kantorovich distance between the original distribution and the reduced distribution is defined by the optimal objective value of the following linear transportation problem

$$
\begin{aligned}
D_{\text{Kan}} = \min_{\eta_{i,i'}} \ & \sum_{i\in I}\sum_{i'\in S}\eta_{i,i'}c_{i,i'} \\
\text{s.t.} \ & \sum_{i\in I}\eta_{i,i'} = p_{i'}^{new} \quad \forall i' \in S \\
& \sum_{i'\in S}\eta_{i,i'} = p_i^{orig} \quad \forall i \in I \\
& \eta_{i,i'} \geq 0 \ \ \forall i \in I \ \ \forall i' \in S
\end{aligned}
\tag{2.13}
$$

where i and i' represent realizations, I is the superset and S is the selected subset, p_i^{orig} and p_i^{new} represent the probability of realization i in the original and the reduced distribution, respectively, $\eta_{i,i'}$ is the decision variables representing the probability mass transportation plan and $c_{i,i'}$ is the dissimilarity between realizations. Dupacova et al. (2003) proved that the optimal objective value of the above problem is

$$D_{\text{Kan}} = \sum_{i \in I-S} p_i^{orig} d_i \tag{2.14}$$

where $d_i = \min_{i' \in S} c_{i,i'}$ represents the transportation cost for a removed realization $i \in I - S$ and it is the minimum dissimilarity between the removed realization i and all of the selected realizations $i' \in S$. The optimal solution of $p_{i'}^{new}$ for problem (2.13) is

$$p_{i'}^{new} = p_{i'}^{orig} + \sum_{i \in J(i')} p_i^{orig} \quad \forall i' \in S \tag{2.15}$$

where $J(i') = \{i \mid i \in I - S, c_{i,i'} \le c_{i,i''}, \forall i'' \in S\}$, meaning that a preserved realization's new probability is the sum of its original probability and the probability mass that has been transported to it. A removed realization is transported to the closest preserved realization.

2.4.3 Realization reduction algorithm

To select representative geological realizations, an optimization based realization reduction method is proposed in this work. The proposed realization selection/reduction method is based on a constrained mixed integer linear optimization technique, and it minimizes the Kantorovich distance between the original distribution and the reduced distribution as explained in previous subsection. Details on the proposed optimization model are stated below.

First, binary variables y_i are introduced to denote whether the realization i is removed ($y_i = 1$) or not ($y_i = 0$). Continuous variables $v_{i,i'}$ ($0 \le v_{i,i'} \le 1$) are introduced to denote the fraction of the probability mass that is transported from realization i to realization i'.

The objective function of the proposed realization reduction algorithm is to minimize the Kantorovich distance between the original distribution and the reduced distribution, which is given in Eq. (2.16)

$$\min D_{Kan} = \sum_{i \in I} p_i^{orig} d_i \tag{2.16}$$

where d_i represents the cost of removing a realization i (i.e., transporting and distributing its probability mass to preserved realizations). This cost is quantified by a weighted summation of

the transported probability mass, where the weight is the dissimilarity $c_{i,i'}$ between realizations. This scheme can be modeled by using Eq. (2.17)

$$d_i = \sum_{i' \in I} c_{i,i'} v_{i,i'} \quad \forall i \in I \tag{2.17}$$

Notice that the Kantorovich distance defined in problem (2.13) is based on a known subset *S*, while the objective in the proposed algorithm here is to find the optimal subset *S* that leads to the minimum Kantorovich distance. With the introduction of variables y_i and $v_{i,i'}$, the proposed optimization model will generate the optimal *S* that leads to the minimum Kantorovich distance as explained by the following constraints. The reader is also referred to Li and Floudas (2014) for detailed proof on this.

The following set of constraints are necessary to enforce the logical relationship between variables y_i and $v_{i,i'}$. First, if a realization i is removed (y_i=1), then all of its probability mass should be transported ($\sum_{i' \in I} v_{i,i'}$=1). If a realization i is selected/preserved (y_i=0), then its probability mass should not be transported to any realization ($\sum_{i' \in I} v_{i,i'}$=0). The above logical relationship is reflected in Eq. (2.18)

$$\sum_{i' \in I} v_{i,i'} = y_i \quad \forall i \in I \tag{2.18}$$

Furthermore, if a realization i' is removed ($y_{i'}$= 1), then no probability mass can be transported to it ($v_{i,i'}$= 0). If a realization i' is selected ($y_{i'}$= 0), then the probability mass can be transported to it ($0 \le v_{i,i'} \le 1$). This condition is modeled in Eq. (2.19) below

$$0 \le v_{i,i'} \le 1 - y_{i'} \quad \forall i, i' \in I \tag{2.19}$$

The next constraint enforces the number of selected realizations. Assume the total number of realizations to be removed is R, then Eq. (2.20) ensures that R realizations are removed

$$\sum_{i \in I} y_i = R \tag{2.20}$$

In the proposed realization reduction model, a subset of realizations representing the potential best and worst performance is also considered. Equation (2.21) below ensures that at least two realizations are selected from subset I_{SB}

$$\sum_{i \in I_{SB}} (1 - y_i) \geq 2 \tag{2.21}$$

where subset I_{SB} has two realizations which are identified using the following steps. For each static measure, the realizations corresponding to the top three highest static measure values are identified. Those identified realizations' IDs are combined into a superset from which the two most frequent realizations are selected to form set I_{SB}. Similarly, Eq. (2.22) ensures that at least two realizations are selected from subset I_{SW} in the reduced distribution

$$\sum_{i \in I_{SW}} (1 - y_i) \geq 2 \tag{2.22}$$

where subset I_{SW} has the top two most frequent realizations that represent the potential worst performance. For each static measure, the realizations corresponding to the top three lowest static measure values are identified. Those identified realizations' IDs are combined into a superset from which the two most frequent realizations are selected to form set I_{SW}.

With the selected realizations (i.e., y_i) and the probability mass transportation plan (i.e., $v_{i,i'}$), the new probability of realizations in the reduced distribution p_i^{new} can be evaluated as follows

$$p_{i'}^{new} = (1 - y_{i'}) p_{i'}^{orig} + \sum_i v_{i,i'} p_i^{orig} \qquad \forall i' \in I \tag{2.23}$$

Notice that if realization i' is removed ($y_{i'} = 1$), then $p_i^{new} = 0$. If realization i' is preserved ($y_{i'} = 0$), then its new probability mass can be calculated as the sum of all of the probability mass that has been transported to it ($\sum_i v_{i,i'} p_i^{orig}$) and its original probability ($p_{i'}^{orig}$).

Finally, the complete optimization model is composed of Eqs. (2.16) to (2.23), and it is a MILP optimization problem. This problem can be solved using a MILP solver such as CPLEX (IBM, 2010).

The complete MILP optimization model for the proposed optimal realization reduction method is summarized as follows

$$\min D_{Kan} = \sum_{i \in I} p_i^{orig} d_i$$

Subject to

$$d_i = \sum_{i' \in I} c_{i,i'} v_{i,i'} \quad \forall i \in I$$

$$\sum_{i' \in I} v_{i,i'} = y_i \quad \forall i \in I$$

$$0 \le v_{i,i'} \le 1 - y_{i'} \quad \forall i, i' \in I$$

$$\sum_{i \in I} y_i = R$$

$$\sum_{i \in I_{SB}} (1 - y_i) \ge 2$$

$$\sum_{i \in I_{SW}} (1 - y_i) \ge 2$$

$$p_{i'}^{new} = (1 - y_{i'}) p_{i'}^{orig} + \sum_i v_{i,i'} p_i^{orig} \quad \forall i' \in I$$

$$y_i \in \{0,1\} \quad \forall i \in I$$

Input Parameters:

R the total number of realizations to be removed

p_i^{orig} the original probabilities of realizations, i, is normally set as equal to $p_i^{orig} = 1/|I|$, where $|I|$ is the size of the set I

$c_{i,i'}$ the distance between two geological realizations

Variables:

y_i binary variables which denote whether a realization is removed ($y_i = 1$) or not ($y_i = 0$)

$v_{i,i'}$ continuous variables ($v_{i,i'} \in [0,1]$) which denote the fraction of its probability mass that is transported from realization i to realization i'

p_i^{new} continuous variables ($p_i^{new} \in [0,1]$) which denote the new probabilities of realizations i after optimal probability mass transportation. Notice that if $p_i^{new} = 0$, it means that realization i is removed

2.5 Case Study

In this study, the proposed realization reduction method is applied to 3 different reservoir grids to quantify geological uncertainty. The grid size, dimension and the number of injector or producer considered in each of the study is different. The case studies demonstrate the applicability of the realization reduction method to reservoirs of different dimensions and complexity.

2.5.1 Realization generation

In all the case studies, a superset of 100 realizations are generated for realization reduction. For each realization, porosity values of the reservoir grid are generated in MRST using a built-in function '*Gaussian Field*' with a range parameter of [0.2 0.4]. The function creates an approximate Gaussian random field by convolving a normal distributed random field with a Gaussian filter with a standard deviation of 2.5 (Lie et al., 2012).

Permeability values are further generated from the porosity values using the Carmen-Kozeny relationship (Lie et al., 2012) as given by Eq. (2.24)

$$k_c = \frac{1}{2\tau A_v^2} \frac{\phi_c^3}{(1-\phi_c)^2} \tag{2.24}$$

In Eq. (2.24), k_c is the permeability of cell c, ϕ_c is the porosity of cell c, A_v is the surface area of spherical uniform grains with a constant diameter of 10×10^{-6} m and τ is the tortuosity with a value of 0.81 (Lie et al. 2012). The irreducible water saturation (S_c) values for each cell c were generated next from the porosity and permeability values using the Wyllie and Rose equation as given in Eq. (2.25)

$$k_c = \left[\frac{100\phi_c^{2.25}}{S_c} \right]^2 \tag{2.25}$$

To evaluate the static measures for different geological realizations in this case study, the threshold porosity is set as $\phi_0 = 0.25$ and the threshold permeability is set as $k_0 = 1\times10^{-13} m^2$ to determine whether a cell is net or non-net.

2.5.2 Static measure based ranking

The static measure based ranking method is applied to the different case studies to select a subset of 10 realizations from the superset of 100 realizations. In the static measure based ranking methods, all of the 100 realizations in the superset are sorted in ascending order based on a single static measure value. Ten realizations are evenly selected from the sorted list corresponding to ranks of 1, 12, 23, 34, 45, 56, 67, 78, 89 and 100. Realizations with ranks of 1 and 100 from the sorted list ensure that the realizations with the best and worst performance, as denoted by the static measures, are incorporated in the selected subset of realizations. In this study, the following static measures are used to perform realization reduction using the ranking based method: K_{net}, ϕ_{net}, S_{net}, F_{net}, F_{LC}, PV_{net}, $OOIP$, OIP_{net} and CHV_{local}.The performance of the selected subset of realizations using the proposed realization reduction framework is compared to the selected realizations using static measure based ranking method.

2.5.3 Case Study 1

The reservoir model used in case sudy 1 consists of a two-dimensional grid with a size of 21 × 21 cells (441 cells) where each grid cell has dimensions of 5m × 5m in the X and Y directions, respectively. To check the performance of the proposed realization reduction method, Matlab Reservoir Simulation Toolbox (MRST) (Lie et al., 2012) is used to perform reservoir simulations on different geological realizations to obtain the production parameters for validation. The reservoir simulation is performed using 3 injector wells and 5 producer wells in MRST to calculate the COP and NPV of oil production for all the 100 geological realizations of the reservoir grid. The injector well locations are fixed at grid positions of [1 1], [1 11] and [1 21]. The producer well locations are fixed at grid positions of [21 1], [21 6], [21 11], [21 16] and [21 21]. The porosity and permeability distribution of the seventy-fifth realization are given in Figs. 2.1 and 2.2, respectively. The injector (I_1, I_2, I_3) and producer (P_1, P_2, P_3, P_4, P_5) well locations for the two dimensional grid is shown in Fig. 2.1.

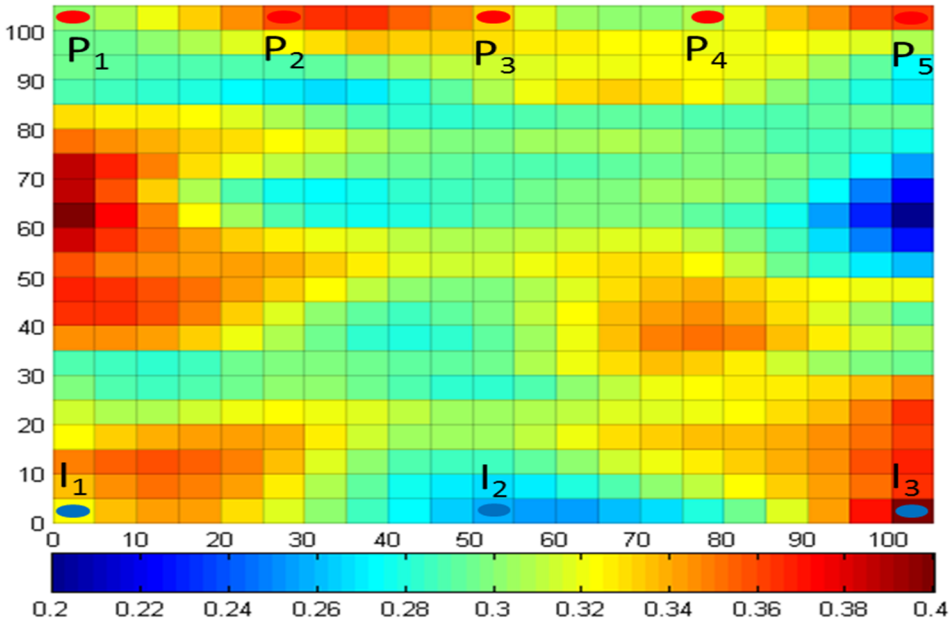

Figure 2.1 Porosity distribution of the Case 1 grid for the seventy-fifth realization from the superset

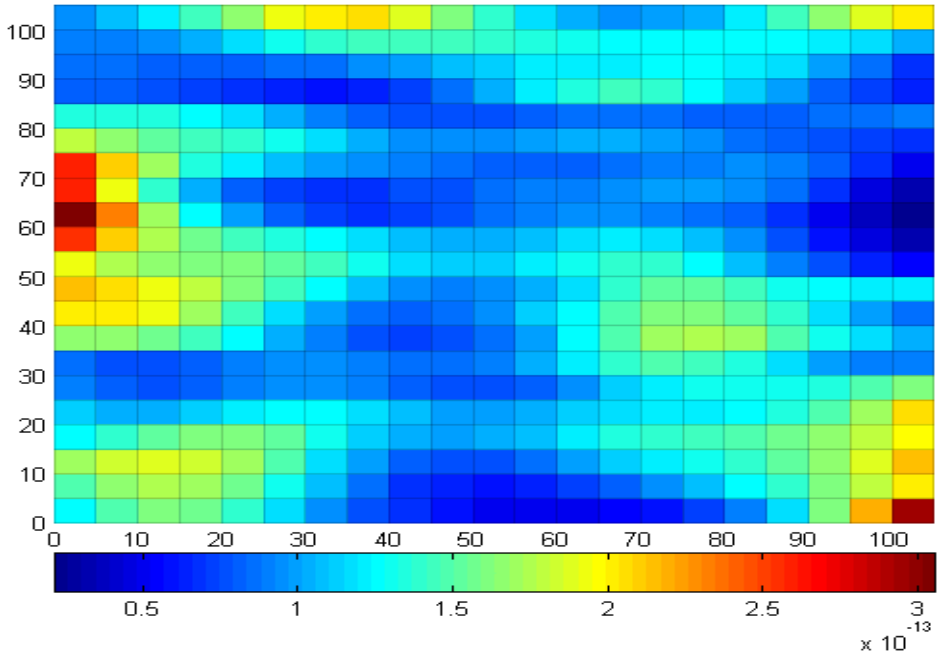

Figure 2.2 Permeability (m^2) distribution of the Case 1 grid for the seventy-fifth realization from the superset

The fluid properties and the economic data used in the reservoir simulation to obtain the NPV and COP for all the realizations are given in Table 2.1.

Table 2.1 Case study 1 parameters

Parameter	Value
Initial pressure p_i	0 psi
Oil viscosity μ_o at p_i	5 cp
Water viscosity μ_w at p_i	1 cp
Oil density ρ_o	859 kg/m^3
Water density ρ_w	1,014 kg/m^3
Relative permeability exponent for oil n_o	2
Relative permeability exponent for water n_w	2
Residual phase saturation for oil Sr_o	0
Residual phase saturation for water Sr_w	0
Relative permeability for oil kwm_o at Sr_o	1
Relative permeability for water kwm_w at Sr_w	1
Oil Price	100$/stb
Water Production Cost	10$/stb
Water Injection Cost	10$/stb
Discount Rate	0%

The total time horizon for the reservoir simulation is 500 days with 10 equal time periods. Oil production is calculated at each time period and the COP value is the cumulative oil production at the final time period.

Applying the proposed realization reduction method, 10 realizations are selected from the superset of 100 realizations. The ID of the 10 selected realizations and the new probabilities of the realizations in the reduced subset are given in Table 2.2. The proposed MILP model had 100 binary variables representing all the realizations in the superset. The CPU time for solving the proposed optimization model, using a computer system with 3.2GHz processor and 8 GB RAM, is less than a second. The NPV and COP values associated with the selected realizations are also provided in Table 2.2.

Table 2.2 Realizations selected using the proposed method for case 1

Realization ID	Probability	NPV ($)	COP (m^3/day)
1	0.15	1,007,970	1,679
3	0.19	941,162	1,618
13	0.03	857,397	1,490
31	0.13	899,902	1,543
32	0.07	854,068	1,455
48	0.02	1,077,550	1,832
63	0.09	1,029,220	1,755
65	0.13	1,004,200	1,719
85	0.01	1,115,370	1,860
94	0.18	946,938	1,605

Static measure based ranking method is applied to obtain a subset of 10 realizations from the superset and the results are reported in Appendix A. The selected realization id, the corresponding static measure value, COP and NPV value from flow simulation for case study 1 are reported in Table A.1 in Appendix A.

Histogram and CDF plot showing the distribution between the original superset of 100 realizations and selected subset of 10 realizations using the proposed method is given in Figs. 2.3 and 2.4, respectively. It is evident from the histograms that the shape of the distributions between all the realizations and selected realizations using the proposed method is very similar. The histogram and CDF plot also shows the distributions of selected subset of realizations from K_{net}, F_{LC} and OIP_{net} based ranking. The other ranking based methods have significantly different distributions compared the full set of realizations.

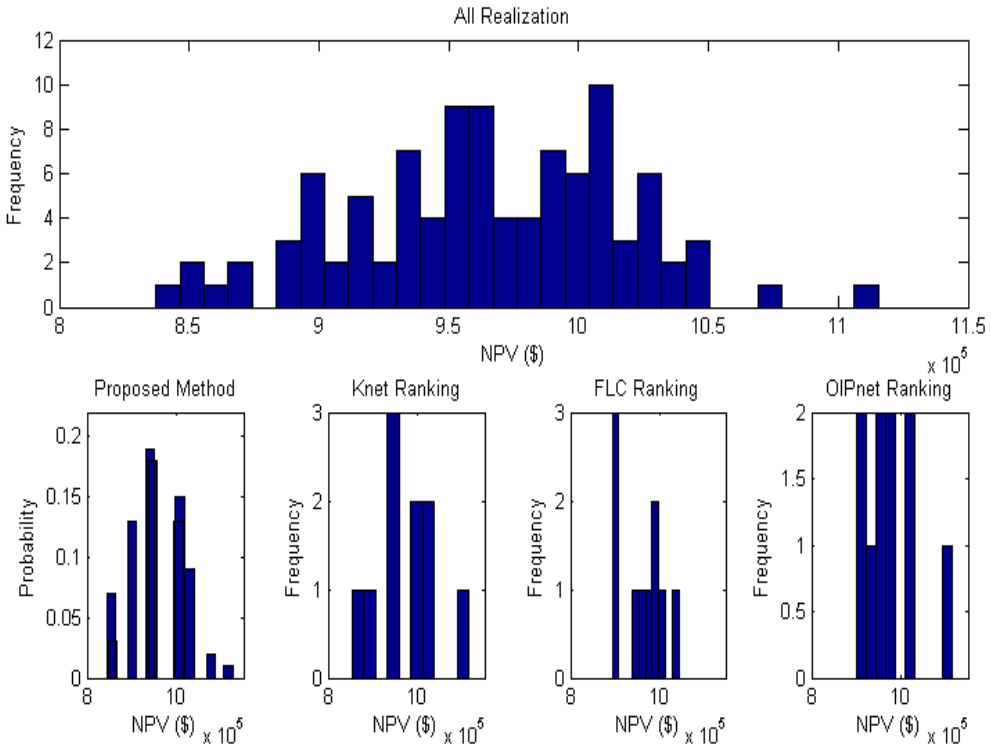

Figure 2.3 Histograms using NPV for (i) superset of all 100 realizations (top) and 10 selected realizations using (ii) the proposed method, (iii) Knet ranking, (iv) FLC ranking and (v) OIPnet ranking

The CDF plot shows that the selected realizations from the proposed method almost cover the entire distribution of the original superset of realizations. F_{LC} based ranking method does not incorporate realizations from the superset which denote the best and worst performances in terms of NPV. On the other hand, K_{net} based ranking method does a good job of incorporating the realizations denoting the best and worst NPV amongst the original full set of realizations.

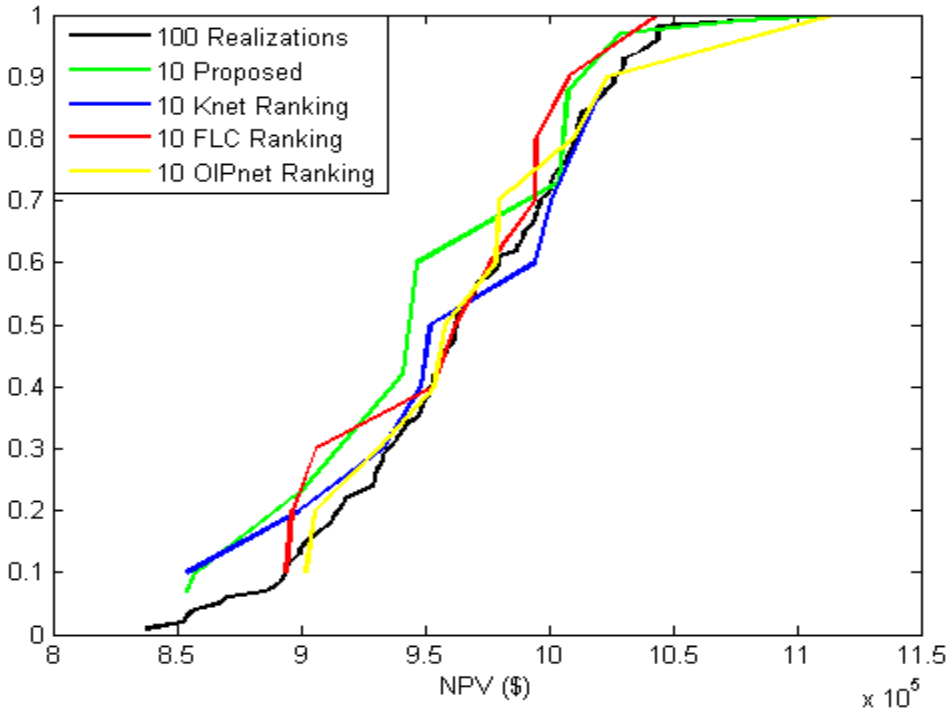

Figure 2.4 CDF plot comparison using NPV between the superset of realizations and selected set of realizations using (i) the proposed method, (iii) Knet ranking, (iv) FLC ranking and (v) OIPnet ranking

Plots of COP versus time period for the selected subset of realizations using the proposed method and different static measure based ranking method are given in Fig. 2.5. The COP plots of the selected realizations (green) are superimposed over the COP plots of all the realizations in the superset (grey) to compare how the selected realizations are distributed amongst the superset of realizations. The COP plots of the selected realizations from the proposed method evenly cover the entire range of COP plots from the full set of realizations. The selected realizations are spread throughout the superset of realizations confirming that the proposed method selects a subset of realization which has identical characteristics to the superset of realizations. The COP plots for the selected realizations using F_{LC} and OIP_{net} ranking does not incorporate realizations which have lower oil production values from the full set of realizations.

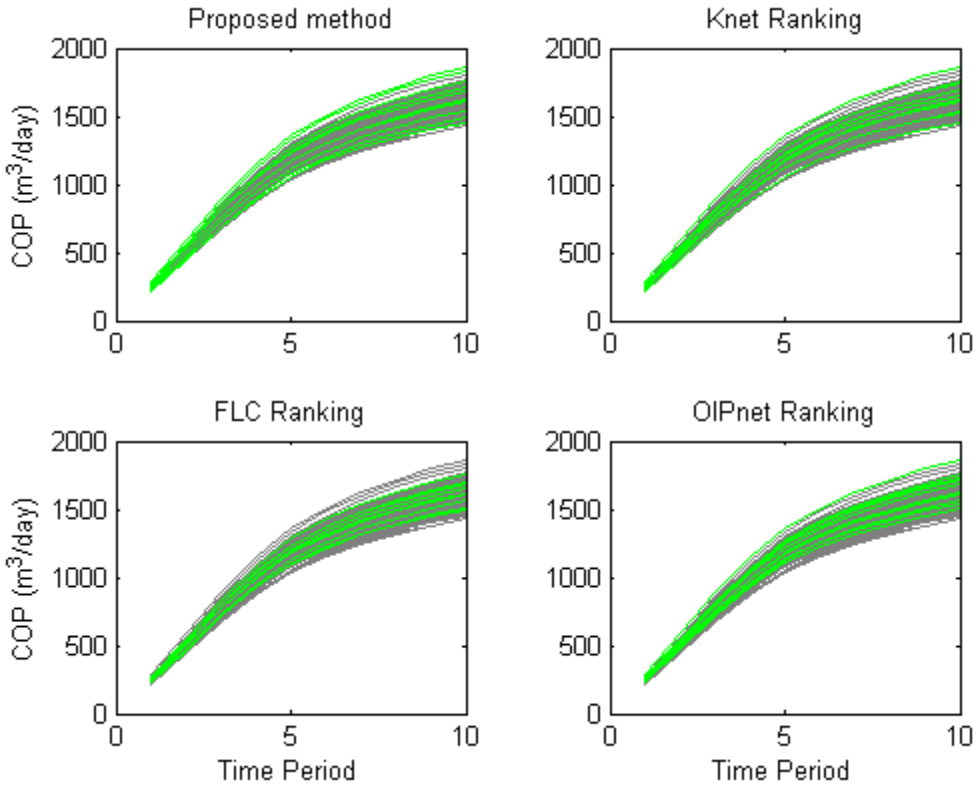

Figure 2.5 COP versus time plot for 10 realizations selected from (i) the proposed method, (iii) Knet ranking, (iv) FLC ranking and (v) OIPnet ranking

To check the quality of the selected realizations, expected production parameters are also calculated for comparison. The expected COP is calculated by the summation of all the products between the probability of selecting a realization and the corresponding COP values of that realization, as given by the following equation

$$COP_{Expected} = \sum_{i} COP_i . p_i \tag{2.26}$$

where p_i is the probability of a selected realization i and COP_i is the corresponding COP value of that selected realization. The expected COP for the subset of realizations obtained using the proposed method is calculated using Eq. (2.26). Selected realizations using the static measure based ranking methods have equal probabilities of being selected, and therefore, the expected COP for the subset of realizations is the mathematical average of the COP values for the selected realizations. Using a similar idea, the expected NPV is calculated using Eq. (2.27)

$$NPV_{Expected} = \sum_i NPV_i . p_i \tag{2.27}$$

where p_i is the probability of a selected realization i and NPV_i is the corresponding NPV value. Similarly, the expected NPV from the static measure based ranking method is the mathematical average of the NPVs of the selected realizations since all the selected realizations have equal probabilities.

The highest, lowest, and expected values of both NPV and COP of the superset of 100 realizations, the subset of 10 realizations using the proposed method and the subset of 10 realizations using ranking method based on various single static measures are given in Table 2.3. The proposed method has an expected NPV and COP value which is close to the expected NPV and COP value of the superset of all the realizations. The realization with the maximum NPV and COP value of the superset of realizations is incorporated in the subset of realizations obtained from the proposed method. In this case study, ranking based on ϕ_{net} and $OOIP$ have the realizations denoting both the best and worst case performance from the superset of realizations.

Table 2.3 Reservoir simulation results of all realizations and selected realizations of case 1

	$NPV_{\max}$ $(\times 10^6)$	$NPV_{\min}$ $(\times 10^6)$	$NPV_{\exp}$ $(\times 10^6)$	$COP_{\max}$ $(\times 10^3)$	$COP_{\min}$ $(\times 10^3)$	$COP_{\exp}$ $(\times 10^3)$
All realizations	1.115	0.837	0.964	1.860	1.429	1.627
Proposed method	1.115	0.854	0.959	1.860	1.455	1.632
Ranking						
K_{net}	1.115	0.854	0.973	1.860	1.455	1.646
ϕ_{net}	1.115	0.837	0.967	1.860	1.429	1.636
$S_{iw,net}$	1.115	0.853	0.971	1.860	1.455	1.640
F_{net}	1.115	0.902	0.978	1.860	1.501	1.648
F_{LC}	1.044	0.894	0.963	1.760	1.494	1.628
PV_{net}	1.115	0.867	0.972	1.860	1.472	1.654
$OOIP$	1.115	0.837	0.966	1.860	1.429	1.646
OIP_{net}	1.115	0.902	0.976	1.860	1.501	1.657
CHV_{local}	1.044	0.894	0.963	1.760	1.494	1.628

Note: $NPV_{\max}$, $NPV_{\min}$ and $NPV_{\exp}$ are the maximum, minimum and expected NPV from all/selected realizations, respectively; $COP_{\max}$, $COP_{\min}$ and $COP_{\exp}$ are the maximum, minimum and expected COP from all/selected realizations, respectively.

An expected COP plot, as calculated using Eq. (2.26), is generated to compare the performance of the proposed realizations reduction method. The expected COP plot which compares the expected COP of the proposed method and the various single static measure based traditional ranking method at each time period is given in Fig. 2.6. The part of the plot at the eight time period is magnified to closely visualize the figure. It is desired to have the expected COP from the realization reduction methods close to the expected COP of the full set of realizations. The magnified part of Fig. 2.6 confirms that the expected COP of the reduced set of realizations using the proposed method at the 8th time period is close to the expected COP from all the realizations. However, the expected COP from F_{LC} and CHV_{local} ranking is the closest to the expected COP of the superset of all the realizations. Other ranking based methods have expected COP values much higher than the expected COP from all the realizations in the superset.

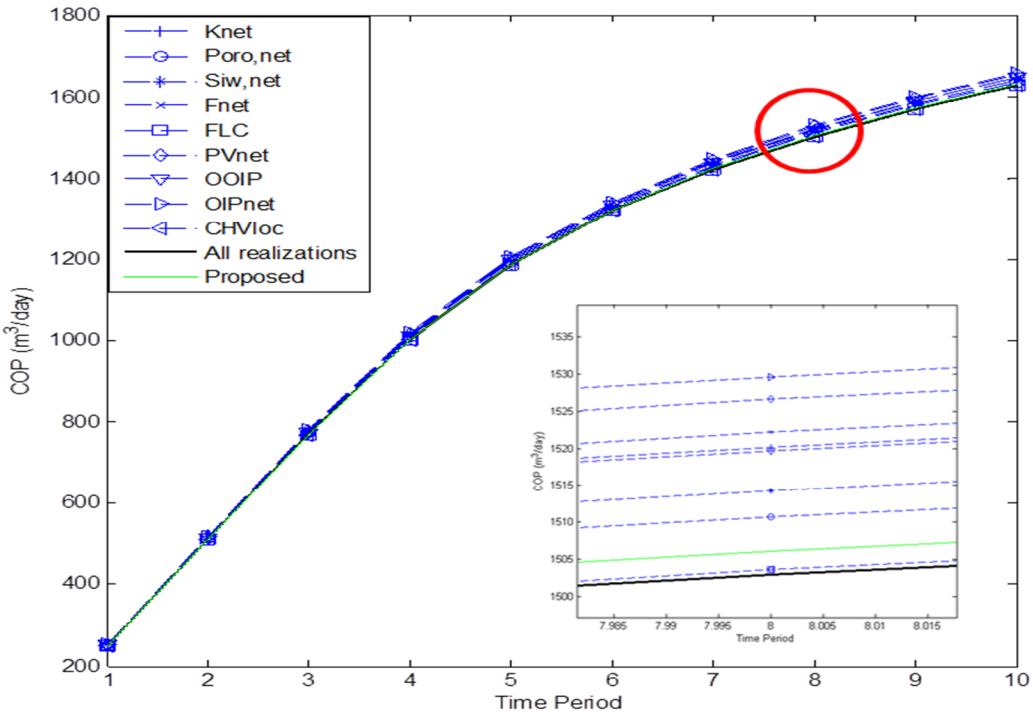

Figure 2.6 Expected COP plots of the different realization reduction methods; the figure inside is a magnified version of the plot to show the details

2.5.4 Case Study 2

Case study 2 has a larger reservoir grid with different number and location of wells as compared to the previous case study. In case study 2, a two-dimensional model consisting of 40 × 40 grid cells (1600 total cells) with dimensions of 5m in both X and Y directions is generated. Grid locations of 4 vertical injectors at [8 35], [16 35], [24 35], [32 35] and 4 vertical producers at [8 5], [16 5], [24 5], [32 5] were fixed in the reservoir. The porosity and permeability distributions of the seventy-fifth realization are given in Figs. 2.7 and 2.8 respectively. In addition, the fixed injector (I_1, I_2, I_3, I_4) and producer (P_1, P_2, P_3, P_4) locations are given in Fig. 2.7.

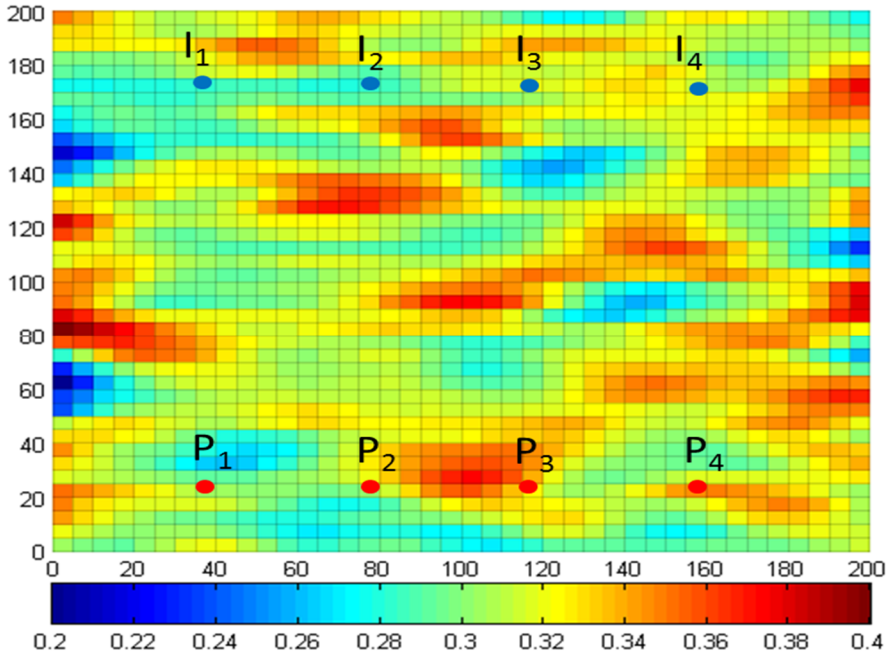

Figure 2.7 Porosity distribution of the Case 2 grid for the seventy-fifth realization from the superset

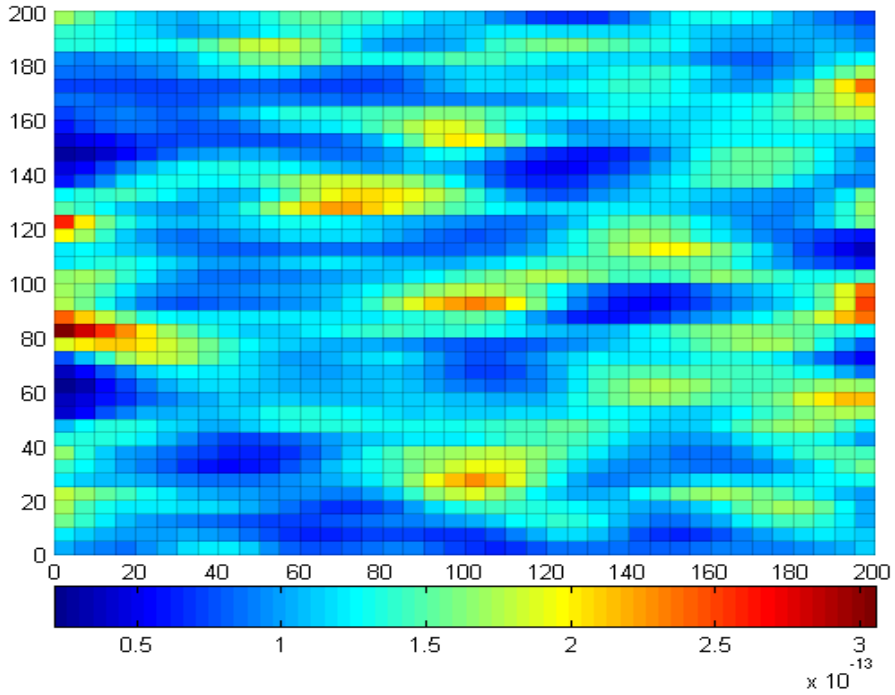

Figure 2.8 Permeability (m^2) distribution of the Case 2 grid for the seventy-fifth realization from the superset

MRST reservoir simulator is used to obtain the performance paramaters of NPV and COP from the oil production data. The fluid properties used in the reservoir simulation for case study 2 are given in Table 2.4. The economic data used for calculation of NPV is also provided in Table 2.4.

Table 2.4 Case study 2 parameters

Parameter	Value
Initial pressure p_i	5,080 psi
Oil viscosity μ_o at p_i	1.18 cp
Water viscosity μ_w at p_i	0.325 cp
Oil density ρ_o	865 kg/m^3
Water density ρ_w	929 kg/m^3
Relative permeability exponent for oil n_o	2
Relative permeability exponent for water n_w	2
Residual phase saturation for oil Sr_o	0
Residual phase saturation for water Sr_w	0
Relative permeability for oil kwm_o at Sr_o	1
Relative permeability for water kwm_w at Sr_w	1
Oil Price	86$/stb
Water Production Cost	36$/stb
Water Injection Cost	18$/stb
Discount Rate	0%

The total reservoir simulation time horizon for case study 2 is 3000 days. The total time is divided into 10 equal periods for the calculation of both NPV and COP.

The static measures for case 2 are calculated in a pre-processing step since the static measure values were used in the distance calculation of the proposed method. The proposed MILP model had 100 binary variables corresponding to each realization in the superset. Similar to the previous case, the computational processing time for solving the proposed MILP realization reduction model is less than a second. Applying the proposed method, the 10 selected realizations' ID and the new probabilities of those realizations obtained from the proposed method are given in Table 2.5, along with the associated flow simulation NPV and COP values. As expected, a broad range of NPV and COP values are covered by the selected realizations from the proposed method.

Table 2.5 Realizations selected using the proposed method for case 2

Realization ID	Probability	NPV ($)	COP (m^3/day)
3	0.17	1,276,140	5,091
25	0.01	1,427,390	5,608
33	0.15	1,344,940	5,212
46	0.14	1,238,330	4,846
59	0.02	1,150,250	4,545
73	0.15	1,342,980	5,269
76	0.03	1,457,430	5,640
89	0.13	1,374,660	5,368
92	0.15	1,230,330	4,959
97	0.05	1,183,520	4,596

The ranking based on a single static measure is applied and the realization ID, corresponding static measure value, COP and NPV value from the flow simulation for case 2 are reported in Table A.2 in Appendix A. Figure 2.9 shows the histogram of the superset of realization and the selected subset of realizations obtained using the proposed method and K_{net}, F_{LC} and OIP_{net} based ranking methods. It is clearly evident from the shape of the frequency distribution that the distribution from the proposed method is very similar to the distribution of the superset of all realizations. The similar shape of both the histograms confirms the similarity in the statistical distribution of the reduced realizations from proposed method and the full set of realizations. Both the extreme NPV values of the histogram for all the realizations are also covered by the histograms of the proposed method. The distributions of other ranking based methods have either significantly different shape than the distribution of the NPV for all the realizations or do not cover both extremes of the histogram for all the realizations.

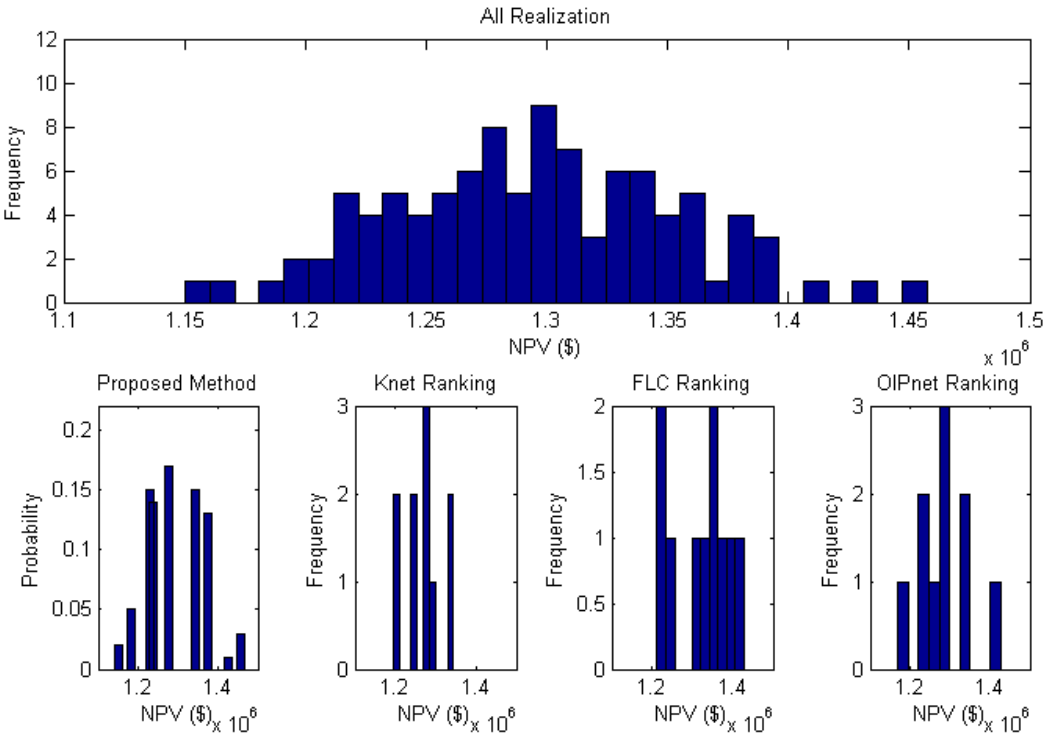

Figure 2.9 Histograms using NPV for (i) superset of all 100 realizations (top) and 10 selected realizations using (ii) the proposed method, (iii) Knet ranking, (iv) FLC ranking and (v) OIPnet ranking

The CDF plot of the full set of realizations and the selected set of realization obtained from the proposed method and other ranking based method is given in Fig. 2.10. The CDF plot further confirms that the proposed method ensures that the realizations representing the best and worst case NPV values from the superset are incorporated in the selected subset of realizations. No other ranking based realization reduction methods contain realizations with both the best and worst case NPVs. The CDF plot for the proposed method does not deviate significantly from the CDF plot of all the realizations. Fig. 2.10 reaffirms the similarity in the distribution of the subset of realizations from the proposed method and the superset of realizations from all the realizations.

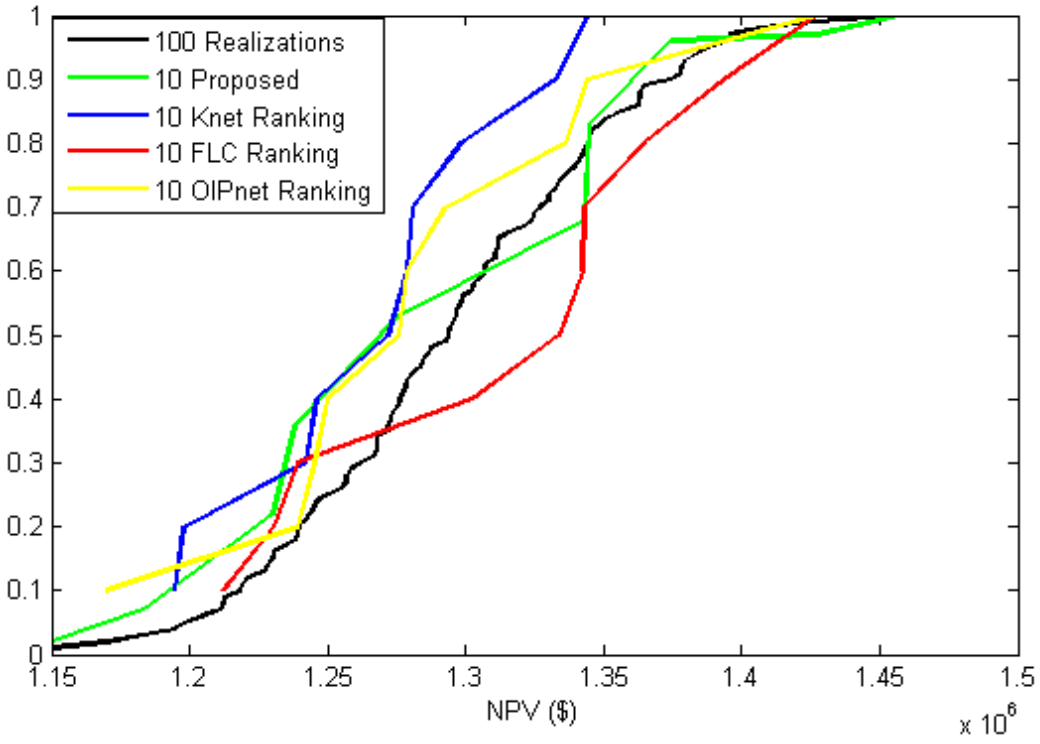

Figure 2.10 CDF plot comparison using NPV between the superset of realizations and selected set of realizations using (i) the proposed method, (iii) Knet ranking, (iv) FLC ranking and (v) OIPnet ranking

The COP versus time period plot for the 10 selected realizations from the proposed method and all 100 realizations from the superset are shown in Fig. 2.11. Figure 2.11 also has the COP versus time period plot for 10 selected realizations obtained from ranking based methods using the following static measures: K_{net}, F_{LC} and OIP_{net}. The selected subset of realizations from the proposed method is evenly spread among the superset of realizations. Figure 2.11 confirms that the reduced distribution from the proposed method is a good representation of the superset of realizations since the reduced subset contains realizations which have the best and worst COP values at each time period. COP plots from selected realizations obtained using K_{net} ranking method shows a very uneven spread of realizations when compared to the superset of all realizations.

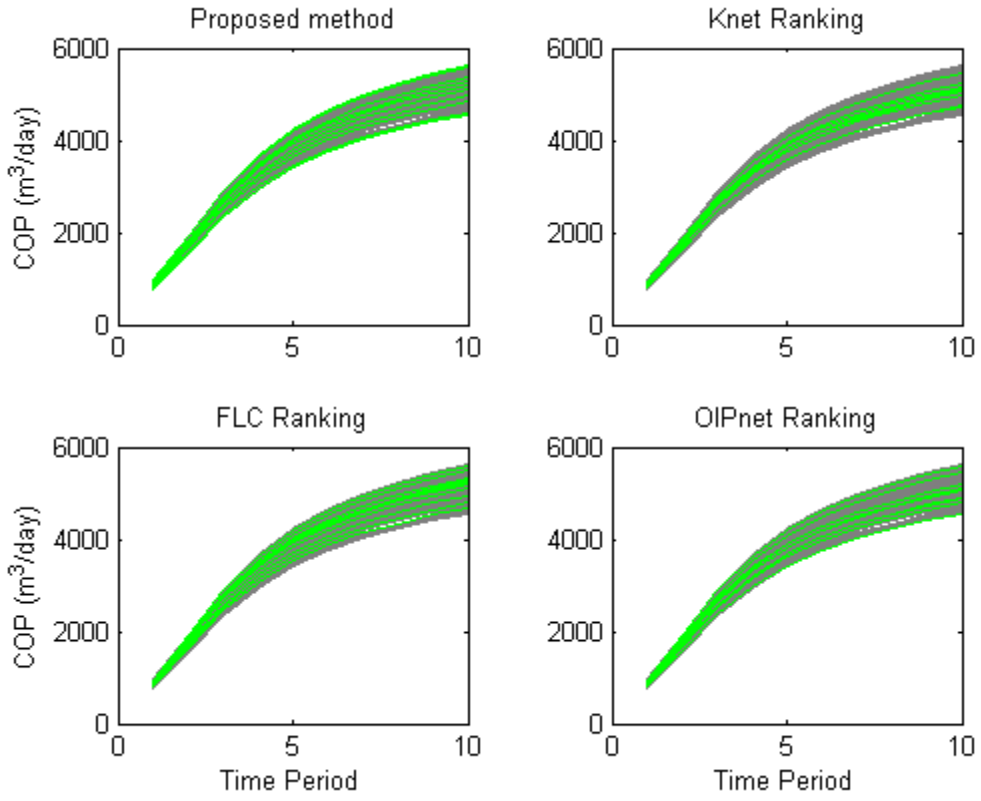

Figure 2.11 COP versus time plot for 10 realizations selected from (i) the proposed method, (iii) Knet ranking, (iv) FLC ranking and (v) OIPnet ranking

The expected COP and NPV values for the reduced subset of realizations using the proposed method and the ranking based methods are calculated using Eq. (2.26) and Eq. (2.27), respectively. The best, worst and expected NPV and COP values for all the realizations in the superset, selected realizations from proposed method and selected realizations from the various static measure based ranking method is given in Table 2.6. Subset of realizations obtained using the proposed method contains both the worst and best NPV and COP values from the superset of realizations. The expected NPV and COP from the 10 selected realizations using the proposed method is very close to the average NPV and COP values of the complete set of 100 realizations. The proposed method selects realization ensuring the best and worst realizations are included and ensures that the expected NPV and COP values of the reduced distribution is close to the expected NPV and COP values of the superset of realizations. Amongst the ranking based methods, *OOIP* based ranking is the only ranking based method containing the realizations

which has both the best and worst NPV/COP from the superset and has an expected NPV/COP close to that of the full set of realization.

Table 2.6 Reservoir simulation results of all realizations and selected realizations for case 2

	$NPV_{\max}$ $(\times 10^6)$	$NPV_{\min}$ $(\times 10^6)$	$NPV_{\exp}$ $(\times 10^6)$	$COP_{\max}$ $(\times 10^3)$	$COP_{\min}$ $(\times 10^3)$	$COP_{\exp}$ $(\times 10^3)$
All realizations	1.457	1.150	1.294	5.640	4.545	5.083
Proposed method	1.457	1.150	1.297	5.640	4.545	5.104
Ranking						
K_{net}	1.344	1.195	1.269	5.455	4.732	5.024
ϕ_{net}	1.344	1.195	1.282	5.455	4.732	5.043
$S_{iw,net}$	1.344	1.150	1.268	5.455	4.545	5.023
F_{net}	1.427	1.169	1.287	5.608	4.557	5.075
F_{LC}	1.427	1.212	1.319	5.608	4.675	5.169
PV_{net}	1.427	1.169	1.299	5.608	4.557	5.089
$OOIP$	1.457	1.150	1.296	5.640	4.545	5.082
OIP_{net}	1.427	1.169	1.286	5.608	4.557	5.072
CHV_{local}	1.427	1.212	1.319	5.608	4.675	5.169

The expected COP at each time period of the 10 selected realizations obtained from the proposed method and all the static measure based ranking methods are given in Fig. 2.12. The magnified section of the plot at the eight time period shows that the expected COP from the subset of realizations obtained from the proposed method is close to the expected COP from all the 100 realizations in the superset. However, for case 2, several ranking based realization reduction methods have expected COP which is closer to the expected COP of the full set of realizations. On the other hand, some ranking based realization reduction methods have expected COP which show significant deviation to the expected COP of all the realizations.

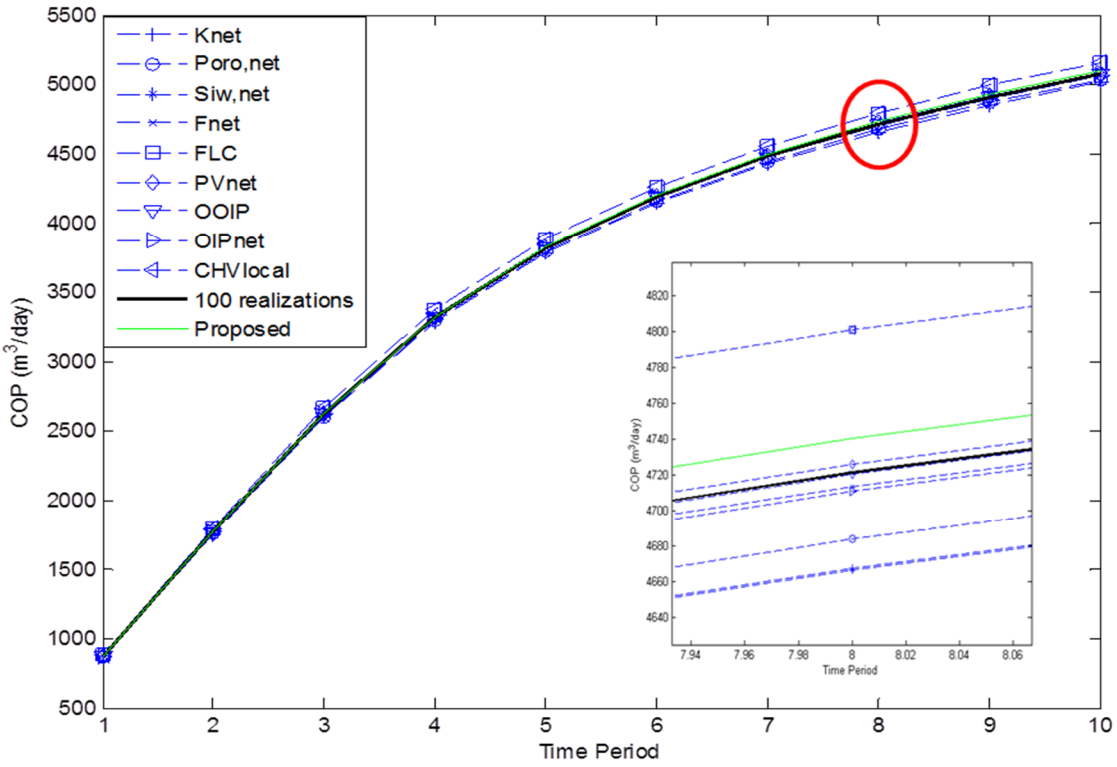

Figure 2.12 Expected COP plots of the different realization reduction methods; the figure inside is a magnified version of the plot to show the details

2.5.5 Case Study 3

Case study 3 is a realistic three dimensional reservoir model with a grid size of 60 × 220 × 5 (66000 total cells) and cell sizes of 6.096 m × 3.048 m × 0.6096 m. The reservoir has one vertical injector well placed at the centre of the grid with position [30 110] and four vertical producer wells placed at the four corners of the grid with positions [1 1], [60 1], [60 220] and [1 220]. The reservoir grid size, fluid properties and well locations for the case study are obtained from the SPE 10 comparative solution project model 2 (Christie and Blunt, 2001). Figure 2.13 shows the three dimensional grid with the mean permeability field calculated from all 100 realizations in the superset. The locations of the vertical injector well (I_1) and the four producer wells (P_1, P_2, P_3, P_4) are also included in Fig. 2.13.

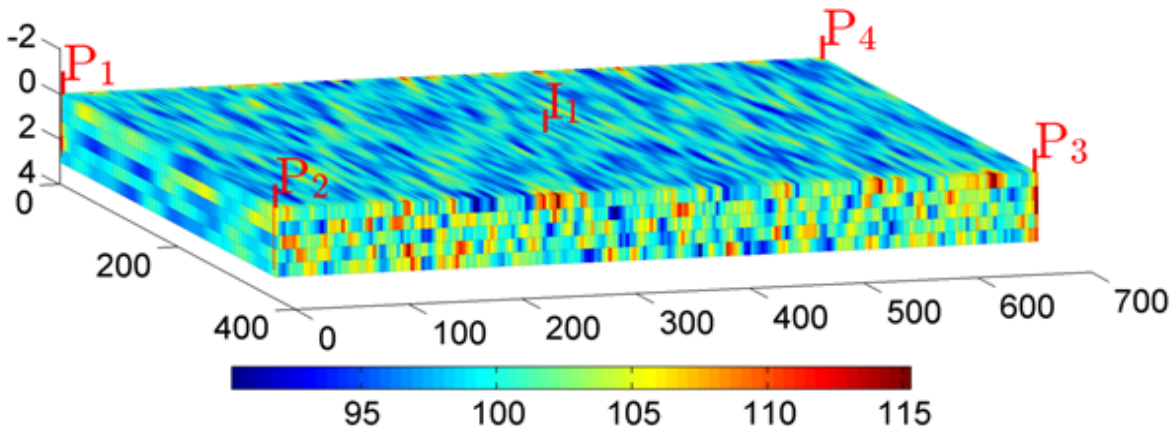

Figure 2.13 Three dimensional grid structure of the mean permeability distribution (mD) of the reservoir with the injector and producer locations

Detailed fluid properties and cost data used for the simulation of the given reservoir are provided in Table 2.7.

Table 2.7 Case study 3 parameters

Parameter	Value
Initial pressure p_i	6,000 psi
Oil viscosity μ_o at p_i	3 cp
Water viscosity μ_w at p_i	0.3 cp
Oil density ρ_o	849 kg/m^3
Water density ρ_w	1,025 kg/m^3
Relative permeability exponent for oil n_o	2
Relative permeability exponent for water n_w	2
Residual phase saturation for oil Sr_o	0.2
Residual phase saturation for water Sr_w	0.2
Relative permeability for oil kwm_o at Sr_o	1
Relative permeability for water kwm_w at Sr_w	1
Oil Price	100$/stb
Water Production Cost	10$/stb
Water Injection Cost	10$/stb
Discount Rate	0%

In addition to NPV and COP, the other production parameter evaluated in the simulator for case 3 is the water cut of the reservoir. The simulation time horizon is set as 360 days and is divided into 12 equal periods.

For illustrative purposes, the porosity distribution of the seventy-fifth realization is given in Fig. 2.14. Each subfigure represents a layer of the three dimensional grid. From left to right, the subfigures represent the porosity distribution of layers 1 to 5 of the grid.

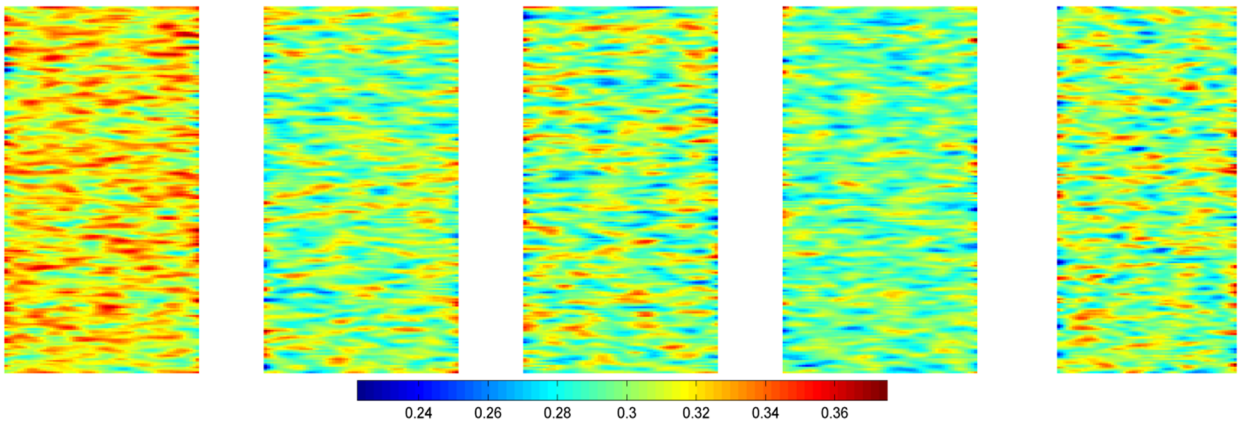

Figure 2.14 Porosity distribution of the Case 3 grid layers for the seventy-fifth realization from the superset

The permeability distribution of all the layers of the seventy-fifth realization, in units of milli-Darcy, is given in Fig. 2.15.

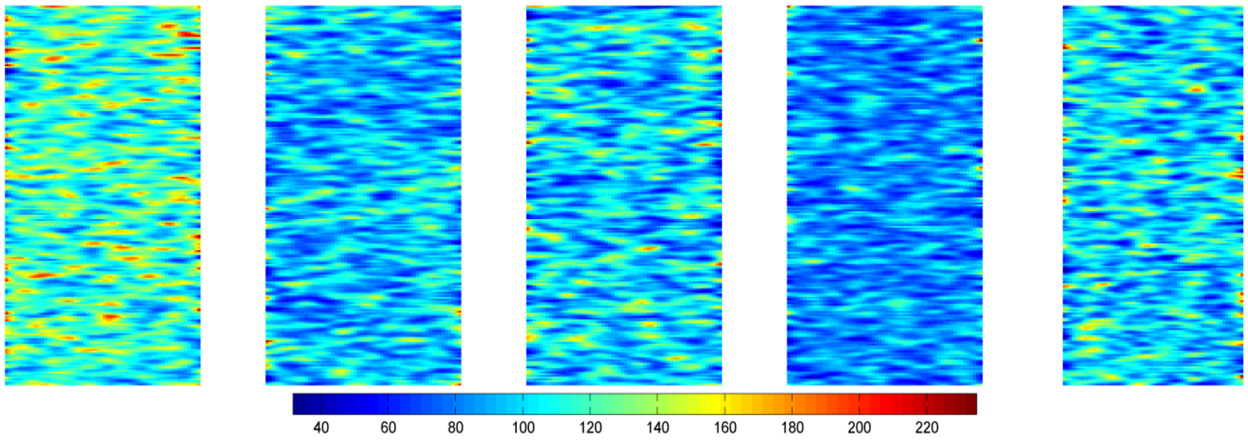

Figure 2.15 Permeability (mD) distribution of the Case 3 grid layers for the seventy-fifth realization from the superset

In this case study, the realization reduction results from the proposed method are compared to the traditional ranking method, kernel k-means clustering method and random selection method. A subset of 10 realizations was selected from the superset of 100 realizations to investigate the effectiveness of the proposed method.

Based on the generated geological realizations, different static measures stated in section 2.3 are calculated in a pre-processing step. Those measures are used to compute the dissimilarities between realizations as defined in Eq. (2.12). The proposed MILP model is built next, which has 100 binary variables corresponding to each realization in the superset. The optimization problem is solved using the CPLEX solver in a desktop computer with a 3.2GHz processor and 8 GB memory in less than one second. It is important to note that the optimization framework for the realization reduction method is solved very efficiently even for a large reservoir grid. The solution of the optimization problem includes the selected realizations' IDs and their new probabilities. For comparison purposes, the selected realizations' IDs, probabilities, NPV and COP values associated with the selected realizations are reported in Table 2.8.

Table 2.8 Realizations selected using the proposed method for case 3

Realization ID	Probability	NPV ($)	COP (m^3/day)
3	0.04	43,207,700	114,482
8	0.2	50,161,200	124,532
20	0.11	46,223,000	118,840
41	0.14	51,491,500	126,455
64	0.01	55,497,500	132,245
76	0.15	47,146,400	120,175
79	0.05	53,198,600	128,922
80	0.01	43,664,800	115,143
85	0.19	49,291,600	123,274
99	0.1	48,695,600	122,414

-

Results from the ranking method are the realizations' IDs. The probabilities of the selected realizations are assumed to be equal (i.e., 0.1 in this case). The selected realizations' IDs, the corresponding static measure values, COP and NPV value from flow simulation are reported in Table A.3 of Appendix A.

2.5.5.1 Kernel k-means clustering

The kernel k-means clustering method proposed by Scheidt and Caers (2009) was applied to this case study. The workflow is as follows:

1. Computation of the dissimilarity matrix. While the literature generally uses simplified flow simulation results to calculate the dissimilarity, the same dissimilarity values used by the proposed method were used for clustering in this study.
2. Classical Multidimensional Scaling (MDS) was used to transform the dissimilarity matrix into reduced dimensional data in Euclidean space.
3. Conversion of the Euclidean space to a feature space by using a Gaussian kernel (radial basis function) given by Eq. (2.28)

$$K_{mn} = \kappa(x_m, x_n) = \exp\left[-\frac{\|x_m - x_n\|}{2\sigma^2}\right] \tag{2.28}$$

   In the Gaussian kernel function, a kernel width, σ, value between 10% and 20% of the range of the distance measures was used based on the recommendation by Shi and Malik (2000). σ = 2000 was used in this study.
4. Ten clusters were generated using k-means clustering. The realization ID closest to the centroid of each cluster was chosen as the representative realization from the kernel k-means clustering.

The realization ID, NPV and COP values from the 10 selected realizations using kernel k-means clustering are given in Table 2.9. All of the selected realizations of the clustering method have equal probabilities.

Table 2.9 Realizations selected using kernel k-means clustering for case 3

Realization ID	NPV ($)	COP (m^3/day)
19	49,887,900	124,137
99	48,695,600	122,414
78	51,281,700	126,152
66	50,017,000	124,324
70	45,745,300	118,150
92	53,209,000	128,937
30	50,347,000	124,801
87	51,628,000	126,652
37	49,306,000	123,296
24	47,640,100	120,888

A subset of realizations is selected randomly to compare with the proposed method. Random permutation is used to generate 10 realization IDs from the superset. The realization ID, NPV and COP values from the 10 equiprobable randomly selected realizations are given in Table 2.10.

Table 2.10 Realizations selected using random selection for case 3

Realization ID	NPV ($)	COP (m^3/day)
12	52,791,900	128,334
15	49,003,702	122,859
44	49,679,300	123,836
36	51,044,700	125,809
51	50,191,100	124,575
2	49,371,500	123,391
81	49,966,000	124,250
61	52,327,100	127,663
75	48,834,300	122,614
67	48,086,500	121,534

Histograms and CDF plots were generated for the reduced subset of realizations obtained using the proposed method and the complete superset of realizations. The reduced subset of realizations obtained using the proposed method was compared to the reduced subset of realizations obtained from the static measure based ranking method, kernel k-means clustering method and random selection method.

Figures 2.16 and 2.17 presents the histogram and CDF plot showing the NPV distribution of the original superset of 100 realizations and the selected subset of 10 realizations using the proposed method, respectively. The shapes of the histogram in Fig. 2.16 between the superset of realizations and the selected subset of realizations obtained using the proposed method confirms similarities in the statistical characteristics between the two distributions. In comparison, the histograms of the selected realizations obtained by k-means clustering, K_{net} based ranking and random selection have a significantly different shape than the histogram from the superset.

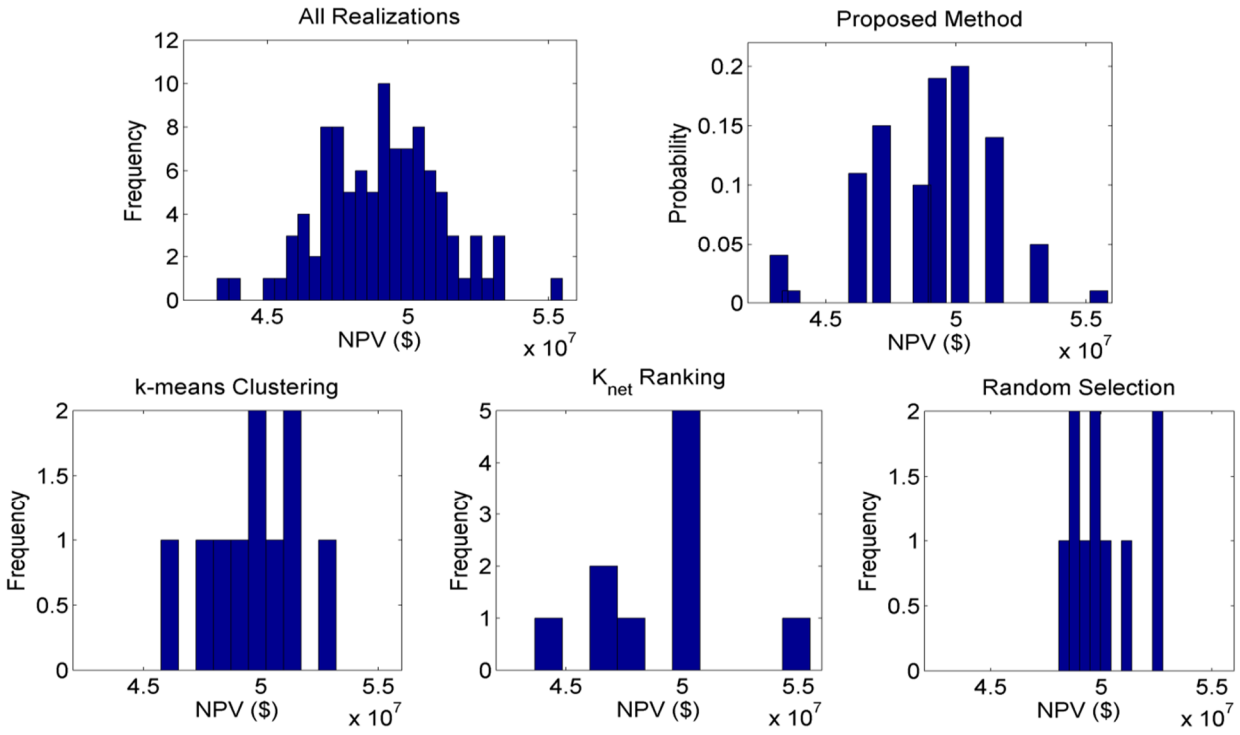

Figure 2.16 Histograms using NPV for (i) superset of 100 realizations (top) and 10 selected realizations using (ii) the proposed method, (iii) kernel k-means clustering, (iv) Knet ranking and (v) random selection

In addition to the CDF plot of the proposed method, Fig. 2.17 also has the CDF plots of the selected realizations obtained by random selection, k-means clustering and K_{net} based ranking. It is evident from the CDF plots that the selected subset of realizations using the proposed method contains the realizations which have the maximum and minimum NPV values of the superset of

realizations. It is clearly evident that the distributions obtained from the subset of realizations using random selection and k-means clustering are a poor representation of the superset and neither of these methods incorporate the maximum or minimum NPV from the superset of realizations.

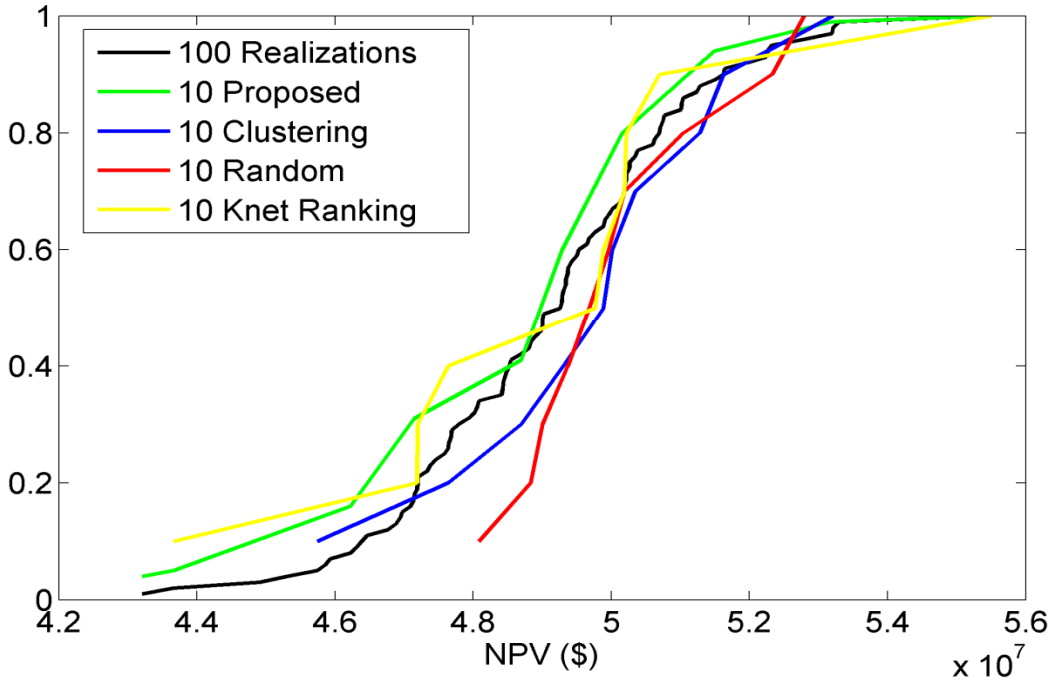

Figure 2.17 CDF plot comparison using NPV between the superset of realizations and selected set of realizations using (i) the proposed method, (ii) kernel k-means clustering, (iii) Knet ranking and (iv) random selection

Figure 2.18 shows the plot of COP versus time period for the 10 realizations selected from the proposed method, kernel k-means clustering, random selection and K_{net} ranking. Plots for the reduced realizations are all superimposed over the COP versus time plots for all 100 realizations from the original set of realizations. Figure 2.18 confirms that the selected subset of realizations from the proposed method generates a distribution that is a good representation of the distribution of the original superset as the selected realizations evenly covers the entire range of the original superset of realizations. The other realizations reduction methods have COP plots which are skewed and as a result not evenly covering the COP plots of the superset of all the realizations.

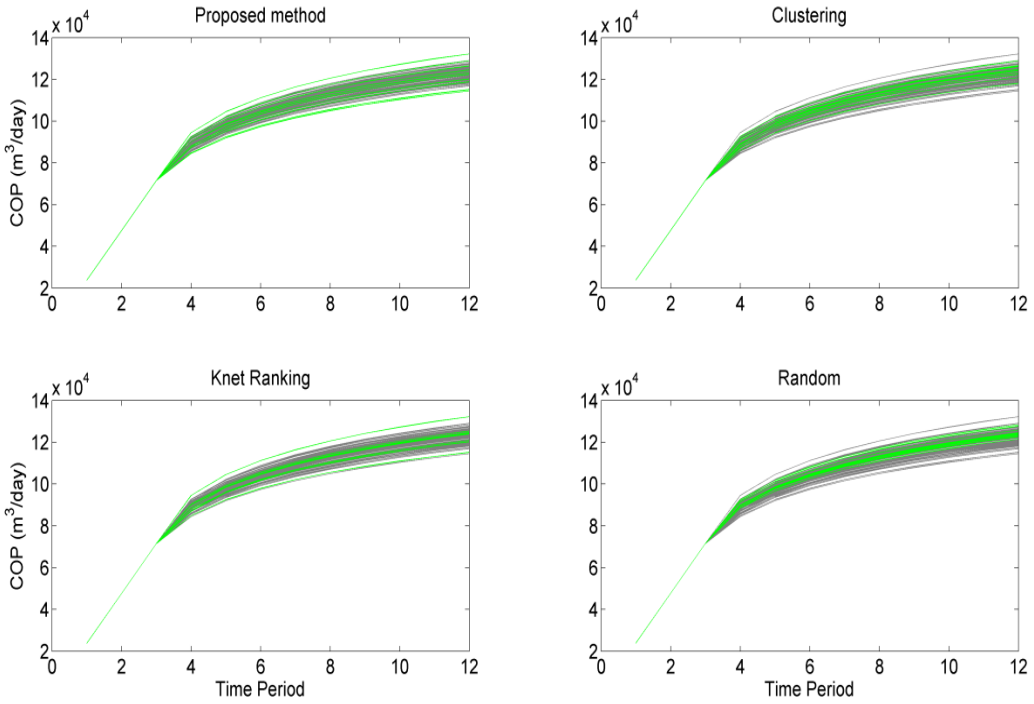

Figure 2.18 COP versus time plot for 10 realizations selected from (i) the proposed method, (ii) kernel k-means clustering, (iii) Knet ranking and (iv) random selection

The maximum, minimum and expected NPV and COP values for the different realization reduction methods are given in Table 2.11. The proposed method selects realizations to preserve the characteristics of the superset, and this is verified by the small difference between the expected NPV value of the selected realizations by the proposed method (i.e., 4.901×10^7) and the expected NPV from all of the realizations (i.e., 4.907×10^7). The expected COP from the selected subset of realizations using the proposed method (1.229×10^7) is also very close to the expected COP from the superset of realizations (1.230×10^7). The proposed method leads to results containing the realization with the maximum and minimum NPV and COP values from the original full set of realizations as can be seen in Table 2.11. The other realization reduction methods' results generally do not contain the realizations representing the maximum and minimum NPV and COP values.

Table 2.11 Reservoir simulation results of all realizations and selected realizations for case 3

	$NPV_{\max}$ $(\times 10^7)$	$NPV_{\min}$ $(\times 10^7)$	$NPV_{\exp}$ $(\times 10^7)$	$COP_{\max}$ $(\times 10^5)$	$COP_{\min}$ $(\times 10^5)$	$COP_{\exp}$ $(\times 10^5)$
All realizations	5.550	4.321	4.907	1.322	1.145	1.230
Proposed method	5.550	4.321	4.901	1.322	1.145	1.229
Ranking						
K_{net}	5.550	4.366	4.920	1.322	1.151	1.231
ϕ_{net}	5.550	4.366	4.941	1.322	1.151	1.234
$S_{iw,net}$	5.550	4.366	4.958	1.322	1.151	1.237
F_{net}	5.550	4.366	4.900	1.322	1.151	1.229
F_{LC}	5.550	4.491	5.007	1.322	1.169	1.244
PV_{net}	5.550	4.366	4.895	1.322	1.151	1.228
$OOIP$	5.550	4.366	4.926	1.322	1.151	1.232
OIP_{net}	5.550	4.366	4.895	1.322	1.151	1.228
CHV_{local}	5.550	4.491	5.007	1.322	1.169	1.244
Clustering	5.321	4.575	4.978	1.289	1.182	1.240
Random	5.279	4.809	5.013	1.283	1.215	1.245

The plots showing the expected COP values for the selected subset of realizations at different time periods using the proposed method, clustering method, random selection and ranking methods are shown in Fig. 2.19. A magnified part of the plot around the tenth time period shows that the expected COP of the selected realizations using the proposed method is closest to the expected COP of the full set of realizations. The expected COP values of the subset of realizations selected using random selection and kernel k-means clustering significantly deviate from the expected COP of the full set of realizations. Compared to the single static measure based ranking method, the proposed method and K_{net} based ranking method provides an expected COP value which is very close to that of the original superset of realizations.

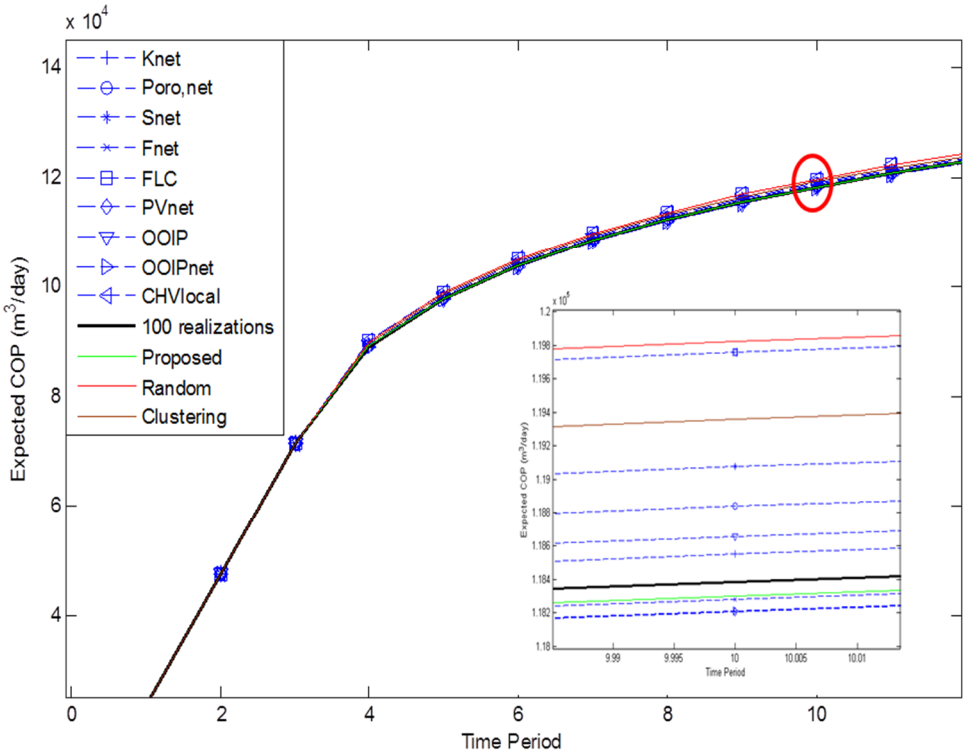

Figure 2.19 Expected COP plots of the different realization reduction methods; the figure inside is a magnified version of the plot to show the details

A further study was generated to check how the proposed realization reduction method represents the superset of realizations in the case of local reservoir performance criteria such as water cut and breakthrough time. The water cut versus the time period plot for the selected realizations using different realization reduction methods is given in Fig. 2.20. To see how similar the distribution of the reduced realization is to that of the original superset of realizations, the water cut plots of selected realizations are superimposed over the water cut plots of all of the realizations in the superset. A magnified version of the water cut plots around the fourth time period is provided in Fig. 2.21 to show the water breakthrough of the selected realizations. The water cut plots confirm that the reduced subset of realizations from the proposed method is a good representation of the superset of realizations. Specifically, the maximum and minimum water cuts at each time period are recovered very well by the proposed method, while the selected realizations using random selection, k-means clustering or K_{net} based ranking do not cover the entire range of water cut plots for all of the realizations in the superset. It is evident

from Fig. 2.21, that the proposed method incorporates realizations which have the highest and lowest water breakthrough time among the superset of realizations.

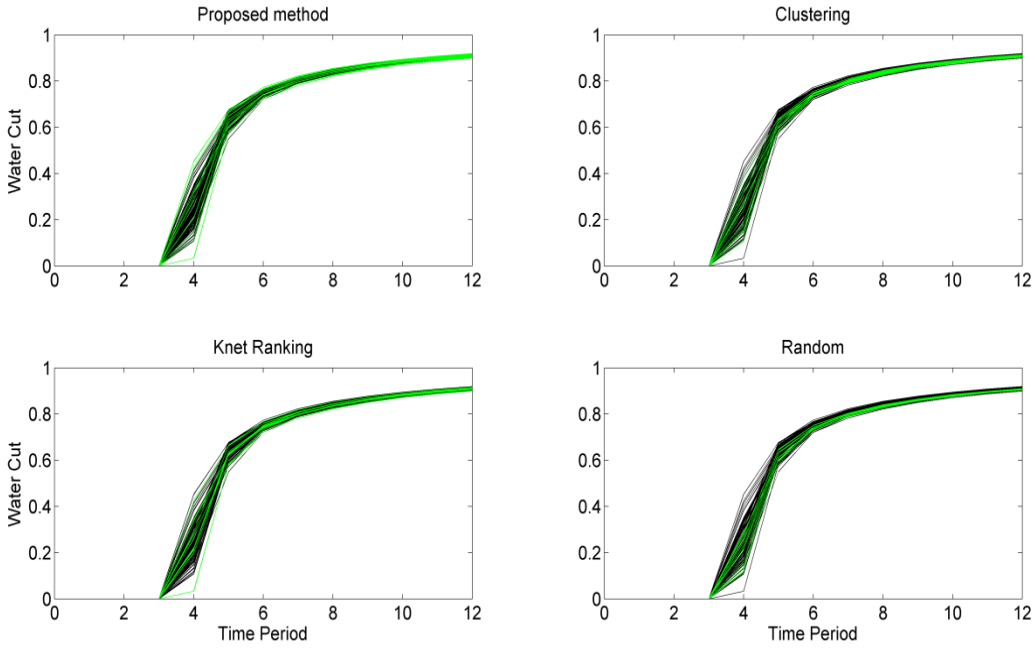

Figure 2.20 Water cut plots for 10 realizations selected from (i) the proposed method, (ii) kernel k-means clustering, (iii) Knet ranking and (iv) random selection.

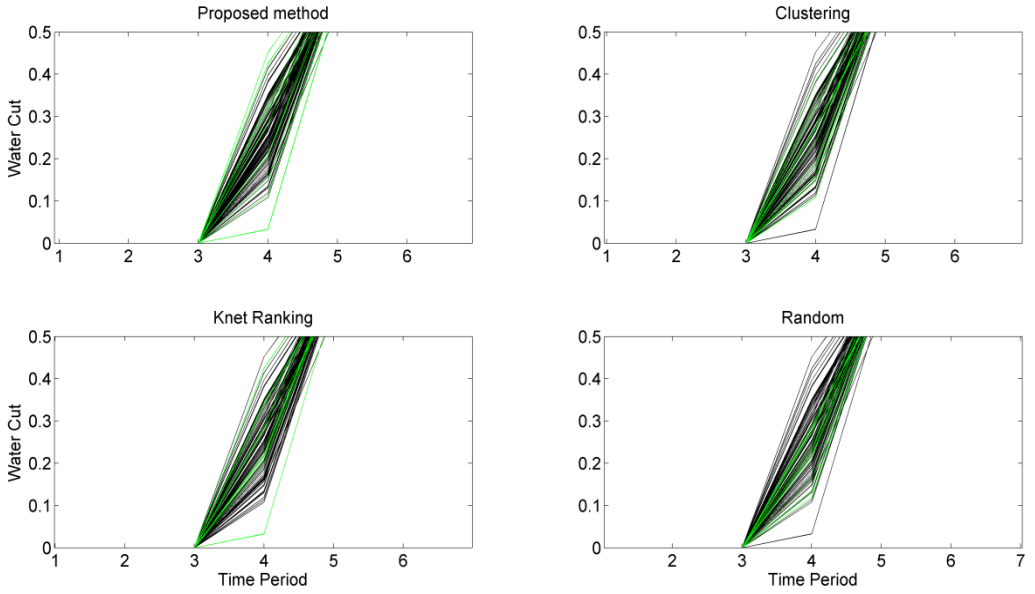

Figure 2.21 Water cut profiles around the fourth period

The results demonstrate that the proposed method generates a subset of realizations which gives a good representation of the superset of realizations in local criterion such as water cut.

An extension of case study 3 is created on a new set of geological realizations to further evaluate the proposed realization reduction method to a realistic reservoir grid. The reservoir size, number and locations of producer/injector wells, fluid properties and economic parameters used in this additional study are same as that of case study 3. A new superset of 200 geological realizations is generated for the reservoir. Two different subset of realization are selected from the superset of 200 geological realizations. The first subset consisted of 10 realizations to be selected from the superset and the second subset consisted of 20 realizations to be selected from the superset. Similar to case study 3, the proposed realization reduction method is compared to realization reduction methods of k-means clustering, random selection and ranking based methods.

The results of the supporting case 3 study are given in Appendix B. The results from selecting 20 realizations from the superset of 200 realizations are given in Figs. B.1 to B.4. Table B.1 gives the maximum, minimum and expected NPV/COP for the different realization reduction methods in selecting 20 realizations from a superset of 200 realizations. The results from selecting 10 realizations from the superset of 200 realizations are given in Figs. B.5 to B.8. The maximum, minimum and expected NPV and COP is given in Table B.2 for the various realization reduction methods in the case of selecting 10 realizations from a superset of 200 realizations.

The results of selecting two different subsets of realization from a superset of 200 realizations consistently shows that the subset of realizations selected using the proposed method has a statistical distribution which is very similar to the superset of all the realizations. In addition, the proposed method ensures the realizations showing the maximum and minimum performance from the superset of all the realizations are incorporated in the selected subset.

2.6 Conclusion

A mixed integer linear optimization model is proposed to reduce the geological uncertainty in reservoir simulations by selecting a small subset of realizations from a larger superset of realizations. The proposed realization reduction method minimizes the probability distance between the original distribution of the superset of realizations and that of the reduced subset of realizations. The proposed realization reduction method calculates the probability distance between realizations using the geological property of the reservoir and static measures. The proposed method not only selects a smaller subset of realizations, but also assigns a new probability to each of those realizations. The proposed method is efficient and computationally inexpensive compared to other simplified flow based methods. As a result, the proposed method is a good candidate for complex realistic reservoirs. The case studies demonstrated that the selected realizations from the proposed method have very close statistical characteristics to the original distribution of the superset of all realizations. In comparison to realizations reduction methods of; ranking, kernel k-means clustering or random selection, the proposed method leads to a distribution which is a closer representation of the distribution obtained from all the realizations in the superset. The selected realizations from the proposed method have a good coverage of the superset of realizations in terms of the maximum, minimum and expected performances. The proposed method will be very useful for quantifying uncertainty in reservoir performance and reservoir development decision making.

Chapter 3
Vertical Well Placement Optimization Under Uncertainty

3.1 Background and Literature Review

The production amount of oil from reservoirs greatly depends on the well locations and the geological property of the reservoir. To achieve the maximum economic benefit, well placement optimization is necessary for determining the best locations for placing wells in a reservoir. Reservoir flow simulation is commonly used in well placement optimization problems. The well positions is determined by maximizing the output variable of interest such as the cumulative oil production (COP) or net present value (NPV) generated by a reservoir flow simulator. The objective function for the well placement optimization at each set of well position is obtained by running the reservoir flow simulator. As a result, the computational time for the flow simulator significantly increases with increasing size of the reservoir grid and the number of wells to be placed. The complexity of the well placement optimization problem is further increased by incorporating uncertainty associated with geological properties of the reservoir. Geological uncertainty in well placement optimization is reduced by incorporating multiple geological realizations of the reservoir in the optimization model. However, using a large number of realizations in well placement optimization is computationally infeasible and hence a smaller subset of realizations are selected and used in the well placement optimization model to account for geological uncertainty.

In the literature, different methods have been used in well placement optimization to determine optimal well positions of a reservoir. In most cases, the objective function for the well placement optimization problem is to maximize the NPV or COP (Nasrabadi et al., 2012). Optimization methods used in well placement include: mixed integer programming (Rosenwald and Green, 1974), gradient-based optimization using finite difference method (Bangerth et al., 2006), genetic algorithms (Bittencourt and Horne, 1997), simulated annealing (Beckner and Song, 1995) and particle swarm optimization (Onwunalu and Durlofsky, 2010), etc. To capture the

geological uncertainty, calculation of COP or NPV is often based on flow simulation on multiple geological realizations. However, since flow simulation for a large number of realizations is a very computationally demanding task and impractical for larger realistic reservoirs with multiple wells, reducing the number of geological realizations for flow simulation becomes an important step in well placement optimization. Yeten et al. (2003) used the approach of using multiple equiprobable geological realizations in the determination of objective function of well placement optimization to account for the geological uncertainty associated in a reservoir. Since the use of multiple realizations in the well placement optimization results in an excessive number of reservoir simulations, Wang et al. (2012) selected a smaller subset of realization to quantify geological uncertainty in well placement optimization using k-means clustering. K-means clustering uses cumulative field oil production which requires to be calculated for every possible locations of well and therefore is computationally intensive. Yasari et al. (2013) used robust well placement optimization under uncertainty using a risk weighted objective function for multiple realizations. They selected a subset of realization from a superset by calculating the NPV for all the realizations using base case well position and then used ranking to select the small subset of realization. Similarly, Yang et al. (2011) combined Steam Assisted Gravity Drainage (SAGD) well production and placement optimization under uncertainty by selecting a subset of realizations using traditional ranking method based on the NPV of all the realizations for a base case scenario.

3.2 Problem Statement

In this chapter, vertical well placement optimization considering geological uncertainty is studied. The well placement optimization problem is solved using derivative free optimization method. Geological uncertainty is considered by selecting and incorporating a reduced subset of geological realization from a superset of realization in the well placement optimization model. An optimal realization reduction method using geological property of the reservoir and static measures is used in selecting the subset of realization. The objective function of the robust well placement optimization is a risk averted expected COP calculated from using a reduced number of realizations obtained from the optimal realization reduction method on a reservoir with fixed

number of wells. The well placement plan and performance parameters (COP and NPV) of well placement optimization results using the selected realizations from the optimal realization reduction method is compared to the well plan and performance parameters of well placement optimization results using all the realizations in the superset.

3.3 Robust Well Placement Optimization

Well placement optimization is a computational intensive task. To evaluate the performance of a certain well placement plan (i.e., the decision variables), a reservoir flow simulation is performed for multiple geological realizations. So it is a simulation based optimization problem. Since there is no explicit objective function of the decision variables, derivative free optimization method is used in this work. Specifically, the derivative free optimization solver NOMAD is used in this work. NOMAD implements the Mesh Adaptive Direct Search (MADS) algorithm for constrained blackbox functions. The MADS algorithm is an extension of pattern search method for nonlinear constrained optimization problems and therefore is a derivative free method (Audet et al., 2009). In this work, the objective function for the well placement optimization problem is designed as maximizing the risk averted expected cumulative oil production from a set of realizations as given by (3.1).

$$\text{Max } COP_{risk} = COP_{Expected} - \gamma \sqrt{\sum_{i=1}^{N_R} p_i (COP_i - COP_{Expected})^2} \tag{3.1}$$

where the expected COP is given by

$$COP_{Expected} = \sum_{i=1}^{N_R} p_i COP_i \tag{3.2}$$

In Eqs. (3.1) and (3.2), N_R is the number of realizations used to determine the geological uncertainty, p_i is the probability of a geological realization i , COP_i is the cumulative oil production of realization i, γ is the risk averted factor. The blackbox function is the reservoir simulator which determines the COP value based on the positions of the producer wells.

The robust well placement optimization used in this study is summarized in a flow diagram as given in Fig. 3.1. The steps in the well placement optimization under uncertainty are:

- Generate large number of geological realizations using a geostatistical method.
- Select a smaller subset from those realizations using the proposed realization reduction model. The realization reduction model minimizes the probability distance between the discrete distribution represented by the superset of realizations and the reduced discrete distribution represented by the selected realizations.
- Using the selected subset of realizations, perform well placement optimization by maximizing the objective function as given by Eq. (3.1). Each function evaluation calls on the reservoir simulator to calculate the COP.
- The optimal well locations using the subset of realizations is obtained when the stopping criteria for the optimizer is satisfied. The stopping criterion for the optimizer is the maximum number of iterations.
- Similarly, robust well placement optimization is also performed using all the realizations in the superset to obtain the optimal well locations from all the realizations. The well placement plan using the reduced subset of realizations obtained from the proposed method is compared to the well placement plan obtained using all the realizations in the superset.

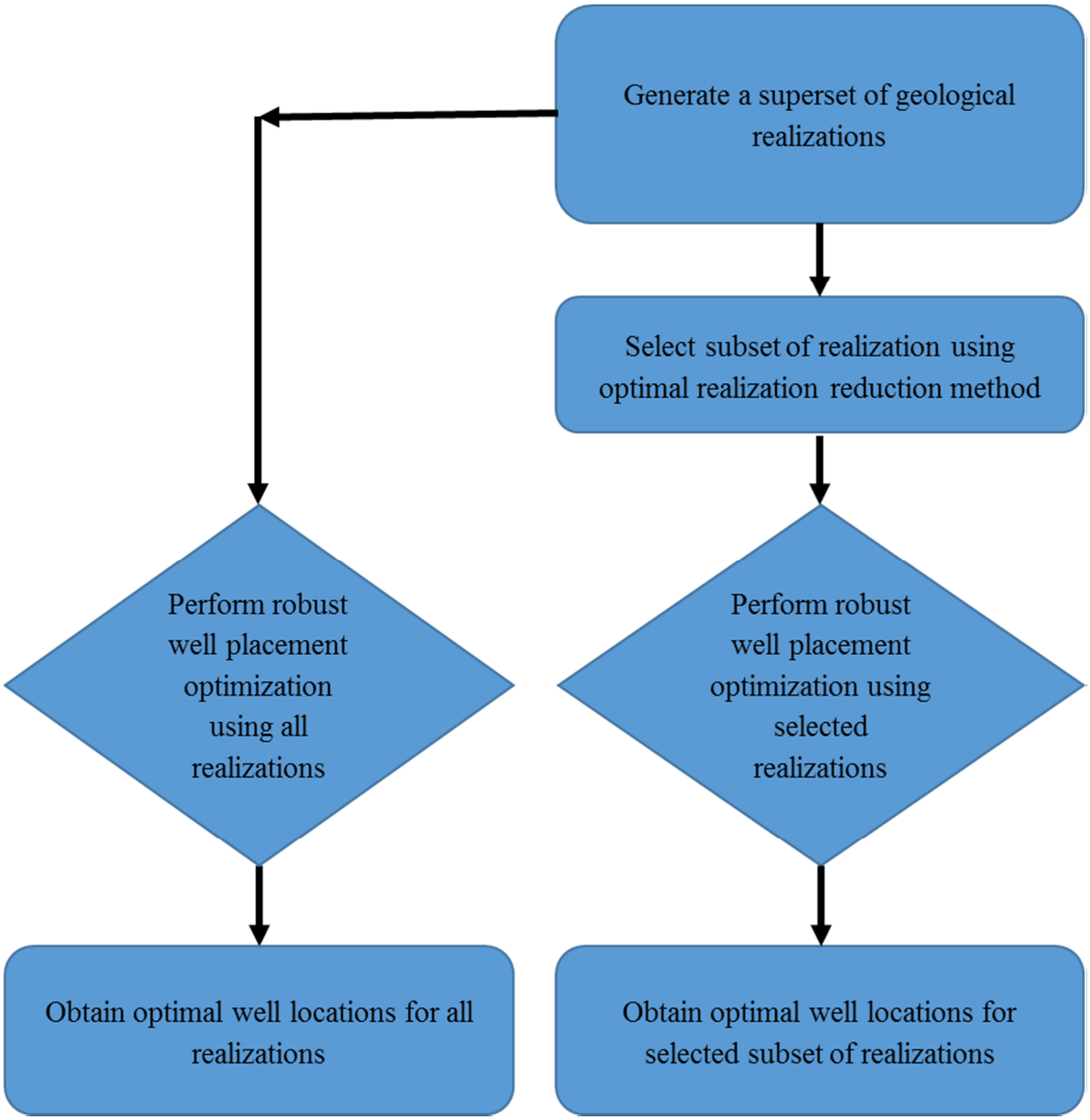

Figure 3.1 Workflow for well placement optimization under uncertainty

3.4 Geological Uncertainty Reduction

Uncertainty associated with the geological properties of a reservoir may result in either higher or lower estimate of the production parameter. As a result, it is very important to consider geological uncertainty in well placement optimization to ensure feasibility and profitability of the

oil extraction process. In this study, the optimal realization reduction model given in Section 2.4 is used to select a subset of realizations. The selected subset of realizations is then used in the evaluation of the objective function of the well placement optimization problem.

The optimal realization reduction model based on mixed integer linear optimization (MILP) technique is used to select a smaller subset of realizations from the superset of realizations (Rahim et al., 2014). The proposed algorithm uses reservoir geological properties and static measures to quantify the dissimilarity between realizations, and uses Kantorovich distance to quantify the probability distance between the superset and the subset of realizations. The objective is to find out the optimal subset which has a similar statistical distribution characteristic to the superset of realizations. The complete MILP optimization model is explained in Section 2.4 and is composed of Eqs. (2.16) to (2.23).

In the calculation of the dissimilarity $c_{i,i'}$ between realizations i and i' for the realization reduction method, both geological properties and static measures are used. The geological properties used for the dissimilarity calculation are the porosity and permeability of the reservoir. The static measures used for the dissimilarity calculation between realizations are: K_{net}, ϕ_{net}, S_{net}, F_{net}, PV_{net}, $OOIP$ and OIP_{net}. Complete definition and equations used to determine the static measures are provided in Section 2.3. The above static measures are selected to determine the dissimilarity between the realizations since these static measures are properties of the reservoir and independent of the location of wells within the reservoir. As a result, the static measures are calculated once in the pre-processing step and therefore not required to be calculated for every set of producer well location evaluated during the well placement optimization. This reduces any additional complexity in the optimal realization reduction method caused by recalculation of the static measure every time a different well placement plan is generated by the blackbox optimizer.

3.5 Case Study

3.5.1 Case Study 1

Application of the proposed geological realization reduction method in well placement optimization is illustrated using a two dimensional reservoir model with 50 × 50 grid size (2500 total cells) and each cell having dimensions of 5m × 5m. The reservoir has 5 fixed vertical injector well placed at grid positions: [8 45], [16 45], [24 45], [32 45] and [40 45]. The numbers of vertical producer well are fixed at 5. The objective function for the well placement optimization is evaluated using Matlab Reservoir Simulation Toolbox (MRST) (Lie et al., 2012) on different geological realizations. MRST provided the COP for each Producer well location plan selected by the optimizer. The simulation time horizon for the simulator is set as 3000 days divided into 10 equal periods. The fluid properties used by the MRST reservoir simulator are provided in Table 3.1.

Table 3.1 Case study 1 parameters

Parameter	Value
Initial pressure p_o	5080 psi
Oil viscosity μ_o at p_o	1.18 cp
Water viscosity μ_w at p_o	0.325 cp
Oil density ρ_o	865 kg/m^3
Water density ρ_w	929 kg/m^3
Relative permeability exponent for oil n_o	2
Relative permeability exponent for water n_w	2
Residual phase saturation for oil Sr_o	0
Residual phase saturation for water Sr_w	0
Relative permeability for oil kwm_o at Sr_o	1
Relative permeability for water kwm_w at Sr_w	1

The NPV was also obtained from the reservoir simulator. The cost data used in the calculation of the NPV are given in Table 3.2.

Table 3.2 Case Study 1 economic parameters

Parameter	Value
Oil Price ($/STB)	86
Water Production Cost ($/STB)	36
Water Injection Cost ($/STB)	18
Discount Rate (%)	0

In this study, 100 realizations are generated to create a superset of realizations. A smaller subset of realization is selected from the superset of realizations to incorporate uncertainty associated with the geological property of the reservoir in the vertical well placement optimization. For each realization, porosity values of the reservoir grid are generated in MRST using a built-in function '*Gaussian Field*' in the range of [0.1, 0.5]. The function creates an approximate Gaussian random field by convolving a normal distributed random field with a Gaussian filter with a standard deviation of 2.5 (Lie et al., 2012). Permeability values are further generated from the porosity values using Carmen-Kozeny relationship (Lie et al., 2012). Mathematically, Carmen-Kozeny relationship is given by Eq. (2.24). In the case study, the well placement optimization results using a subset of realizations from the proposed method are compared to optimization results from subset of realizations obtained using static measure based ranking method and random selection. 10 realizations are selected for the subset of realizations. In random selection, 10 realizations are arbitrarily selected from the superset of realizations.

To evaluate the static measures for different geological realizations, a constant threshold porosity of $\phi_0 = 0.3$ and threshold permeability of $k_0 = 3 \times 10^{-13} m^2$ is used to determine whether a cell is a net or non-net cell. Static measure based ranking method is applied next to obtain a subset of 10 selected realizations from the superset of 100 realizations. In the ranking based methods, all the 100 realizations in the superset are sorted in ascending order based on the static measure values. 10 realizations are evenly selected from the sorted list with ranks 1, 12, 23, 34, 45, 56, 67, 78, 89, 100. In this study, static measures of PV_{net} and $OOIP$ are used to perform realization reduction using the ranking based method. PV_{net} and $OOIP$ are calculated from Eqs. (2.8) and (2.9) respectively.

The decision variables for the case study are the X and Y locations of the 5 producer wells to be placed. The objective is to maximize the risk averted expected cumulative oil production after 3000 days of simulation period. The well placement optimization problem is simulated in an Intel Core i5 system using a 3.2GHz processor with 8 GB of installed memory. The well placement plans obtained from the well placement optimization under uncertainty for the case study using the subset of realizations from the optimal realization reduction method and all the realizations from the original superset are provided in Fig. 3.2. In Fig. 3.2, the fixed injector wells are denoted by blue dot and the producer well locations are denoted by red dot.

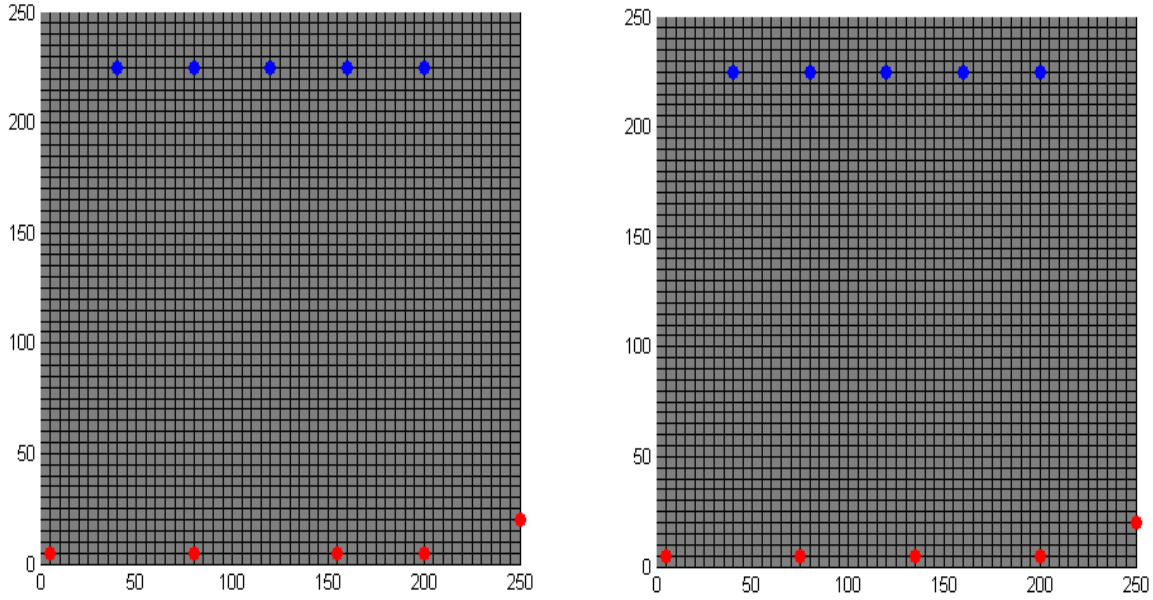

Figure 3.2 (a) Well placement plan using selected realizations from proposed method; (b) Well placement plan using full set of realizations

It is evident from Fig. 3.2 that the producer well placement plan using a subset of realizations from the optimal realization reduction method is very similar to the producer locations from the well placement plan using all the realizations. Some of the producer wells have the same locations between the two different well placement plans obtained using optimization. The optimal producer well placement plans using selected realizations from *OOIP* ranking, PV_{net} ranking and random selection are given in Figs. 3.3 to 3.4.

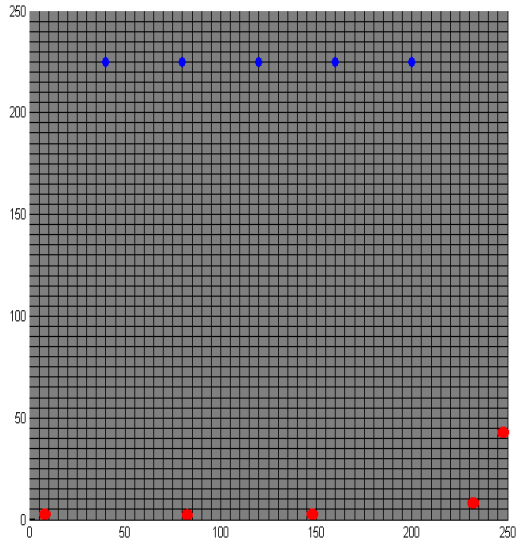

Figure 3.3 Well placement plan using selected realizations from OOIP ranking

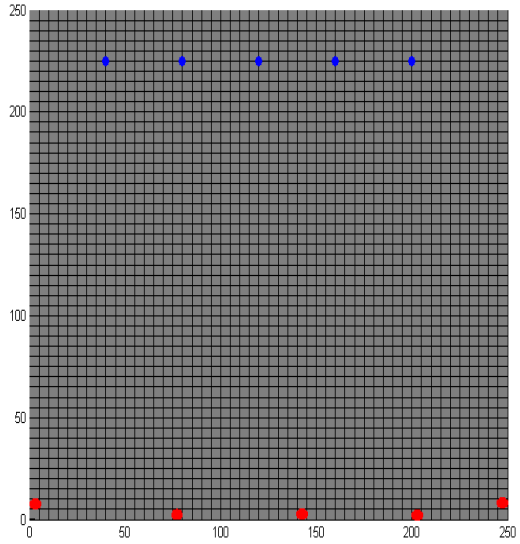

Figure 3.4 Well placement plan using selected realizations from PVnet ranking

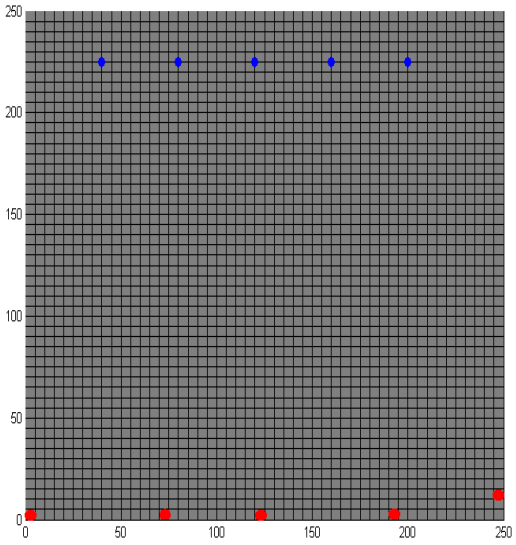

Figure 3.5 Well placement plan using selected realizations from random selection

The well placement plans obtained by using realizations selected from the ranking based and random selection method are not significantly different from the well placement plan obtained by using all the realizations in the superset.

The expected COP, expected NPV, standard deviation between the COP values, standard deviation between the NPV values and the computational time for the well placement optimization methods by using the subset of realizations using different realizations reduction methods and by using all the realizations in the the superset are given in Table 3.3.

Table 3.3 Reservoir simulation results of all realizations and selected realizations of case 1

	$COP_{\exp}$ ($\times 10^4$)	$NPV_{\exp}$ ($\times 10^6$)	COP_{SD} ($\times 10^3$)	NPV_{SD} ($\times 10^5$)	Simulation time (hours)
All realizations	1.1529	2.5382	1.0004	2.2140	25
Proposed method	1.1535	2.5482	0.9403	2.0042	2.5
PVnet	1.1556	2.5438	1.4023	2.9852	2.5
OOIP	1.1472	2.5200	1.4749	3.0709	2.5
Random	1.1310	2.4983	1.2354	2.6118	2.5

It can be seen from Table 3.3 that the expected COP and NPV obtained from the well placement optimization plan from a subset of realizations obtained using the proposed optimal realization reduction method is very close to the expected COP and NPV from the well placement optimization plan obntained using all the realizations in the superset. Similarly, the standard deviation between the COP and NPV values obtained using the producer well plan from the subset of realizations using the proposed method and the producer well plan from the superset of realizations are very similar. Compared to the other realization reduction methods, the proposed method provides results which are closest to the results from using all the realizations. More importantly, the well placement optimization problem using a subset of realization takes only one-tenth of the computational time since the reservoir simulation time is greatly reduced by using a fraction of the realizations.

The results for the well placement optimization are given in Figs 3.3 to 3.7. For all the results, the x-axis shows the number of iterations used by the NOMAD optimizer and the y-axis shows the output performance parameter. It is important to note that for each number of iterations used by the optimizer, 100 function evaluations have to be evaluated by the reservoir simulator in the case of using the full set of realizations in the superset. In the case of the reduced subset of 10 realizations, 10 function evaluations have to be evaluated by calling on the reservoir simulator, per iteration used by the optimizer. Each of the figures contain a subplot, on the right, which shows the absolute difference between the output performance parameter of the well plans using the different realizations reduction methods with the output performance parameter of the well plan using all the realizations in the superset. This absolute error term is a good representation of the closeness of the output performance parameter obtained from the realization reduction methods with respect to the output performance parameter from using all the realizations in the superset.

The objective function in the well placement optimization is the risk averted expected COP. The objective function versus the number of iterations used by the NOMAD optimizer for the different realization reduction methods are given in Fig. 3.3. As the number of iterations increases, the objective function of the well placement optimization between the superset of

realizations and subset of realization using the proposed method gets closer. The decrease in the objective function error as the number of iteration increases is evident from Fig. 3.3(b). Realization reduction using PV_{net} ranking has an objective function which is also very close to that of the full set of realizations as evident from Fig. 3.3(b), as it coincides with the objective function error of the proposed method.

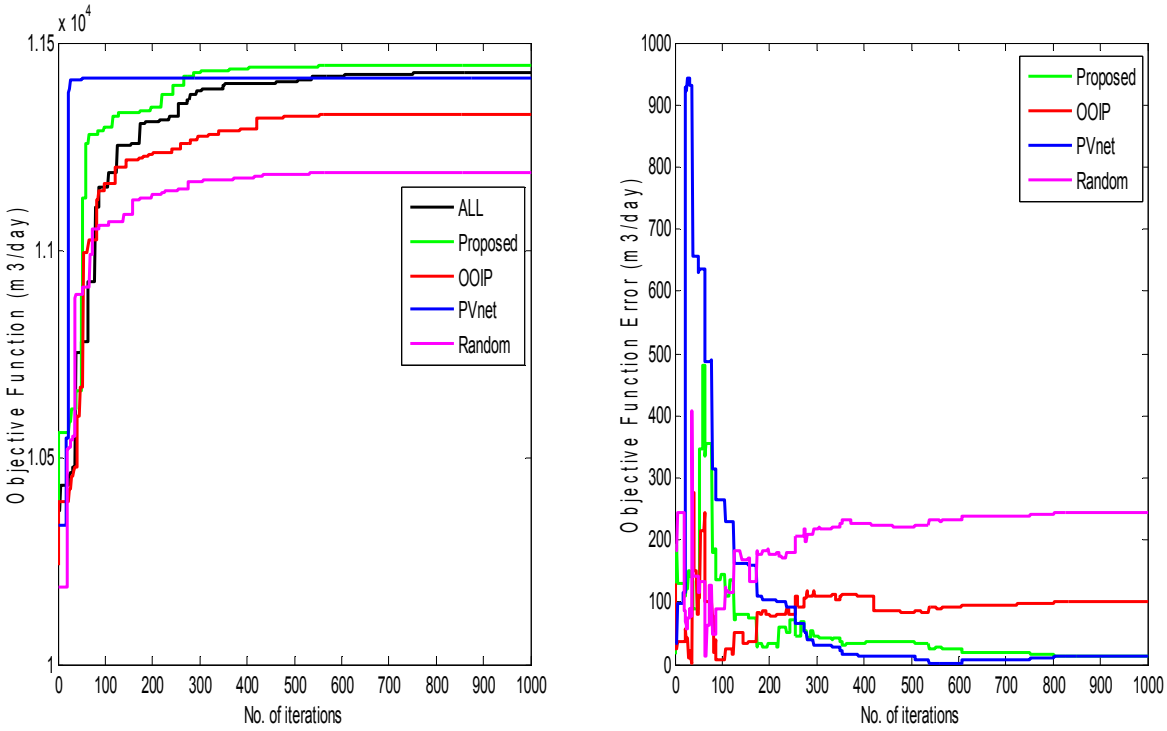

(a) (b)

Figure 3.6 (a) Objective function versus number of iterations using different realization reduction methods; (b) Error in objective function versus number of iterations using different realization reduction methods

The expected COP versus the number of iterations for the optimizer of the different realization reduction methods is given in Fig. 3.4. It is clear that the the expected COP of the well placement plan using subset of realizations from the proposed method comes closest to the expected COP of the well placement plan using all the realizations as the number of iterations increases. It can be seen from Fig. 3.4(b) that the expected COP error from the proposed realization reduction method is very close to zero, confirming the similarity with the expected COP of the well plan using all the realizations in the superset.

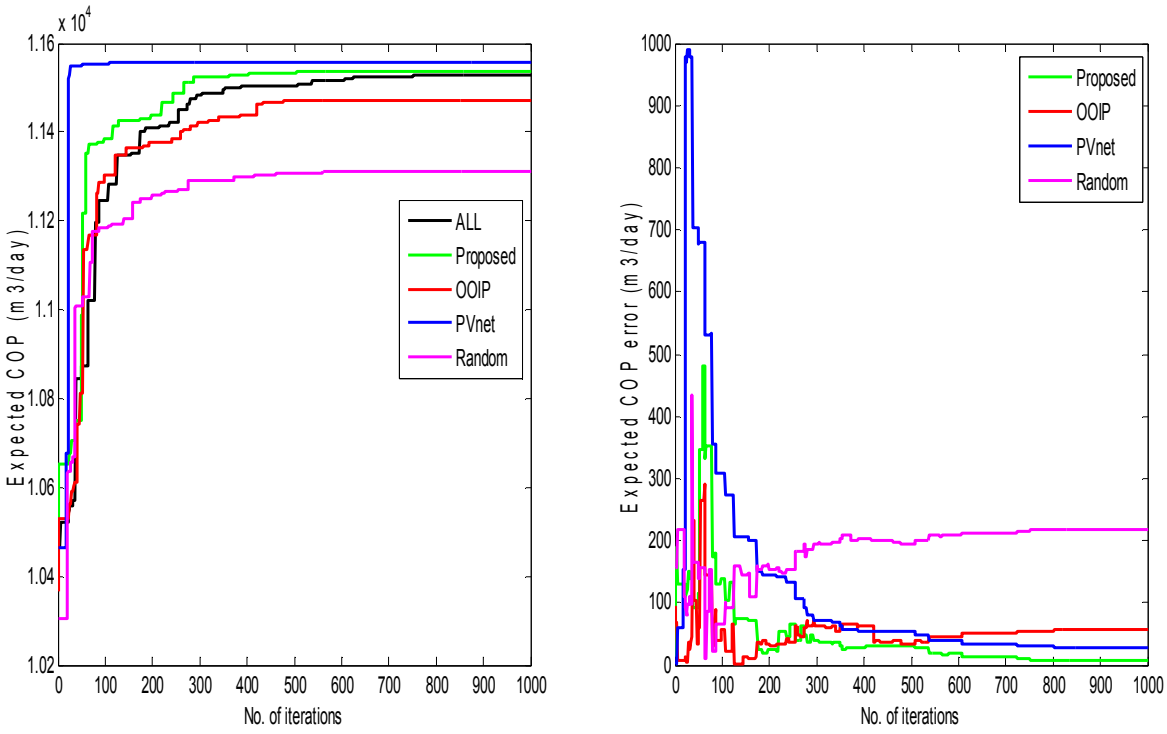

(a) (b)

Figure 3.7 (a) Expected COP versus number of iterations using different realization reduction methods; (b) Error in expected COP versus number of iterations using different realization reduction methods

Figure 3.5 provides the plot of COP standard deviation and error in the COP standard deviation versus the number of iterations used by the optimizer for the different realization reduction methods. Figure 3.5 confirms that amongst the realization reduction methods, the subset of realizations selected by the proposed method has COP standard deviation values which are closest to the standard deviation obtained using all the realizations in the superset. The COP standard deviation plot shows that all the other realization reduction methods have COP standard deviations which deviate significantly from the standard deviation obtained using the superset of all realizations.

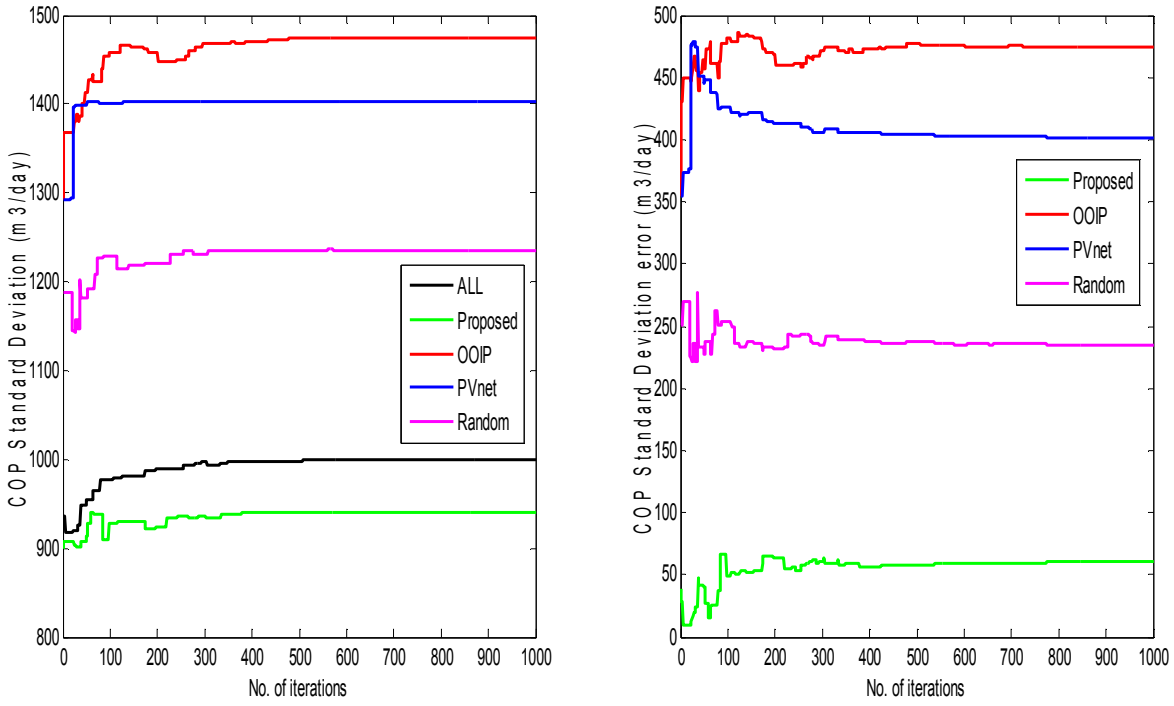

(a) (b)

Figure 3.8 (a) COP Standard deviation versus number of iterations using different realization reduction methods; (b) Error in COP standard deviation versus number of iterations using different realization reduction methods

The expected NPV and NPV standard deviation plots versus the number of iterations used by the optimizer are given in Figs. 3.6 and 3.7, respectively. The expected NPV obtained from the proposed realization reduction method and PV_{net} ranking method are both very close to the expected NPV of the full set of realization as shown in Fig. 3.6. Less variability is observed between the expected NPV values when compard to the expected COP values of all the different realization reduction methods.

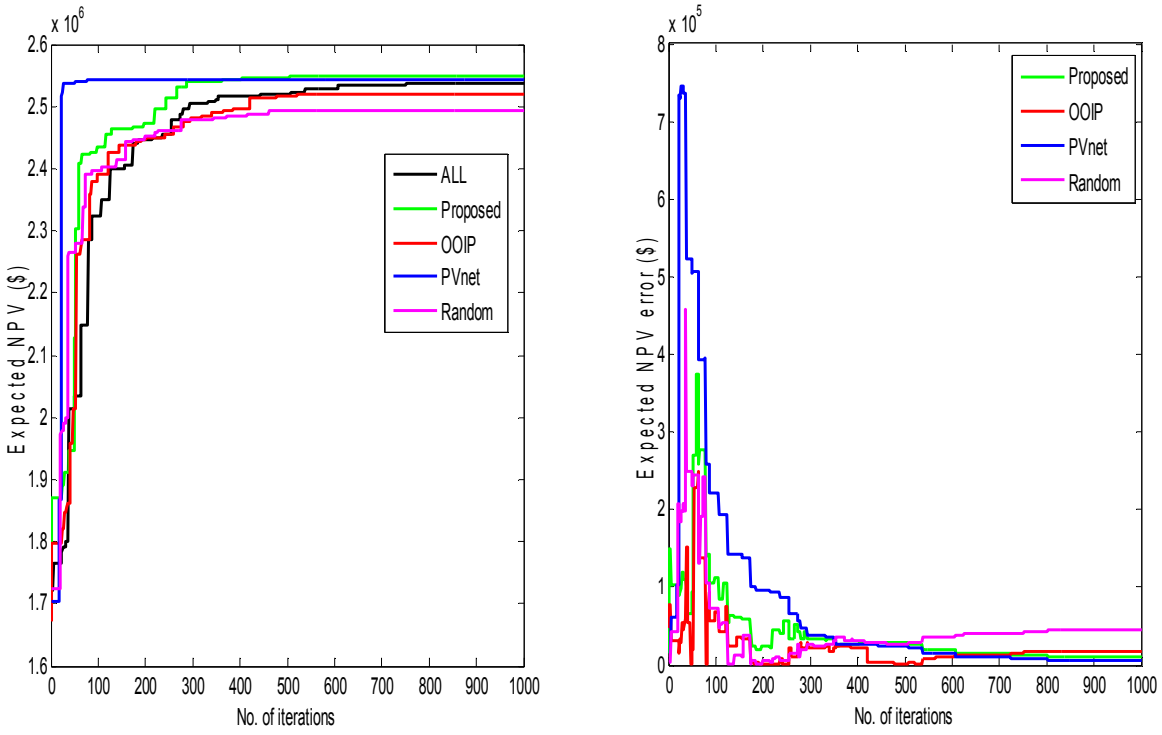

(a) (b)

Figure 3.9 (a) Expected NPV versus number of iterations using different realization reduction methods; (b) Error in expected NPV versus number of iterations using different realization reduction methods

However, the standard deviation of the NPV values between the different realization reduction methods shows the proximity of the proposed method to the full set of realizations. It is evident that the well placement plan obtained using the subset of realizations from the proposed method has the closest standard deviation amongst the NPV values when compared to the standard deviation of NPV values from the well placement obtained using all the realizations in the superset. In comparison to the full set of realizations, other realization reduction methods have significantly different standard deviation values of the NPV.

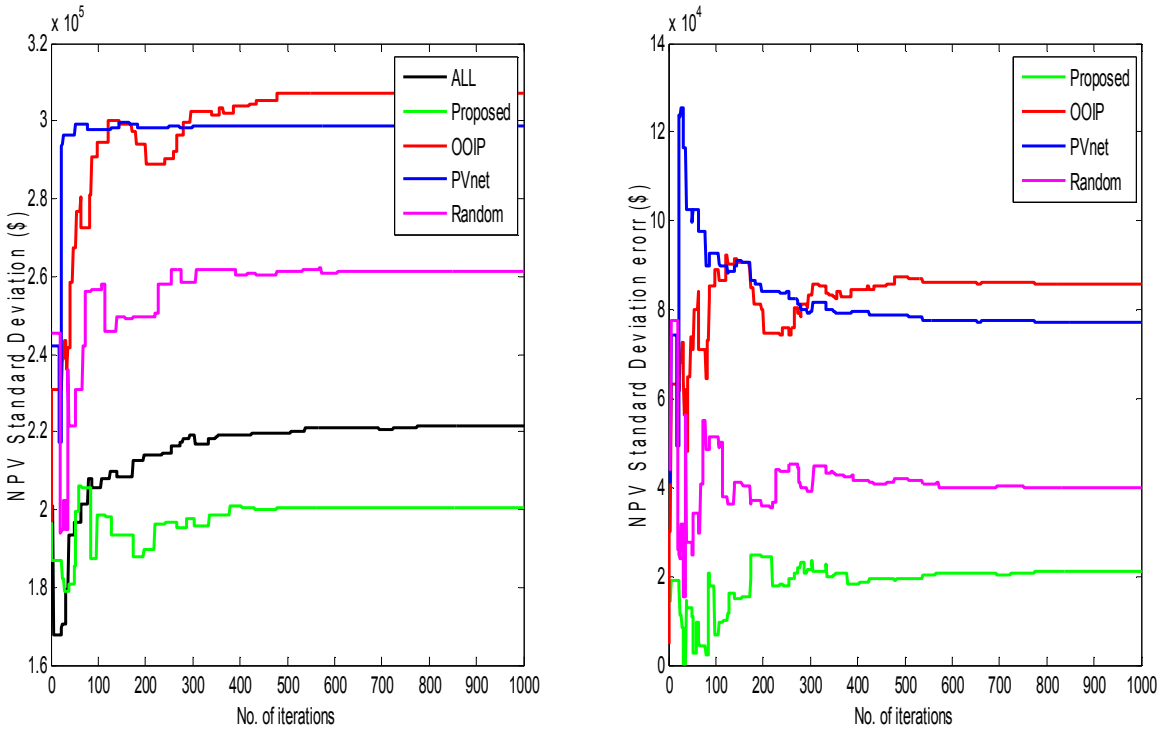

(a) (b)

Figure 3.10 (a) NPV standard deviation versus number of iterations using different realization reduction methods; (b) Error in the NPV standard deviation versus number of iterations using different realization reduction methods

3.5.2 Case Study 2

A three dimensional reservoir model with 30 × 30 × 5 grid size (4500 total cells) and each cell having dimensions of 10m × 10m × 5m is investigated to illustrate the use of the proposed geological realization reduction method in well placement optimization. The reservoir has 3 fixed vertical injector well placed at grid positions: [1 1], [15 15] and [30 30].The numbers of vertical producer well are fixed at 4. Similarly, MRST is used to evaluate the objective function for the well placement optimization problem on different geological realizations. COP and NPV are evaluated by MRST for each Producer well location plan selected by the optimizer. The simulation time horizon for the simulator is set as 3000 days divided into 10 equal periods. The fluid properties used by the MRST reservoir simulator are provided in Table 3.4.

Table 3.4 Case study 2 parameters

Parameter	Value
Initial pressure p_o	6000 psi
Oil viscosity μ_o at p_o	3 cp
Water viscosity μ_w at p_o	0.3 cp
Oil density ρ_o	849 kg/m^3
Water density ρ_w	1025 kg/m^3
Relative permeability exponent for oil n_o	2
Relative permeability exponent for water n_w	2
Residual phase saturation for oil Sr_o	0
Residual phase saturation for water Sr_w	0
Relative permeability for oil kwm_o at Sr_o	1
Relative permeability for water kwm_w at Sr_w	1

The cost data used in the calculation of the NPV are given in Table 3.5.

Table 3.5 Case Study 2 economic parameters

Parameter	Value
Oil Price ($/STB)	86
Water Production Cost ($/STB)	36
Water Injection Cost ($/STB)	18
Discount Rate (%)	0

A superset of 100 geological realizations consisting of porosity and permeability for the reservoir grid are generated using a built in MRST tool and Carmen-Kozeny relationship (Lie et al., 2012). A subset of 10 realizations are selected from the superset using the following; proposed realization reduction method, PV_{net} based ranking method, $OOIP$ based ranking method and random selection. The robust well placement optimization plan obtained using a subset of realization from the proposed method and the well plan obtained using the full set of realization is given in Fig. 3.8. In Fig. 3.8, fixed injector locations are given by the blue dot and the producer locations are given by the red dot. It can be seen from Fig. 3.8 that the two producer positions in the upper y-axis between both the well plans are close to each other.

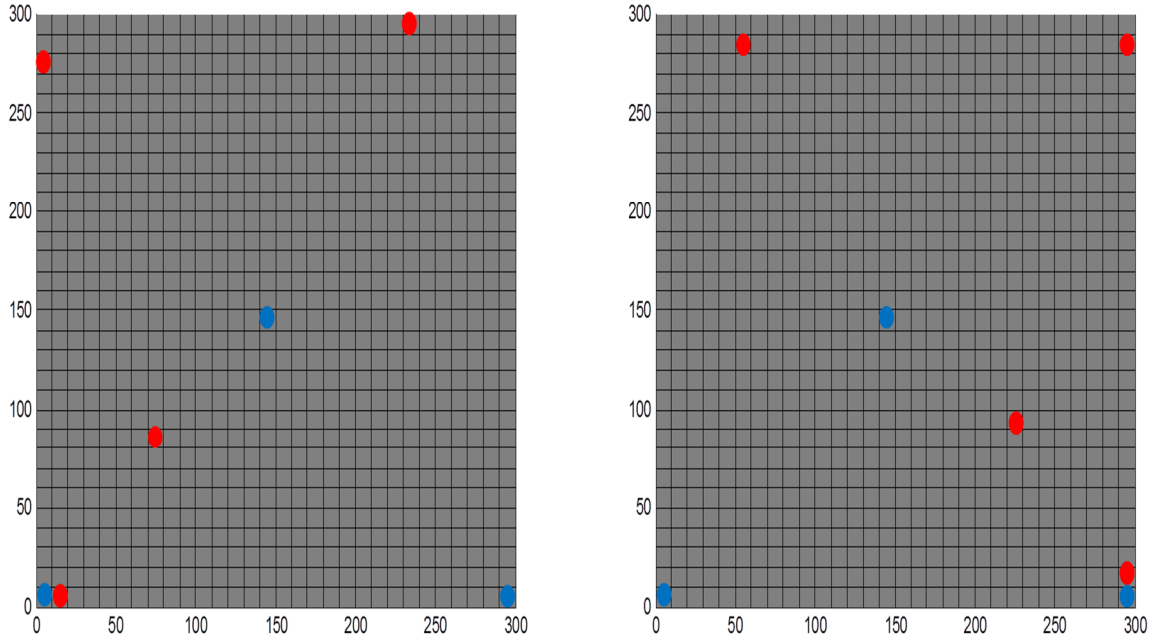

(a) (b)

Figure 3.11 (a) Well placement plan using selected realizations from proposed method; (b) Well placement plan using full set of realizations

The mean and variance of the COP and NPV results from well placement optimization between different realization reduction methods are given in Table 3.6. Both the expected COP and expected NPV calculated from the well placement optimization results using subset of realization from the proposed method is very close to the expected COP/NPV value obtained from the well placement optimization result using all the realizations in the superset. As expected, the simulation time for the optimization is significantly reduced by using one-tenth of the realizations from the superset. Compared to case study 1 given in section 3.5.1, the computational time is higher for this case study since a larger three-dimensional reservoir grid with higher number of cells is used. The standard deviation of the COP and NPV results from the proposed method are also very close to that of all the realization as well.

Table 3.6 Reservoir simulation results of all realizations and selected realizations of case 2

	$COP_{\exp}$ ($\times 10^5$)	$NPV_{\exp}$ ($\times 10^7$)	COP_{SD} ($\times 10^4$)	NPV_{SD} ($\times 10^6$)	Simulation time (hours)
All realizations	3.1381	1.3192	2.4042	1.3049	30
Proposed method	3.1333	1.2215	2.4573	1.4816	3
PVnet	3.1630	1.8554	3.3463	2.1002	3
OOIP	3.1719	1.8612	3.2948	2.1153	3
Random	3.1279	1.8404	3.4044	1.9742	3

The objective function of the well placement optimization versus the number of iterations for the superset of all realizations and different realization reduction methods are given in Fig. 3.9. As the number of iterations of the optimizer increases, the objective function of the different realization reduction methods converge to the objective function value from the superset of all the realizations as shown clearly in the objective function error plot of Fig. 3.9 (b).

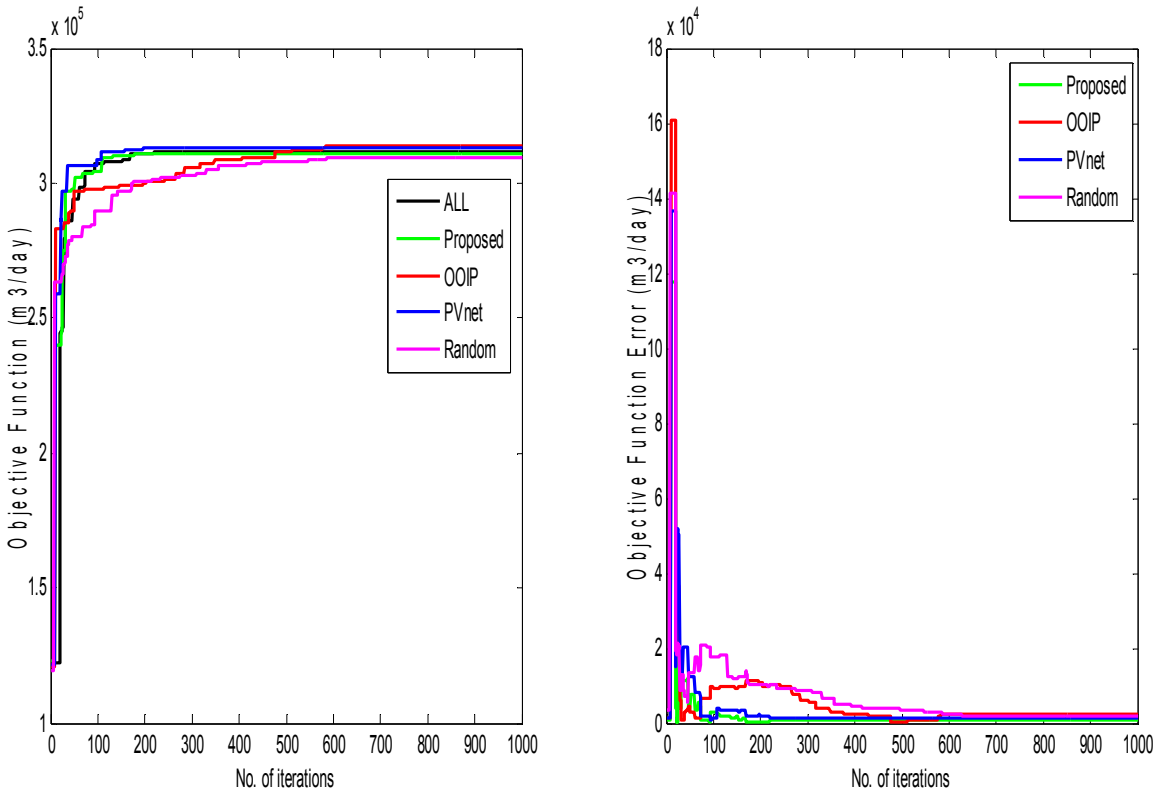

(a) (b)

Figure 3.12 (a) Objective function versus number of iterations using different realization reduction methods; (b) Error in objective function versus number of iterations using different realization reduction methods

Figure 3.10 shows the plot of expected COP and expected COP error versus number of iterations for the superset of realizations and the subset of realizations. A similar trend is observed as the expected COP of all the different realization reduction method almost converges to the expected COP from all the realization as the number of iterations increases. However, from the expected COP error plot of Fig. 3.10 (b), the COP error of the proposed method is the closest to 0 confirming its similarity to the expected COP of the full set of realizations.

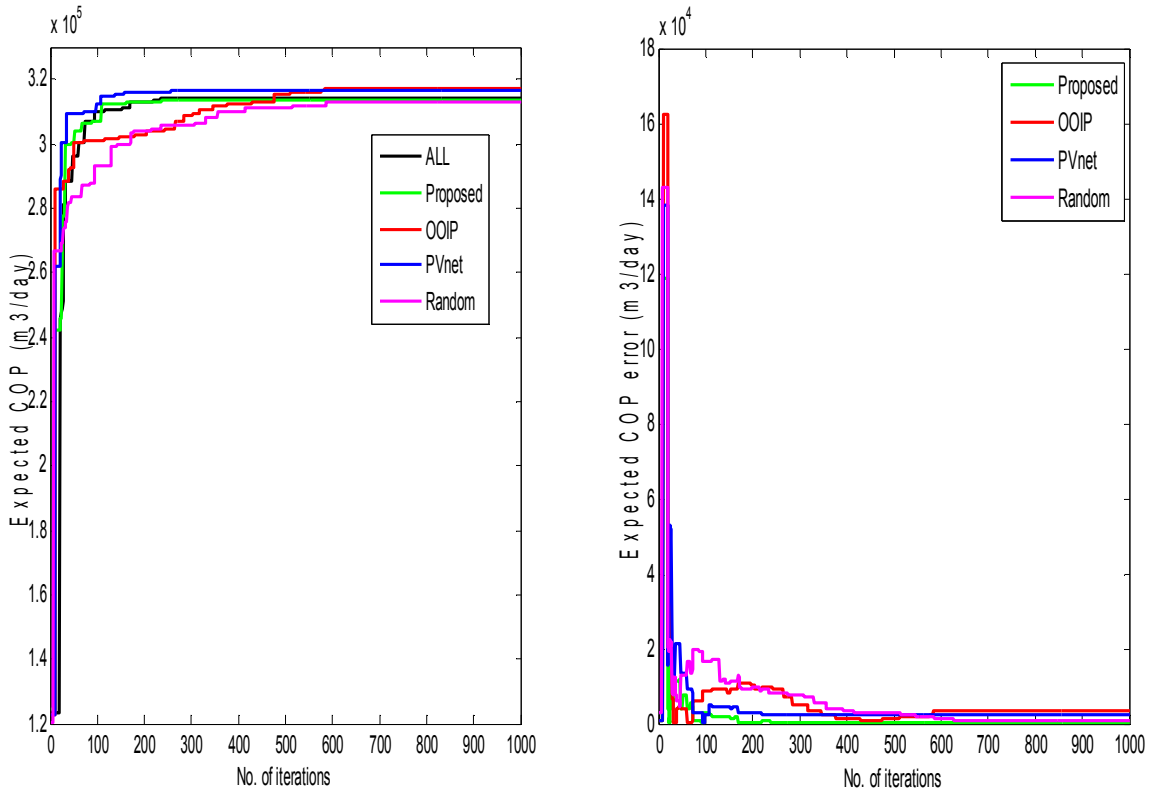

(a) (b)

Figure 3.13 (a) Expected COP versus number of iterations using different realization reduction methods; (b) Error in expected COP versus number of iterations using different realization reduction methods

The standard deviation of the COP values and the COP standard devation error versus the number of iterations for the superset of realizations and subset of selected realizations are given in Fig. 3.11. It is clearly evident from the figure that the COP standard deviation of the proposed method has the closest resemblance to the standard deviation of the superset of all realization. The COP standard deviation error plot shows that all the other realization reduction methods have a significant deviation when compared to the COP standard deviation from all the realization.

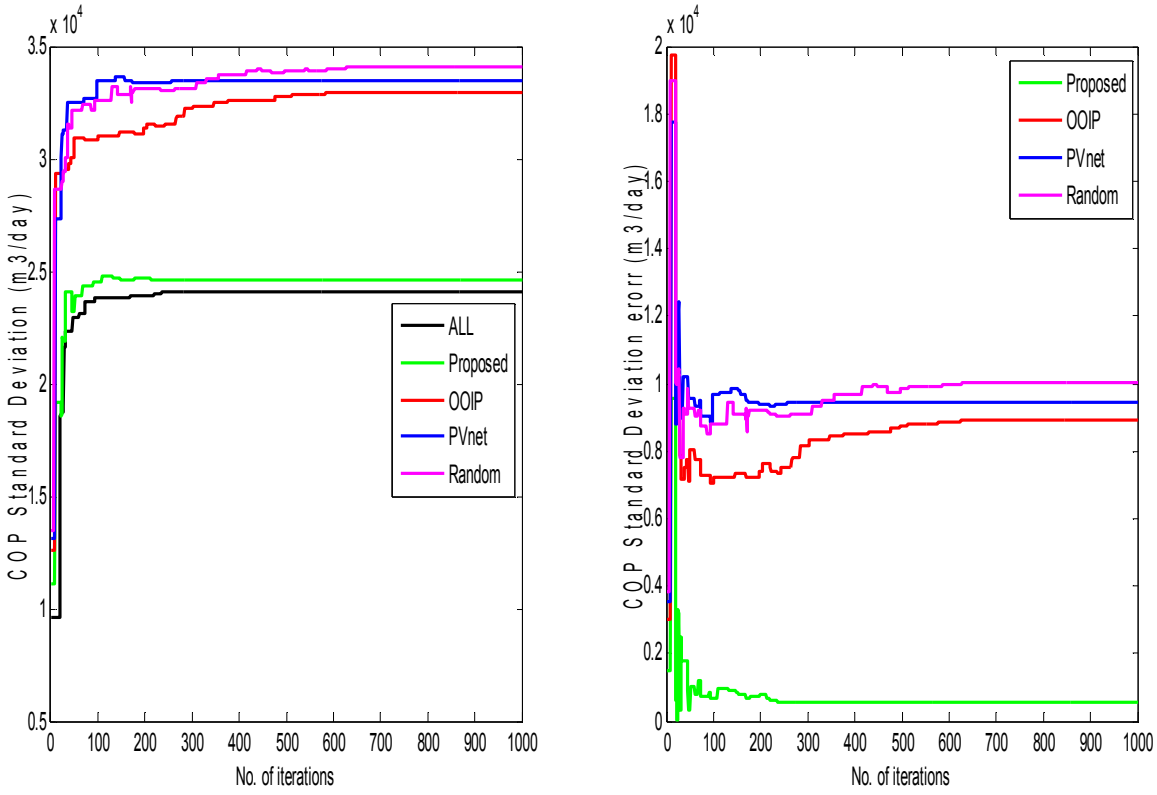

(a) (b)

Figure 3.14 (a) COP Standard deviation versus number of iterations using different realization reduction methods; (b) Error in COP standard deviation versus number of iterations using different realization reduction methods

The expected NPV and NPV error versus the number of iteration of the optimizer for different methods are given in Fig. 3.12. Figure 3.12 confirms the close proximity of the expected NPV value of the subset of relaiztion selected from the proposed method and expected NPV of the full set of realizations. The proposed method shows superior performance in comparison to the other realization reduction methods.

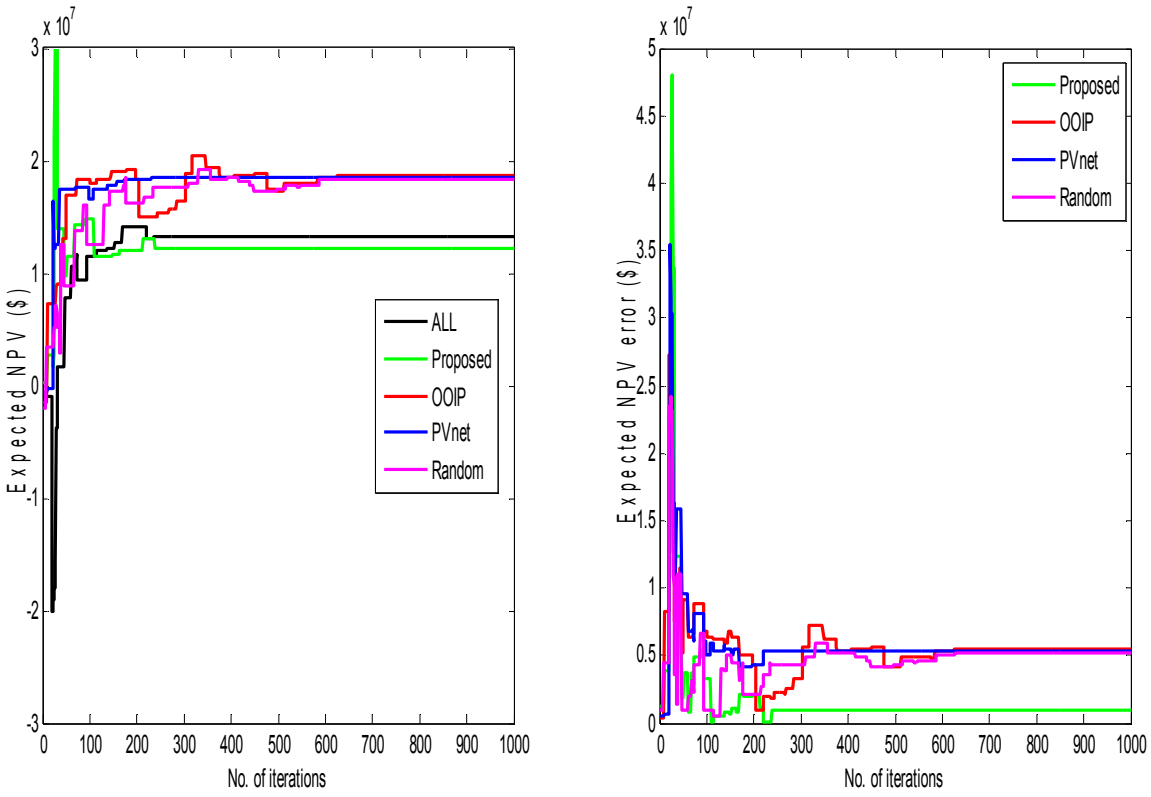

(a) (b)

Figure 3.15 (a) Expected NPV versus number of iterations using different realization reduction methods; (b) Error in expected NPV versus number of iterations using different realization reduction methods

Finally, the standard deviation for the NPV values versus the number of iterations is given in Fig. 3.13. Furthermore, the standard deviation of the NPV values from the proposed realization reduction method is closest to the standard deviation of the NPV values from all the realizations as evident from the NPV standard deviation error plot of Fig. 3.13 (b). All the other realization reduction method have a large error in the standard deviation of the NPV values.

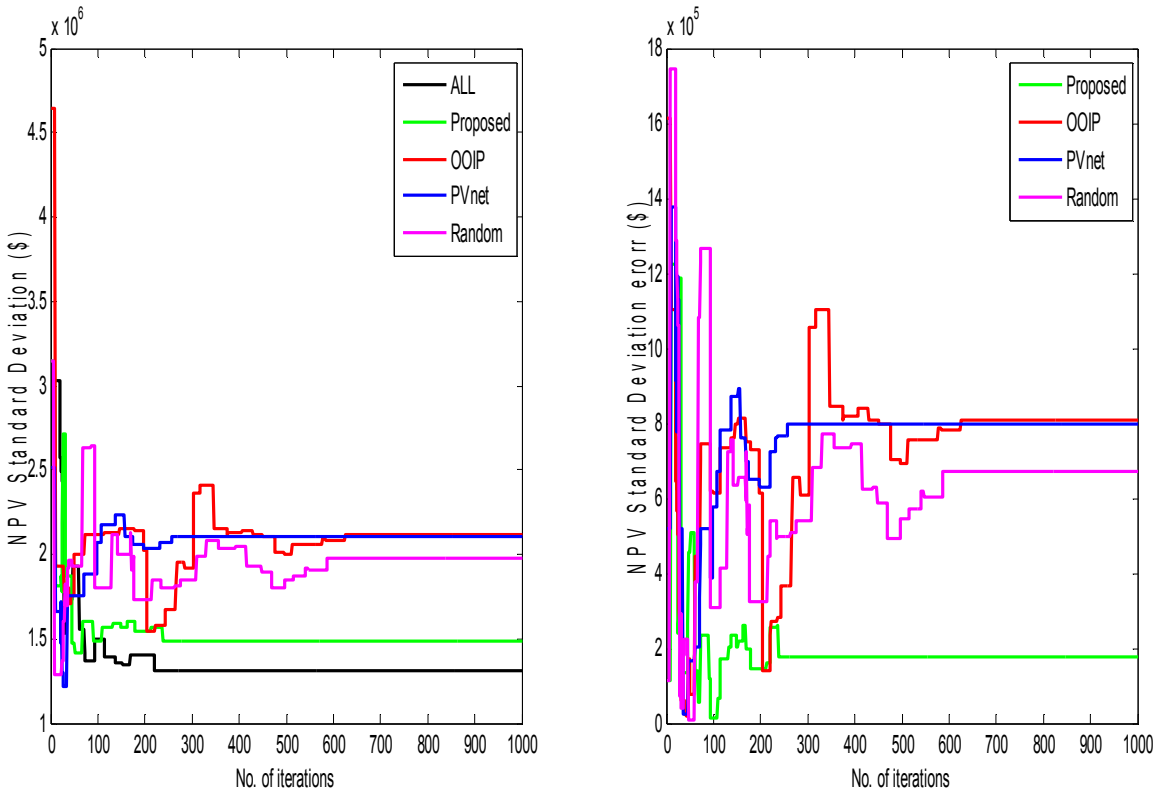

(a) (b)

Figure 3.16 (a) NPV standard deviation versus number of iterations using different realization reduction methods; (b) Error in the NPV standard deviation versus number of iterations using different realization reduction methods

Both the case study demonstrate that the proposed realization reduction method can be applied in the application of vertical well placement optimization for geological uncertainty reduction. The proposed realization reduction method has both the mean-variance values of performance parameters such as COP and NPV very close to the mean-variance value of performance paramaters such as COP and NPV from the full set of relaizations. As a result, the subset of realization selected from the proposed method creates a distribution with very similar performance parameter to that of the full set of realization. Using the subset of realization from the proposed method ensures similarity to the superset of all realization and at the same time significantly reducing the simulation time of the well placement optimization.

3.6 Conclusion

A framework for vertical well placement optimization with geological uncertainty reduction is proposed in this section. The well placement optimization is formulated as a risk averted optimization problem by considering geological uncertainty. The optimization problem is solved using a derivative free optimization method. Geological uncertainty is incorporated into the robust optimization model which calculates the objective function based on a set of realizations obtained from the optimal realization reduction method. The optimal realization reduction method is a mixed integer linear optimization model provides a subset of realization with a similar statistical distribution characteristic to the superset of realizations. The realization reduction model used in the well placement framework is independent of well positions and depends on the reservoir geology. Results from the case studies show that the well placement optimization problem using the optimal realization reduction method is computationally very efficient. The well placement plan obtained using the smaller subset of realization and the well placement plan obtained from the superset of realizations have similar; expected COP, expected NPV, standard deviation of COP and standard deviation of NPV values. Using a reduced number of realizations obtained from the optimal realization reduction method resulted in a significant reduction in the computational time for the well placement optimization problem due to a substantial decrease in the number of function evaluations required by the optimizer.

Chapter 4
SAGD Drainage Area Arrangement Optimization

4.1 Background and Literature Review

Alberta's oil sands are the third largest proven global reserves of oil with current estimates of 26.6 billion cubic meter of crude oil (AER, 2014). Majority of the oil sands in Alberta are divided into three geological areas of Athabasca, Peace River and Cold Lake. In terms of area, Athabasca oil sands are the largest. Most of the bitumen reserves in Alberta's oil sands are deep underground and therefore cannot be extracted using mining methods. 80% of the reserves in the oil sands are extractable using in situ methods whereas the remaining 20% are extractable using surface mining methods. The prominent in situ methods used currently in the oil sands are; Cyclic steam simulation (CSS), Steam assisted gravity drainage (SAGD) and primary development methods. SAGD accounts for almost 52% of the in situ method used to extract bitumen currently from the oil sands. Currently, around 16 SAGD projects are operational in Alberta's oil sands and many more are under development. Examples of some of the prominent SAGD operations with significant bitumen production are: MacKay River and Firebag operation of Suncor Energy, Foster Creek and Christina Lake operations of Cenovus Energy and Jackfish operations of Devon energy (AER, 2014).

SAGD operations use super-heated steam to decrease the viscosity of the bitumen in the underground reservoir. As a result, the bitumen can easily flow and pumped up to the surface. SAGD wells consist of 2 horizontal wells which are in parallel. Steam is injected to the upper injector well and the melted bitumen flows to the lower producer well by gravity. The Bitumen from the producer well is pumped to the surface and transported to bitumen processing facilities. The major SAGD facilities are; Surface pad (SP), Drainage Area (DA) and Central Processing Facility. The SP is the surface facilities from which multiple producer and injector well pair are drilled. DA is the set of parallel wells under the reservoir attached to the same SP. Central processing facility is a surface facility which produces the super-heated steam required by each

of the injector wells. Steam is supplied from the central processing facility to each of the SP through pipelines. SAGD well pairs are drilled in areas which have a higher amount of bitumen as determined by the geological properties, such as porosity and permeability, of the reservoir.

Optimization methods for the placement of SAGD DA and SP are relatively new in academia. Current practice of commercial placement of SAGD wells rely on reservoir characterization and engineering judgement. Kumar (2011) developed an optimal SAGD well arrangement using a space packing optimization of a compact and non-overlapping set of DA. Geometric transformations of global rotation, global translation and column translation are used by the space packing algorithm to maximize the recoverable bitumen. Restrictions such as non-placement of SP over surface restrictions or non-placement of DA in thief zones are avoided by incorporating a penalty function in the objective function equation. Manchuk and Deutsch (2013) used an adaptive grid search algorithm to determine the optimal arrangement of DAs. The optimization algorithm determines the positions and orientations of the SPs and DAs over a reservoir area to economically maximize the recoverable bitumen. The objective function is maximized by the optimization algorithm by performing possible geometric transformations of global rotation, global translation, column rotation and column translation to a compact set of DA. The optimization algorithm ensures a DA is not selected if a SP cannot be placed on either side of that DA due to surface constraint.

4.2 Problem Statement

A two-stage optimization method is formulated for selecting the DA and SP arrangement of SAGD wells in this chapter of the thesis. The objective of the first stage is to obtain an optimal compact arrangement of all the DAs and SPs within the reservoir lease area by maximizing the available bitumen. The compact arrangement is defined by the angle of rotation and amount of translation in both the x and y directions of the compact set of DAs which maximize the total available bitumen. Objective of the second-stage of the optimization method is to provide a plan for initially selecting a set of DAs and SPs from the compact arrangement of all the DAs. A

dynamic DA and SP selection plan, which maximizes the available bitumen and at the same time minimizes the distance between the selected SPs, is obtained. A blackbox based derivative free optimization is used for the first stage and a MILP optimization model is proposed for the second stage of the SAGD DA arrangement optimization. Furthermore, geological uncertainty is incorporated to the first stage of the optimization method by using a subset of realizations obtained from the optimal realization reduction method.

4.3 Available Bitumen

In Alberta's oil sands, bitumen deposits are found in underground porous mediums between impermeable rocks. The impermeable rocks play a crucial part to trap and deposit the bitumen under the ground. The top surface of the bitumen deposit below the impermeable section of rocks is defined as the top continuous bitumen (TCB) and the bottom surface of the bitumen deposit is defined as the bottom continuous bitumen (BCB). The BCB and TCB of a bitumen deposit are determined from data obtained from well logs or exploratory drills. Net continuous bitumen (NCB) is the total thickness between the TCB and BCB that meets certain minimum criteria for reservoir quality. In this study, NCB is calculated for cells which are above a critical threshold porosity and permeability value. A higher permeability value ensures better flow of bitumen and therefore higher recovery of bitumen whereas a higher porosity value ensures a higher amount of bitumen. As a result, NCB is a good indication of the amount of bitumen available for extraction by the SAGD wells. Figure 4.1 illustrates how NCB is calculated along the elevation of the reservoir. In Fig. 4.1, black portions of the reservoir have lower porosity and permeability value and therefore not included in the determination of NCB.

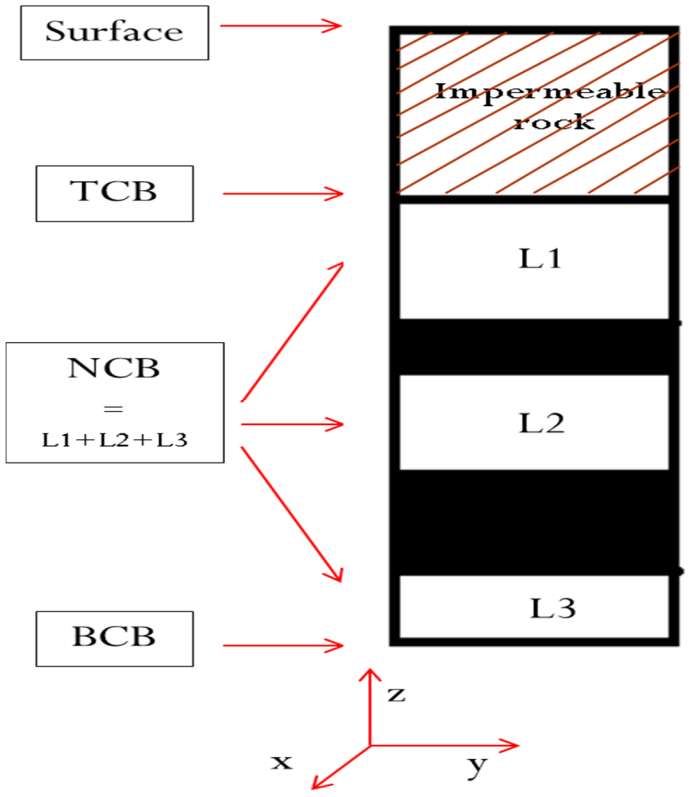

Figure 4.1 Net Continuous Bitumen Calculation

The NCB value is used to calculate the available bitumen. Available bitumen is the quantity of bitumen available for production along all the wells in a single DA. It is calculated by summing up the NCB of all the cells inside the rectangular DA. Mathematically, available bitumen is given by the following expression

$$R_i^{available} = \sum_{c \in DA_i} NCB_c . ar_c \tag{4.1}$$

where, $R_i^{available}$ is the available bitumen for i DA, NCB_c is the net continuous bitumen for cell c and ar_c is the fraction of area of cell c inside i DA. Available bitumen is calculated for each of the DA. It is desired to place a DA which would maximize the available bitumen. This will ensure that the placement of SAGD wells will produce the highest amount of bitumen. In this study, the reservoir quality in terms of bitumen production is represented by the available bitumen.

4.4 Optimization Model

In the optimization model, a compact and non-overlapping arrangement of DA is considered. Commercial SAGD well placement uses a compact arrangement of DAs to ensure maximum accessibility of the available resources. The compact arrangement of DAs ensures that the available bitumen between any 2 DAs are included in the calculation of total available bitumen. The DAs and SPs are rectangle in shape and two possible locations of SP are considered for each DA. The DA and SP dimensions are considered to be fixed in this study and as a result, fixed numbers of parallel injector/producer wells per DA are considered. The first step of the optimization model determines the position and orientation of the compact set of all the DAs, which can be packed within the lease area, by maximizing the available bitumen. The input from the first step of the optimization model is used in the second step of the optimization model to develop a selection plan for DAs and SPs. The detailed explanation of the optimization method is provided in the following subsections.

4.4.1 Optimization workflow

The overview of the two stages of the SAGD DA arrangement optimization method is given in Fig. 4.2. The optimization workflow of Fig. 4.2 is summarized as follows:

- Initially the input to the blackbox optimizer has to be provided. The input includes the reservoir grid, geological data of the reservoir, any surface restrictions on the reservoir grid and the fixed dimensions of each DA and SP in the compact arrangement.

- The objective function of the blackbox optimizer is to determine the optimal orientation and position of the compact arrangement of the entire set of DAs which maximizes the total available bitumen. The orientation is represented by the angle of the compact DA arrangement from the horizontal x direction. The position is represented by the translation of the compact DA arrangement along both the x and y direction.

- The blackbox optimizer runs till the stop criteria of the optimizer is satisfied. The results of the blackbox optimizer are the optimal orientation and location of the compact set of

DAs. Two possible locations for SPs are fixed with respect to the location of each DA in the compact arrangement. The output from the blackbox optimizer is the optimal arrangement of all the DAs and SPs in the compact set.

- The inputs to the second stage of the optimization method are the fixed locations of all the DAs and possible SPs in the compact arrangement and the number of DAs to be selected at a given time period. A MILP optimization model is used for the second stage of the optimization method.

- The MILP optimizer selects DAs and SPs by maximizing the available bitumen and at the same time reducing the distance between the SPs. The MILP optimizer can be run multiple times to select DA and SP from the compact arrangement. This enables a dynamic selection plan for DAs and SPs at different time periods.

- The outputs from the MILP optimizer are the locations of the selected DAs and the corresponding SPs at the given time period.

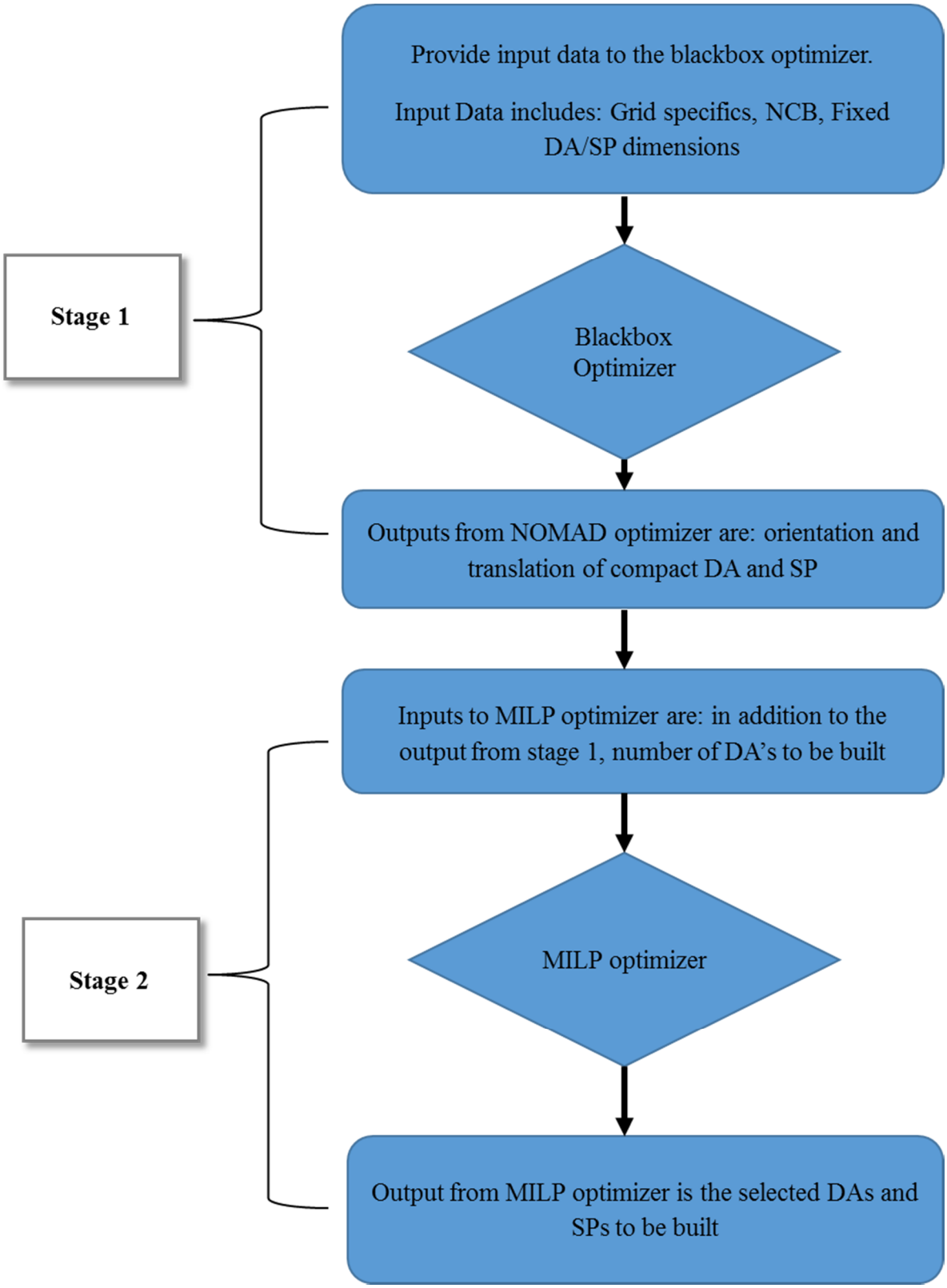

Figure 4.2 Overview of Optimization method

4.4.2 Stage 1 - Compact arrangement of DA

The first stage in the optimization method is to generate an initial compact arrangement of DA which would cover the entire grid. There is no explicit equation for the objective function representing the available bitumen being a function of the decision variables of orientation and translation of the compact set of DAs. Instead, a Matlab program (Matlab, 2012) is developed which calculated the total available bitumen as a function of the orientation and position of the compact set of DAs. Therefore, a derivative free blackbox based optimization method is used in this work which calls on the developed Matlab program for total available bitumen calculation. The derivative free optimization solver NOMAD is used in this work. NOMAD implements the Mesh Adaptive Direct Search (MADS) algorithm for constrained blackbox functions. The MADS algorithm is an extension of pattern search method for nonlinear constrained optimization problems (Audet et al., 2009).

In this step, the objective function for the compact DA arrangement optimization problem is designed as maximizing the total available bitumen and is given by Eq. (4.2)

$$\text{Max} \sum_{i=1}^{allDA} R_i^{available}(\theta, \Delta x, \Delta y) \tag{4.2}$$

Where $R_i^{available}$ is the available bitumen for i DA, $allDA$ is the total number of DAs in the compact arrangement. In addition, upper and lower bounds for the following decision variables were applied: orientation, translation along x direction and translation along y direction, as given by Eqs. (4.3) to (4.5), respectively.

$$\theta_{ub} \geq \theta \geq \theta_{lb} \tag{4.3}$$

$$\Delta x_{ub} \geq \Delta x \geq \Delta x_{lb} \tag{4.4}$$

$$\Delta y_{ub} \geq \Delta y \geq \Delta y_{lb} \tag{4.5}$$

The following restrictions were also applied to the optimization problem:

- A DA was considered only if it's area was 80% or more inside the lease boundary

- A DA was considered only if its total available bitumen was above a certain threshold value
- A DA was considered only if it had at least one possible location for placing a SP. For a feasible SP location, the SP had to be placed inside the lease boundary and could not be placed on top of any surface restrictions. Surface restrictions are areas on the surface ground level where SPs cannot be built. Examples of surface restriction could be rivers, lakes, roads or conserved forest areas.

Stage 1 of the optimization method can be represented by the following pseudo code.

Algorithm: Generate a compact DA-SP arrangement plan for SAGD wells

Input: Grid size with the lease area boundaries, surface restriction on the grid, NCB for each cell in the x-y plane, DA dimensions, SP dimensions, DA-SP spacing, upper and lower bound on the geometric transformations applied to the compact arrangement of all DAs by the optimizer, stopping criteria for the optimizer

Output: Optimal orientation (θ) and positions (Δx, Δy) of the compact arrangement of all DAs

1. Initialize a compact DA arrangement based on the grid specifications
2. If the stopping criterion for the blackbox optimization (ε) is not satisfied then,
    - Optimize the orientation (θ) of the DA arrangement
    - Optimize the translation (Δx, Δy) of the DA arrangement

    a. Compute $\mathrm{R}_i^{available}(\theta, \Delta x, \Delta y)$ of each DA

    b. Make a summation of the available bitumen from all the DA in the compact arrangement $R_{tot} = \sum_{i=1}^{allDA} \mathrm{R}_i^{available}(\theta, \Delta x, \Delta y)$

c. If $R_{tot} > R_{tot}^{k}$ then $R_{tot}^{k} = R_{tot}(\theta, \Delta x, \Delta y)$ and save the corresponding configuration. k is the index representing the number of iteration as used by the optimizer.

d. If $R_{tot}^{k} > R_{tot}^{k-1}$ then save the corresponding $(\theta, \Delta x, \Delta y)$ configuration

3. Update the orientation and position parameters

4. Use the optimal configuration of the compact set of DAs and SPs $(\theta_{opt}, \Delta x_{opt}, \Delta y_{opt})$ to fix the compact DA arrangement and then perform the next step of the optimization

4.4.3 Stage 2 - DA and SP selection plan

The objective of the second optimization step is to select a smaller number of DAs and SPs from the compact arrangement of all the DAs. The objective of the second step of optimization is to provide an insight on which DAs and SPs to construct since commercial development of SAGD wells initially start by developing a smaller number of DA for producing bitumen from the oil sands. Additional development of DAs and corresponding SPs at a later time period occurs after oil production begins from the initially selected SAGD wells. The initial number of DAs to be developed is selected such that the amount of available bitumen is maximized but at the same time costs associated with pipelines are minimized. Having SPs close to each other ensures that a smaller length of pipeline supplying steam to each SP from the central processing facility is required. Similarly, smaller amount of pipeline is required to transfer the bitumen mixture from the SPs. As a result, the MILP optimization model maximizes the available bitumen from the selected DAs and at the same time minimizes distance between SPs. The inputs to the MILP model are: orientation of the compact set of DA, translation of the compact set of DA and the user specified number of DAs to be selected. Fixed compact arrangement of all the possible DAs and SPs is obtained from the optimal orientation and translation parameters of the compact arrangement. The complete MILP model is explained as follows.

The objective function of the second stage of the SAGD DA arrangement is given by Eq. (4.6)

$$\text{Max} \sum_{i \in I} x_i R_i^{available} - \gamma \sum_{i,i' \in I} d_{i,i'} \tag{4.6}$$

Where x_i is a binary variable denoting whether i DA is selected ($x_i = 1$) or not ($x_i = 0$), $R_i^{available}$ is the available bitumen for i DA, γ is a weight parameter which reflects the contribution given to minimizing the distance between SPs (γ = 0.001 used in this study), $d_{i,i'}$ is the distance between the SPs of i and i' DAs, I is the number of DAs in the compact DA arrangement plan obtained from the previous stage. The decision variables of the MILP model are the binary variables of x_i and $y_{i,j}$ which denote whether a DA is selected or not and whether a SP is selected or not, respectively. The weight parameter γ can be changed based on the importance of minimizing the distance, and therefore the cost, between all the SPs in the optimization problem.

Equation (4.7) ensures the number of DAs selected is based on the user specified information

$$\sum_{i \in I} x_i = nDA \quad \forall i \in I \tag{4.7}$$

Where nDA is the number of DAs to be selected as provided by the user.

Equation (4.8) ensures that 1 SP location is selected per DA

$$x_i = \sum_{i \in I} y_{i,j} \quad \forall i \in I \tag{4.8}$$

Where $y_{i,j}$ is a binary variable denoting whether the SP will be placed on j position for i DA ($y_{i,j}$=1) or not ($y_{i,j}$=0). There are 2 possible j positions considered for each SP and denoted by either position 1 or position 2. The j positions are along the 2 edges of the width of the DAs.

The center x and y position of the SPs are given by the next set of Eqs. (4.9) and (4.10)

$$SPx_i = SP1Centerx.y_{i,1} + SP2Centerx.y_{i,2} \quad \forall i \in I \tag{4.9}$$

$$SPy_i = SP1Centery.y_{i,1} + SP2Centery.y_{i,2} \quad \forall i \in I \tag{4.10}$$

Where SPx_i is the x center position of the i selected DA, SPy_i is the y center position of the i selected DA, $SP1Centerx$ and $SP2Centerx$ are the x center position of SP along the *1* and *2*

positions respectively, $SP1Centery$ and $SP2Centery$ are they center position of SP along the *1* and *2* positions respectively, $y_{i,1}$ denoting whether the SP will be placed on *1* position for i DA ($y_{i,1}=1$) or not ($y_{i,1}=0$) and $y_{i,2}$ denoting whether the SP will be placed on *2* position for i DA ($y_{i,2}=1$) or not ($y_{i,2}=0$). The following parameters are obtained from the compact arrangement of DAs as obtained from the output of the first stage of the optimization: $SP1Centerx$, $SP2Centerx$, $SP1Centery$ and $SP2Centery$.

The distance between the x and y center points of any two SPs can be linearized by Eqs. (4.11) and (4.12)

$$d_{i,i'} \geq \left| SPy_i - SPy_{i'} \right| \quad \forall i,i' \in I \tag{4.11}$$

$$d_{i,i'} \geq \left| SPx_i - SPx_{i'} \right| \quad \forall i,i' \in I \tag{4.12}$$

The complete MILP model is given by Eqs. (4.6) to (4.12). This problem can be solved using a MILP solver such as CPLEX (IBM, 2010).

The complete MILP optimization model for stage two of the DA-SP selection plan is summarized as follows

$$\max \sum_{i \in I} x_i R_i^{available} - \gamma \sum_{i,i' \in I} d_{i,i'}$$

Subject to

$$\sum_{i \in I} x_i = nDA \quad \forall i \in I$$

$$x_i = \sum_{i \in I} y_{i,j} \quad \forall i \in I$$

$$SPx_i = SP1Centerx.y_{i,1} + SP2Centerx.y_{i,2} \quad \forall i \in I$$

$$SPy_i = SP1Centery.y_{i,1} + SP2Centery.y_{i,2} \quad \forall i \in I$$

$$d_{i,i'} \geq \left| SPy_i - SPy_{i'} \right| \quad \forall i,i' \in I$$

$$d_{i,i'} \geq \left| SPx_i - SPx_{i'} \right| \quad \forall i,i' \in I$$

$$x_i \in \{0,1\} \quad \forall i \in I$$

$$y_{i,j} \in \{0,1\} \quad \forall i \in I$$

Input Parameters:

*SP*1*Centerx*	x center position of SP along the *1* edge of the DA
*SP*2*Centerx*	x center position of SP along the *2* edge of the DA
*SP*1*Centery*	y center position of SP along the *1* edge of the DA
*SP*2*Centery*	y center position of SP along the *2* edge of the DA

Variables:

x_i	binary variables which denote whether a DA is selected ($x_i = 1$) or not ($x_i = 0$)
$y_{i,j}$	binary variables which denote whether a SP at j location for i DA is selected ($y_{i,j} = 1$) or not ($y_{i,j} = 0$)

4.5 Case Study

4.5.1 Application of DA arrangement optimization

A realistic case study with a three dimensional reservoir grid is used to demonstrate the practicality of the optimization model used for SAGD DA and SP placement. A relatively large reservoir model with a grid size of 55 × 62 × 10 cells with cell dimensions of 100m × 100m × 5m is considered for the case study. Matlab Reservoir Simulation Toolbox (MRST) is used to create the grid and the geological properties. The three dimensional grid is given in Fig. 4.3.

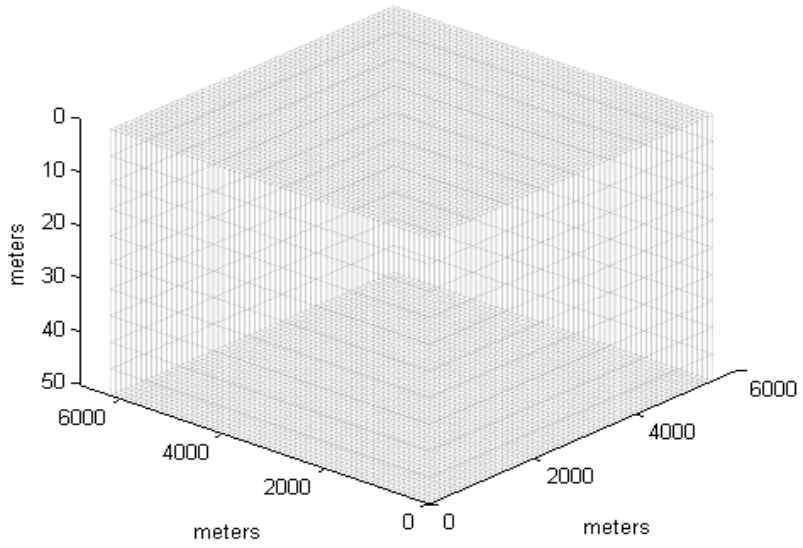

Figure 4.3 Grid representation of case study

The geological data considered for the case study are the porosity and permeability of the reservoir. Porosity and permeability are generated for every cell of the grid using a MRST built in function of Gaussian Field (Lie et al., 2012). The porosity values are in the range of 0.1 to 0.5. Permeability is calculated from the porosity data using Carmen-Kozeny relationship. Commercial companies developing SAGD wells in the oil sands have reservoirs with irregular shaped lease boundary. Therefore, in this case study an irregular shaped leased boundary is used. The optimization model should not put a DA or SP outside the lease boundary. Areas on the ground level of the reservoir where a SP cannot be placed are known as surface restrictions. Examples of possible surface restrictions on oil sand reservoirs are lakes, rivers, roads and conservation areas. Therefore, surface restrictions were created within the lease boundary to demonstrate that the optimization model avoids placing a SP on top of any surface restrictions. The aerial view of the lease boundary and the surface restriction is given in Fig. 4.4. In Fig. 4.4, the leased area is represented as the white section, surface restriction is represented by the blue area and the grey parts represent the area outside the lease boundary.

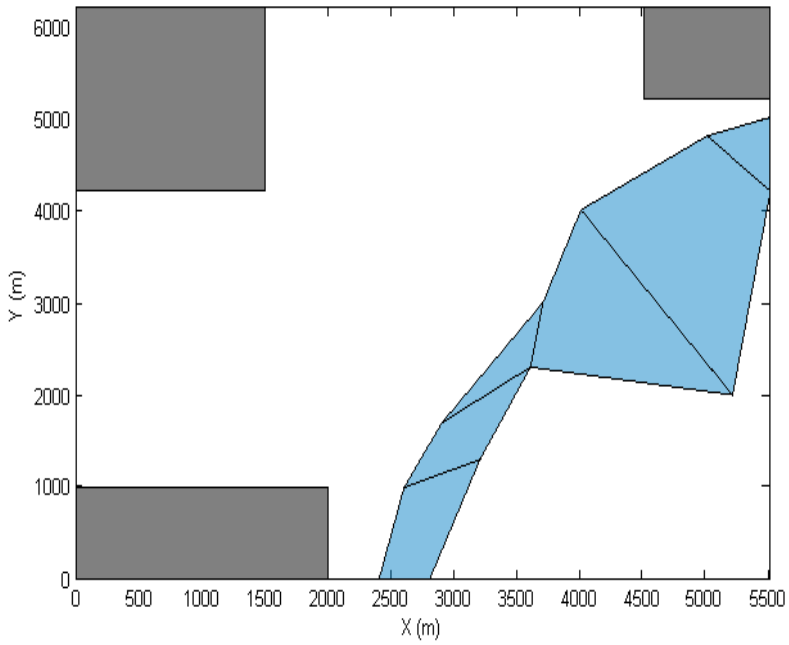

Figure 4.4 Leased area with surface restriction of the reservoir for well placement

The porosity and permeability distribution of the three dimensional grid is given in Figs. 4.5 and 4.6 respectively. The dark blue regions in those figures represent the unleased area. Geological data is not available for the unleased area and therefore the porosity and permeability in that area is considered to be zero.

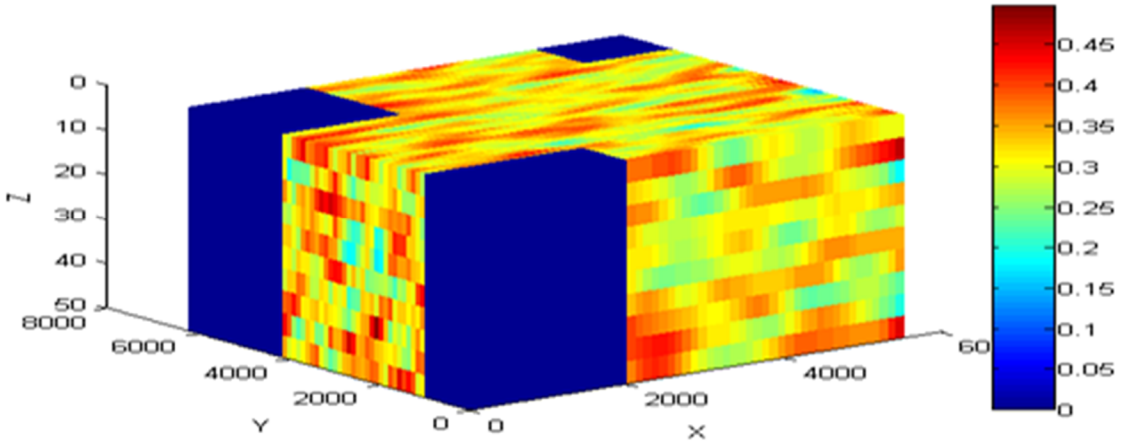

Figure 4.5 Porosity distribution of the leased area

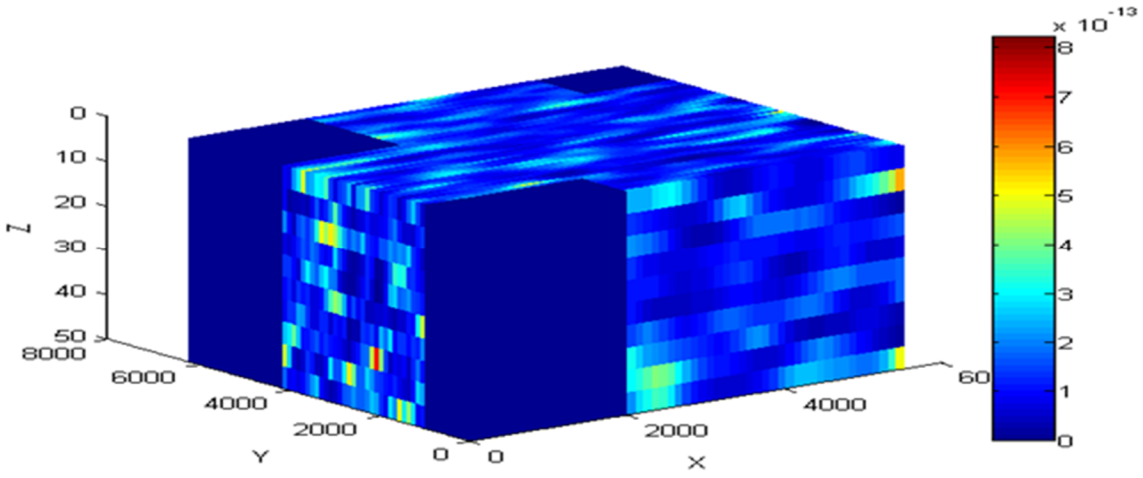

Figure 4.6 Permeability (m^2) distribution of the leased area

The geological data is used to calculate the NCB of the reservoir. The available bitumen of each possible DA location can then be calculated from the NCB of a section of the reservoir. NCB is calculated by summing the number of net cells along the z-direction (height) of the reservoir. In this case study, any cell with a porosity and permeability above a threshold value of 0.25 and $1.1x10^{-13}$ m^2 respectively, were considered to be a net cell. The aerial view of the NCB of the reservoir grid is given in Fig. 4.7.

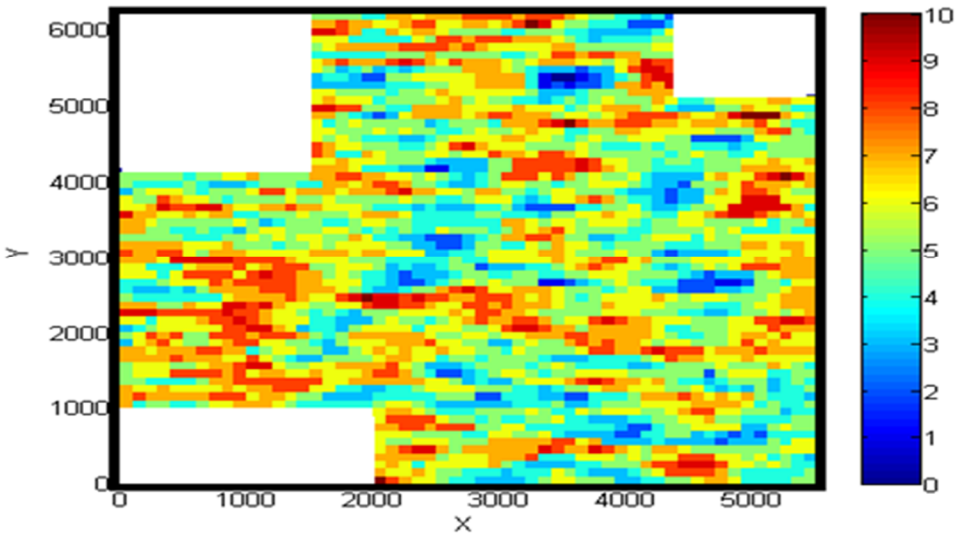

Figure 4.7 Aerial representation of the Net Continuous Bitumen

As expected, the maximum possible NCB value in Fig. 4.7 is 10. This is due to the fact that there are 10 cells along the z-direction of the grid.

In order to provide SAGD well arrangement plan, a list of parameters specific to all the DAs and SPs in the compact arrangement are fixed. The fixed dimensions of the DA and SP are given in Table 4.1. Two possible locations of SP with respect to a specific DA were considered with a fixed DA-SP spacing. Fixing the dimension of the DAs and SPs resulted in a significant reduction in the complexity of SAGD well placement problem.

Table 4.1 Fixed DA and SP dimensions

Parameter	Value (m)
DA length	850
DA width	600
SP length	150
SP width	50
DA – SP spacing	50

The proposed two stage optimization method is applied to the reservoir. The results from the first step of the optimization method representing the orientation and translation along the x and y direction for the compact set of DA which maximizes the total available bitumen is given in Table 4.2. The black box optimization method provides an optimal compact arrangement of DAs and SPs. The total available bitumen in Table 4.2 is the sum of the available bitumen values of all the DAs in the compact arrangement.

Table 4.2 First stage optimization results

Optimization Result	Value
θ	0.7229 rad
Δx	-64.45 m
Δy	-273.1 m
Total Available Bitumen	16720

The plan for the compact arrangement of all the DAs from the first stage of the optimization is given in Fig. 4.8. The numbers on each of the DA quantifies the amount of available bitumen from that particular DA. The following observations can be made from Fig. 4.8:

- A DA is not placed outside the lease area
- A DA is not placed on areas which would result in a significant fraction of the DA area to be outside the lease boundary
- A SP is not placed outside the lease area
- A SP is not placed on any of the surface restrictions
- A DA is not placed if there are no corresponding SP locations available due to either the surface restriction issue or the lease area issue

It is important to note that due to surface restriction and lease boundaries, some DAs have only one possible location for the placement of SP.

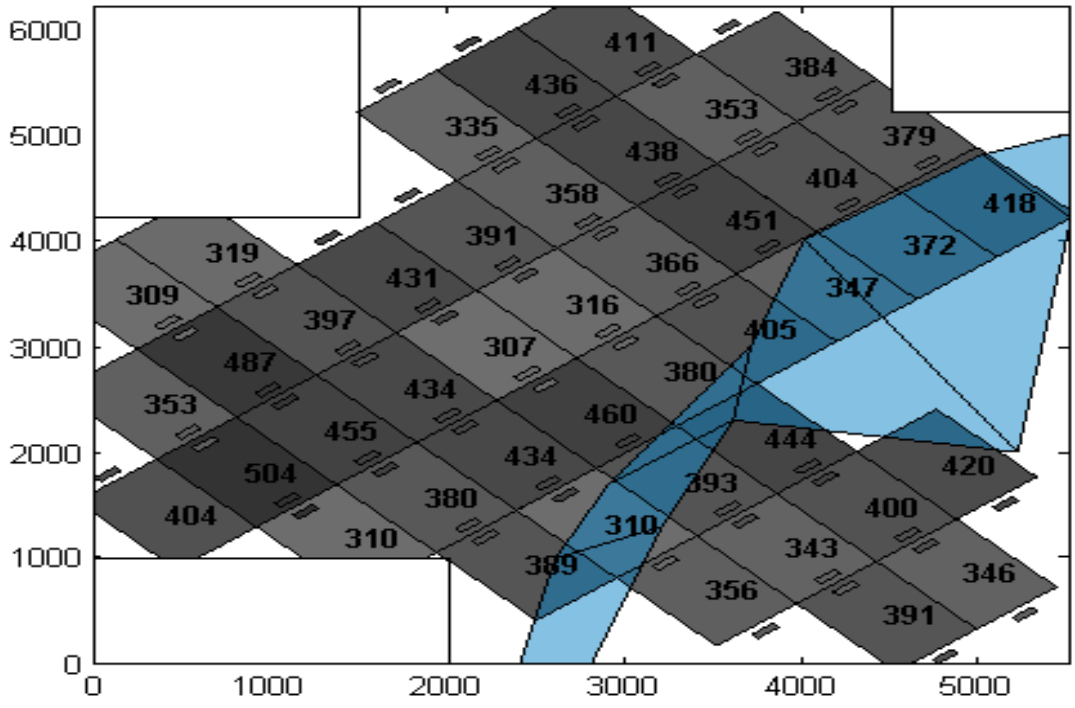

Figure 4.8 Compact DA placement plan from first step of optimization method

The next step of the optimization model uses all the possible DA and SP locations, as given in Fig. 4.8, obtained from the first stage of the optimization method as an input to provide a selected DA and SP placement plan. Initially, companies developing SAGD wells build a smaller number of DA and SP. Hence, DAs representing higher available bitumen are developed initially. In order to reduce financial impact, SPs are selected close to each other. Selecting SPs close to each other ensures a reduced cost associated with the piping which brings super-heated steam to the SPs from the central processing facility. Four time periods were considered in this case study. At each time period, 5 DA and corresponding SP locations were chosen for developing the SAGD area. Therefore, by the end of the fourth time period, a total of 20 $\left(4period \times 5\frac{DA}{period}\right)$ DAs and SPs are selected. The results of the selected DA and SP at each time period are given in Fig. 4.9. DA and SP placement at each time period is represented by different color combination in Fig. 4.9. The DA and SP locations selected during the first, second, third and fourth time periods are given by red, blue, green and yellow colors respectively. As evident from Fig. 4.9, 5 DAs selected in the first time period have the highest available bitumen values and the SPs are placed as close to each other as possible. A similar trend is observed in the DA and SP placement plans for the other time periods as well. Generally, well plans are created with DAs having higher available bitumen and at the same time minimizing the distance between all the selected SPs.

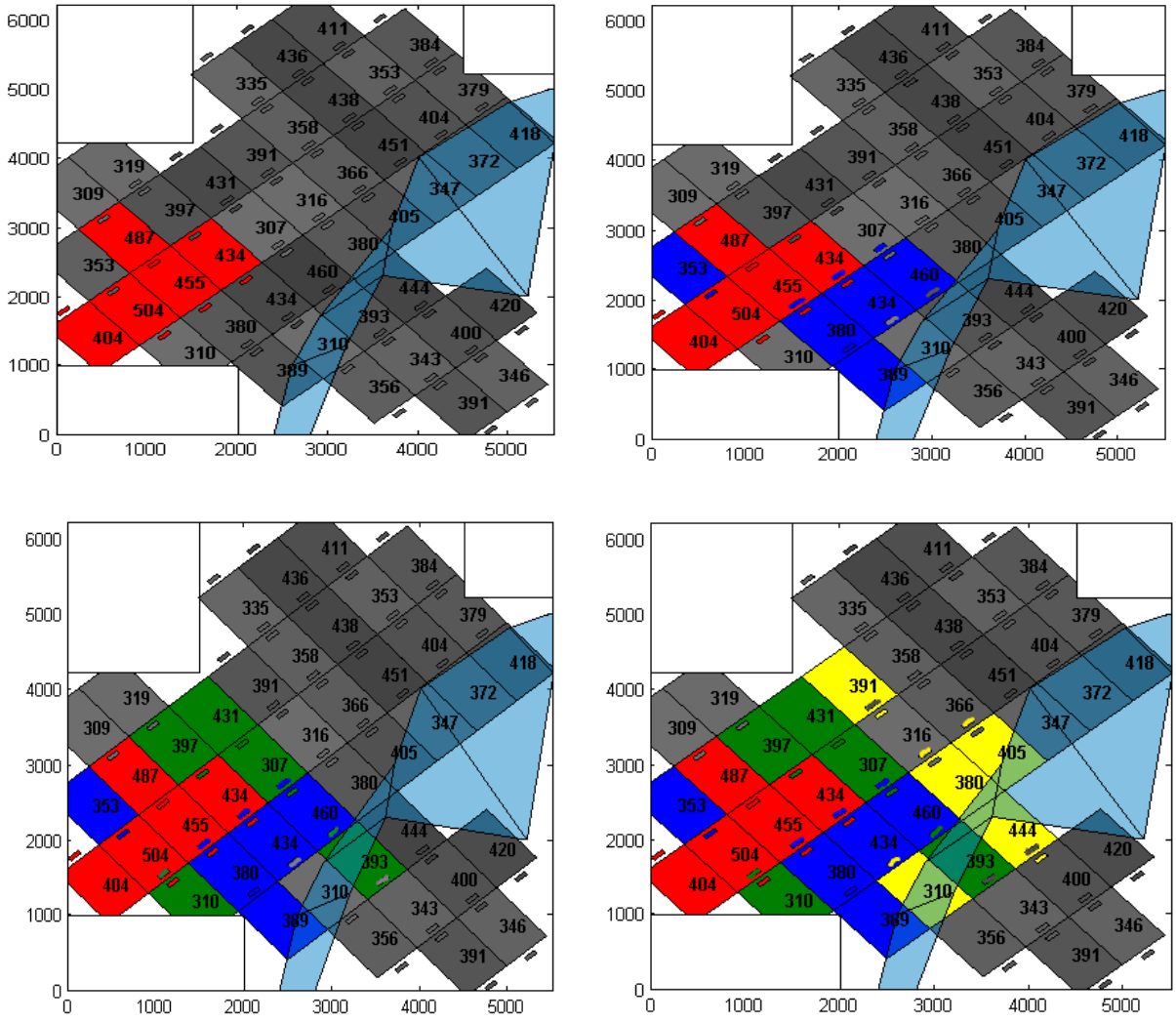

Figure 4.9 DA and SP selection plan at different time periods from the second step of optimization method

4.5.2 Decomposition of lease area

The first stage of the optimization method was further tested by decomposing and breaking down the reservoir area into 3 different sections and applying the optimization method to each of the divided areas separately to obtain 3 different sets of compact DA arrangement plans. The first step of the optimization method is applied to each of those 3 areas to determine the optimal orientation and position for the compact set of DAs. Table 4.3 provides the results of the first stage of the optimization for the 3 different sets of compact DA arrangement plan. The optimal angle of rotation, translation along the x direction and translation along the y direction for the 3

areas are given in Table 4.3. The total available bitumen of each of the areas and the cumulative sum of the total available bitumen from all the 3 areas are also given in Table 4.3.

Table 4.3 First stage optimization results using decomposed areas

Optimization results	Area 1	Area 2	Area 3
θ (rad)	0.6283	0.7362	0.5642
Δx (m)	71.05	25.25	-66.45
Δy (m)	386.2	-169.5	-395.6
Available Bitumen	4056	5646	5970
Total Available Bitumen		15681	

The compact arrangement of DAs and SPs obtained by breaking the total lease area into 3 different sections is given in Fig. 4.10. The red dotted lines divide the lease area into 3 different areas. As expected, no DA or SP is placed outside the lease boundary and no SP is placed on any of the surface restricted areas. Furthermore, a DA was not placed in the compact arrangement if the DA did not have any corresponding position for the placement of at least one SP.

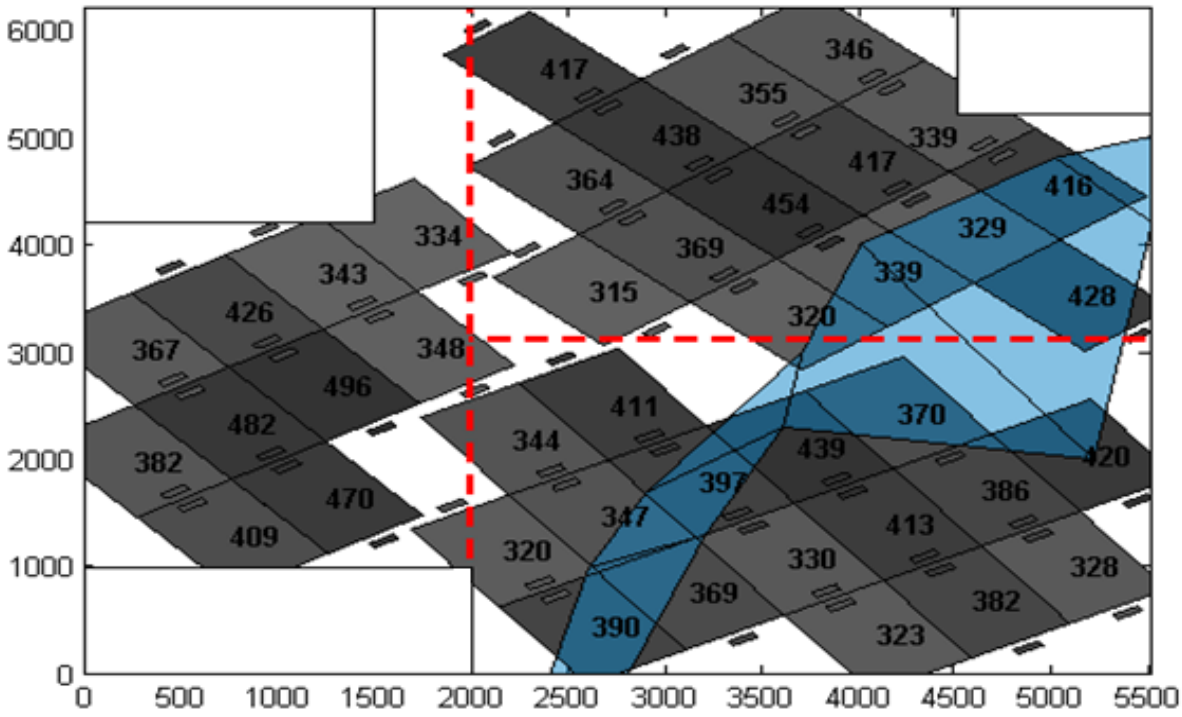

Figure 4.10 Compact DA placement plan from first stage of optimization method using decomposed area

However, it is important to note that the cumulative total available bitumen from the 3 divided areas (15,681) is lower than the total available bitumen from the undivided compact DA arrangement plan of Fig. 4.8 (16,720). The reason behind the lower total available bitumen from the optimization of the decomposed lease area is due to suboptimal division of the lease area into 3 sections. The suboptimal division of the lease area results in more constrained and restricted positions available for the placement of a DA and a SP. As a result less number of DAs can be placed within the leased area.

Another study is performed to validate the reasoning provided for the lower total available bitumen from the decomposed area as given in Fig 4.10. In this case, the only difference was in how the lease area is divided into 3 different decomposed sections. Stage 1 of the compact DA arrangement optimization is then performed on the 3 sections of the lease area separately. Figure 4.11 shows how the lease area is decomposed into 3 different sections as shown by the red dotted lines and the DA arrangement plan obtained from stage 1 optimization. The stage 1 optimization results and the total available bitumen from the 3 different sections are given in Table 4.4.

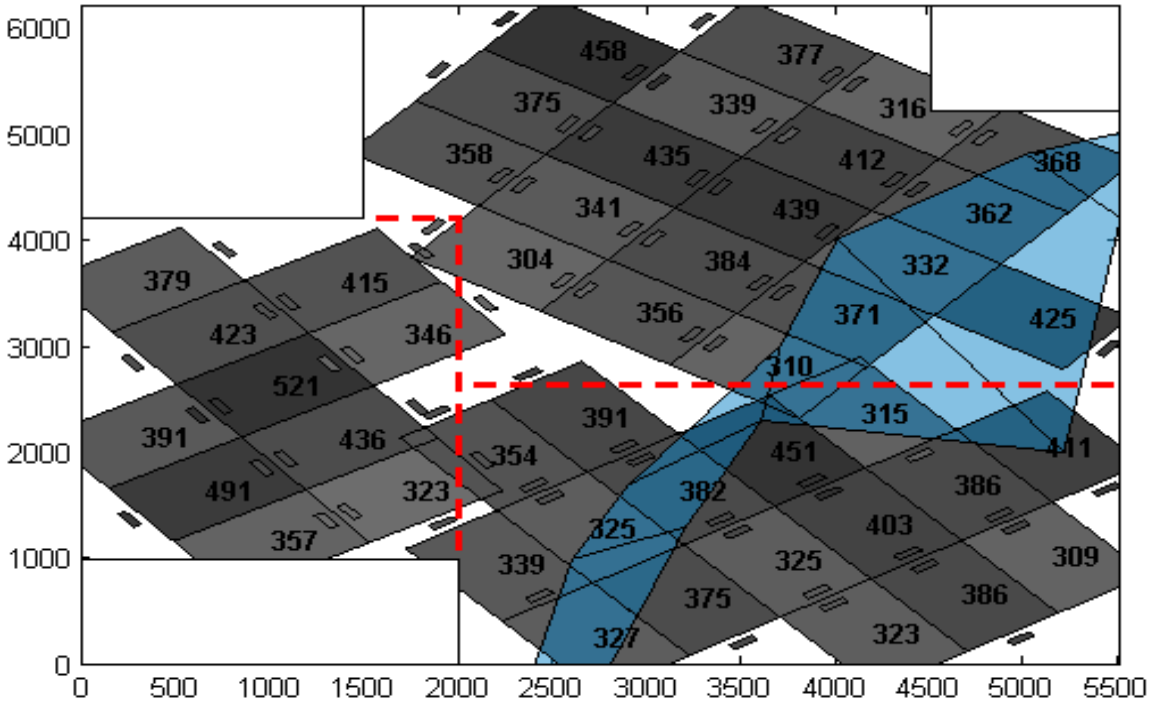

Figure 4.11 Compact DA placement plan from first step of optimization method using decomposed area

It is evident from the plan in Fig. 4.11 that the DA arrangement between the 3 different areas are much compact than the DA arrangement plan in Fig. 4.10. The total available bitumen calculated by the summation of the available bitumen from all the different areas in Table 4.4 (16,947) is higher than the total available bitumen from the DA arrangement obtained from the undivided lease area of Table 4.2 (16,720).

Table 4.4 First stage optimization results using decomposed areas

Optimization results	Area 1	Area 2	Area 3
θ (rad)	-0.9675	0.9362	0.6429
Δx (m)	103.55	108.75	-178.45
Δy (m)	-421	226.7	59.4
Available Bitumen	4082	7063	5802
Total Available Bitumen		16947	

As expected, decomposing a larger lease area into smaller sections and then applying the compact DA arrangement optimization method separately to those areas results in higher total available bitumen. However, it is important to ensure that the lease area is divided in a way as to ensure maximum DA placement.

4.6 DA Arrangement Optimization Under Uncertainty

Uncertainty associated with the geological data of the reservoir was incorporated to the first stage of the SAGD DA arrangement optimization by modifying the objective function of the blackbox optimizer given in Eq. (4.2). A robust optimization method was developed which used multiple geological realizations in the evaluation of the objective function value of the optimizer. The objective function for the DA arrangement optimization problem is designed as maximizing the risk averted expected total available bitumen from a set of realizations as given by Eqs. (4.13) and (4.14).

$$\max R_{risk} = R_{Expected} - \gamma \sqrt{\sum_{i=1}^{N_R} p_i (R_i^{available} - R_{Expected})^2} \tag{4.13}$$

where the expected available bitumen is given by

$$R_{Expected} = \sum_{i=1}^{N_R} p_i R_i^{available} \tag{4.14}$$

In Eqs. (4.13) and (4.14), N_R is the number of realizations used to determine the geological uncertainty, p_i is the probability of a geological realization i , $R_i^{available}$ is the total available bitumen of realization i, γ is the risk averted factor. The blackbox function determines the total available bitumen value based on the orientation and location of the compact set of DAs. A superset of 100 equiprobable realizations of the reservoir lease area is generated using MRST built in function 'GaussianField'. The reservoir dimensions, lease area boundary and surface restrictions of section 4.5.1 are used in generating the superset of realizations. The optimal realization reduction method proposed in section 2.4 is used to select a subset of 10 realization from the superset (Rahim et al., 2014). The dissimilarity between two realizations (Eq. (2.12)) is

represented by the geological properties of the reservoir and the following static measures: K_{net}, ϕ_{net}, S_{net}, F_{net}, PV_{net}, $OOIP$ and OIP_{net}. The static measures are properties of the reservoir grid and hence easily calculated in a preprocessing step. For comparisonal purpose, 10 realizations are selected using OIP_{net} based ranking method and 10 realizations are selected randomly. The selected realizations are used in the objective function evaluation using Eq. (4.13) of the blackbox optimizer to obtain a compact DA arrangement plan. In the robust optimization, only DAs that have available bitumen above the threshold value are considered in the calculation of the objective function of the optimizer. The robust DA arrangement optimization using the different realization reduction methods are performed using 2 different available bitumen threshold values. The results of the optimization showing the orientation and location of the compact DA arranagement obtained using the 3 different realization reduction methods are given in Table 4.5.

Table 4.5 First stage optimization results for the different realization reduction methods

Optimization results	Optimal reduction	OIPnet ranking	Random selection
Available bitumen threshold		>300	
θ (rad)	0.7854	0.7291	0.4712
Δx (m)	271.15	206.8	-2.45
Δy(m)	157.3	-192.9	-68.2
Available bitumen threshold		>100	
θ (rad)	0.3142	1.1854	0.4712
Δx (m)	-291.9	-106.8	-28.6
Δy(m)	-186.2	-177.6	-320.7

The optimization results on Table 4.5 for the different realization reduction methods are used to calculate the total available bitumen from all the realizations in the superset. The results of the compact DA arrangement plan from the different realization reduction methods given in Table 4.5 are used on all 100 realizations of the superset. The compact DA arrangement variables of the different realization reduction methods are applied to each realization in the superset and the expected total available bitumen and the standard deviation of the total available bitumen values

are calculated, as given in Table 4.6. As expected, increasing the available bitumen threshold value significantly decreases the expected total bitumen since less DAs are considered in the calculation of the expected bitumen. The optimal realization reduction method has the highest expected total available bitumen when compared to any the other realization reduction methods.

Table 4.6 Comparison of optimization results for the different realization reduction methods

Results	Optimal reduction	OIPnet ranking	Random selection
Available bitumen threshold		>300	
Total expected bitumen	5445.7	5350.1	5102.2
Standard deviation of total bitumen	7460.5	7236	7129
Available bitumen threshold		>100	
Total expected bitumen	11,359	11,009	11,117
Standard deviation of total bitumen	5878.2	5670	5768.9

The standard deviation of the total available bitumen is also the largest for the optimal realization reduction method. A possible reason for the higher standard deviation can be due to the fact that the optimal realization reduction method incorporates realization which represents the maximum and minimum performance parameter from the superset. As a result, the compact DA arrangement plan from the optimal realization reduction method creates a greater variability when all the realizations of the superset are considered.

Histograms and the compact DA arrangement plan for the different realization reduction methods for available bitumen threshold value of greater than 100 are given in Figs. 4.12 to 4.17. Distributions and DA plans for available bitumen threshold value of 100 are considered because an available bitumen threshold value of 300 results in many realizations with a total bitumen value of 0 since many DAs are not included in the evaluation. A histogram of the total bitumen values of all the realizations in the superset obtained by using robust optimization results from the optimal realization reduction method is given in Fig. 4.12.

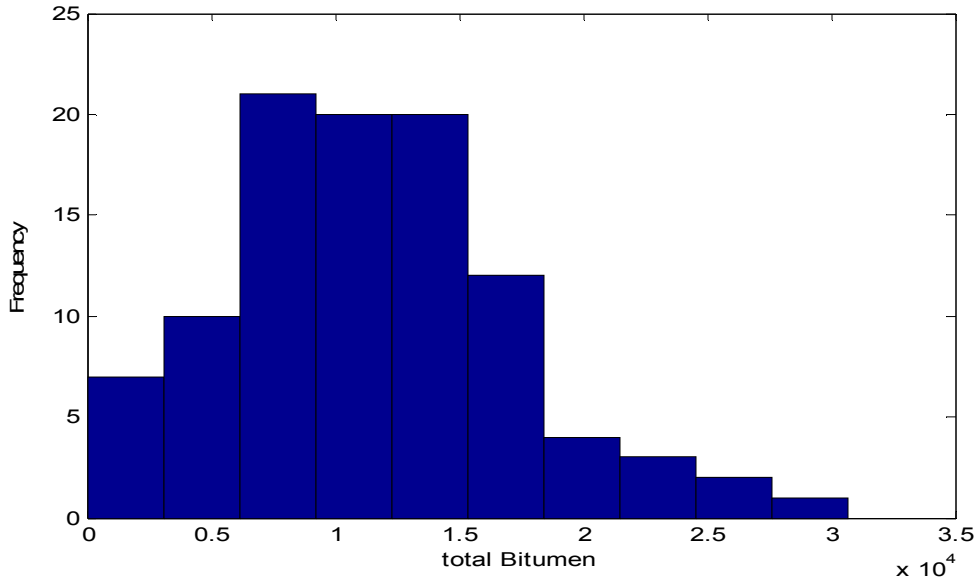

Figure 4.12 Histogram of total Bitumen of all the realization in the superset using robust optimization results from the optimal realization reduction method

The histogram of the total bitumen of all the realizations in the superset obtained using robust optimization results from OIP_{net} ranking based realization reduction method is given in Fig. 4.13.

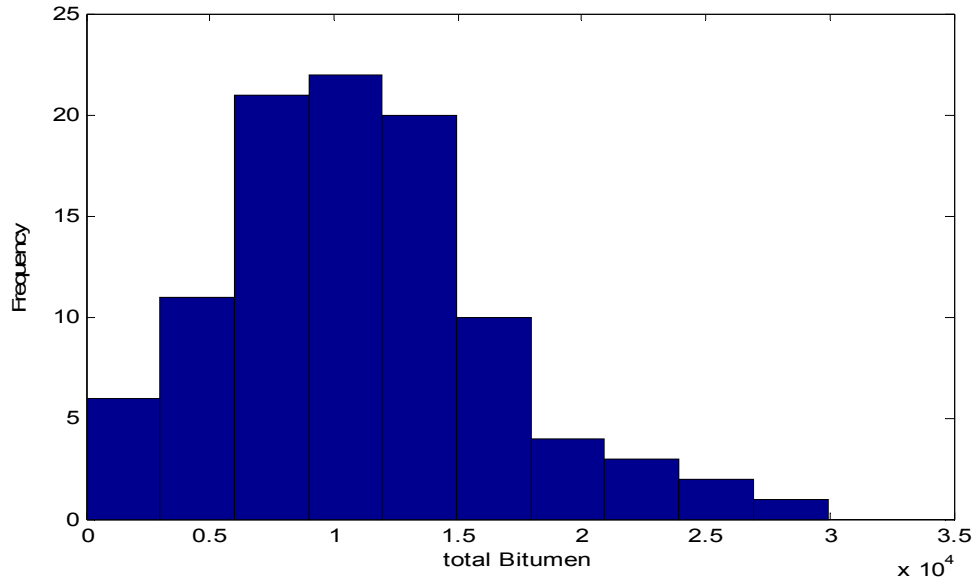

Figure 4.13 Histogram of total Bitumen of all the realization in the superset using robust optimization results from the OIPnet ranking method

The histogram of the total available bitumen of all the realizations in the superset obtained using the compact DA arrangement plan obtained from randomly selected a subset of realization is given in Fig. 4.14.

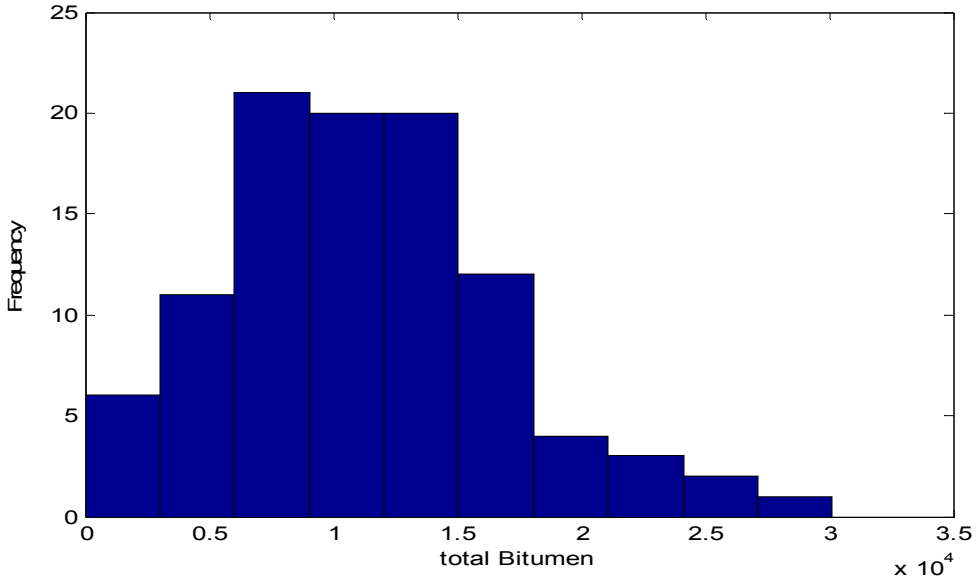

Figure 4.14 Histogram of total Bitumen of all the realization in the superset using robust optimization results from random selection

The compact DA placement plan from the robust SAGD DA arrangement optimization using a subset of realizations obtained from the optimal realization reduction method is given in Fig. 4.15. The compact arrange of the DA is ensured since most of the available area within the lease boundary has been used for placing a DA. Each number on DA is the expected total available bitumen calculated from the 10 selected realizations and the corresponding probabilities obtained from the optimal realization reduction method.

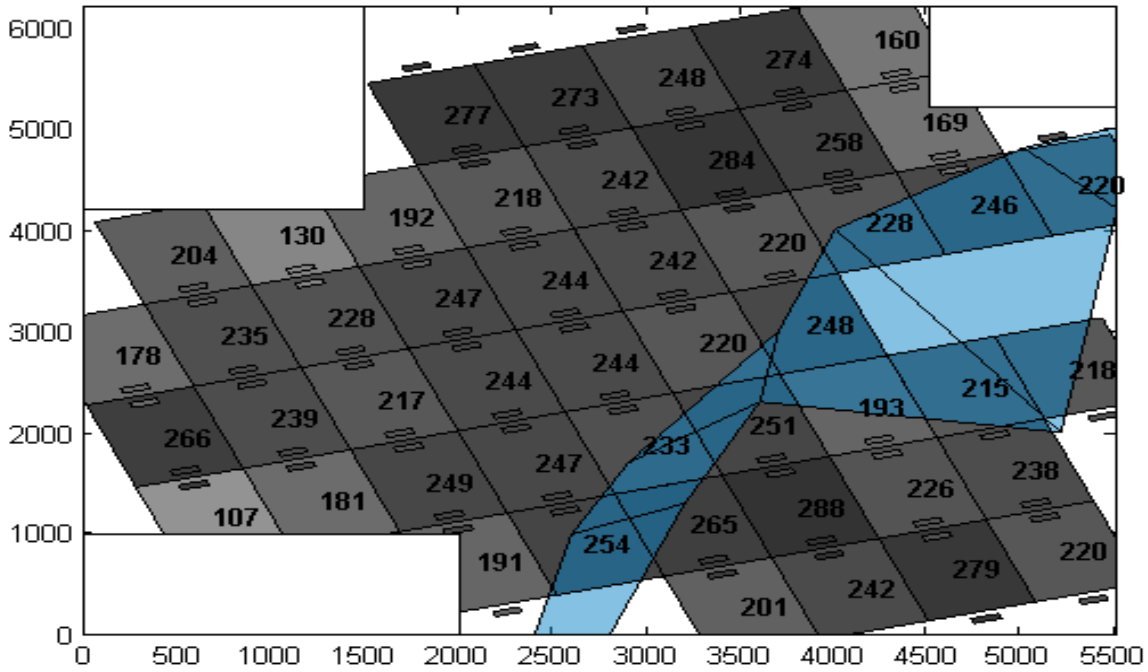

Figure 4.15 Compact DA placement plan from robust SAGD DA arrangement optimization with a subset of realizations selected from optimal realization reduction method

Similarly, the DA arrangement plan obtained from the robust optimization using a subset of realizations from the OIP_{net} ranking based method is given in Fig. 5.16. In the calculation of the total available bitumen of each DA in Fig. 4.16, mathematical averages of the 10 selected realizations with equal probabilities were used.

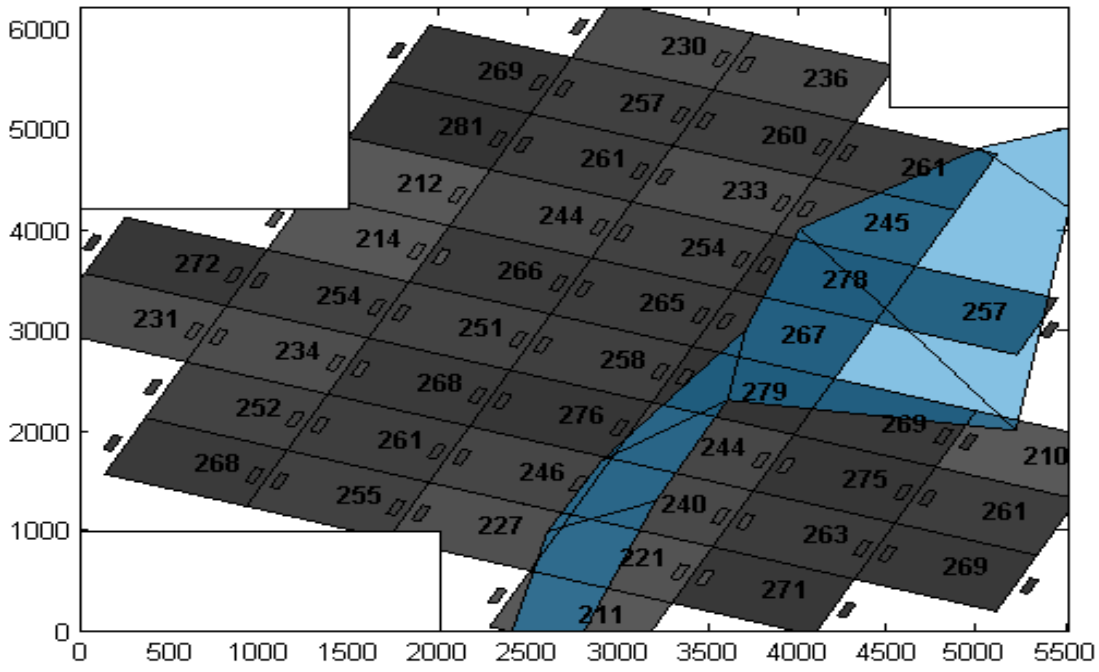

Figure 4.16 Compact DA placement plan from robust SAGD DA arrangement optimization with a subset of realizations selected from OIPnet ranking method

The SAGD DA placement plan for the robust placement optimization using a randomly selected subset of 10 realizations is given in Fig. 4.17. Equal probabilities are considered in the calculation of the mean total available bitumen value for each DA in the case of randomly selected realizations.

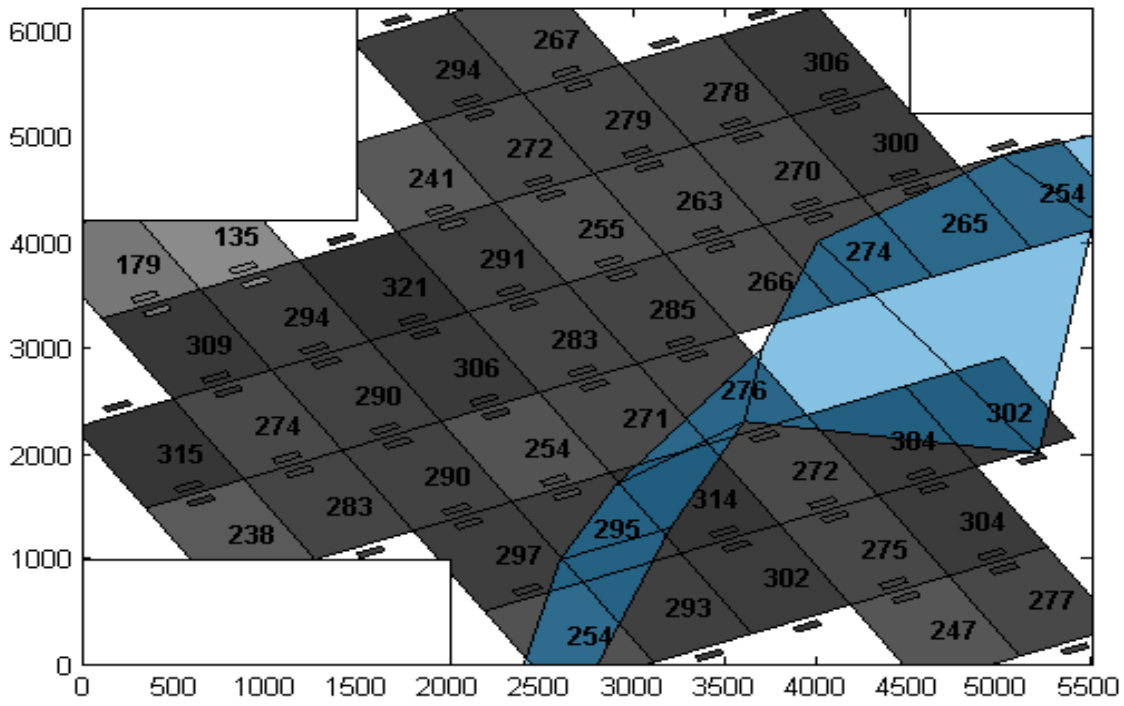

Figure 4.17 Compact DA placement plan from robust SAGD DA arrangement optimization with a subset of realizations selected from random selection

In comparison of all the compact DA arrangement plans given in Figs. 4.15 to 4.17, the DA arrangement plan obtained using the optimal realization reduction method has the highest number of DAs within the lease boundary. The DA arrangement plans using optimal realization reduction method, OIP_{net} ranking method and random selection method has 49, 45 and 46 DAs respectively. Highest number of DAs are fitted in the compact arrangement obtained from using the optimal realization reduction method.

4.7 Conclusion

A two-stage optimization model for selecting optimal SAGD well plan proposed in this chapter selects optimal positions of the Drainage Area (DA) and a Surface Pad (SP) of SAGD wells. In the study, the reservoir quality in terms of the quantity of bitumen present is quantified using the

concept of net cells to determine the total available bitumen. The first stage of the proposed optimization method determines the optimal orientation and position of a compact set of all the DAs and SPs that can be packed within the lease area of the reservoir. The second stage of the proposed optimization method selects a user defined number of DAs and SPs from the compact arrangement of all the DAs which would result in maximum total available bitumen and at the same time decrease the distance between all the selected SPs. Limitations, such as surface restrictions and irregular shaped lease areas, are taken into consideration in the placement of DAs and SPs by the optimization model. The optimization method was applied to a realistic case study to determine a DA and SP placement plan for a lease area to develop SAGD facilities. The SAGD arrangement optimization model produced a plan with DAs being placed at areas with higher available bitumen content and ensured that the selected SPs were close to each other. Furthermore, the SAGD DA arrangement optimization method under geological uncertainty was studied by incorporating multiple geological realizations from the optimal realization reduction method. The results of the SAGD DA arrangement optimization under geological uncertainty showed that a higher expected total available bitumen and a more compact DA arrangement plan with higher number of packed DAs, was obtained using the optimal realization reduction method

Chapter 5
Conclusion

Geological uncertainty reduction and its application in reservoir development optimization are investigated in this thesis. An optimal realization reduction method is proposed which reduces geological uncertainty by selecting a smaller subset of realizations and incorporating them in reservoir studies. The realization reduction method is used to determine optimal producer well locations from a robust well placement optimization method. Additionally, an optimal SAGD well arrangement is determined using a two stage DA arrangement optimization model in this thesis. The optimal realization reduction method is applied to incorporate geological uncertainty in the proposed SAGD DA arrangement optimization model.

The optimal realization reduction method is a MILP optimization model which uses geological properties of the reservoir and simple static measures to quantify the difference between the realizations. The optimal realization reduction method is studied using different reservoir models. The subset of realizations obtained from the proposed realization reduction method has a distribution with similar statistical characteristic as the distribution from the superset of all the realizations. In the calculation of the dissimilarity between two realizations in the optimal realization reduction method, various static measures and geological properties of the reservoir were considered. Static measures of CHV_{local} and F_{LC} are dependent on the producer well locations and were calculated for vertical wells. In future, CHV_{local} and F_{LC} could be modified to calculate for horizontal wells. These static measures could be added to the optimal realization reduction method for use in horizontal well applications. In addition to porosity and permeability, additional geological property of the reservoir, such as, water saturation could be incorporated in the calculation of the dissimilarity used in the optimal realization reduction method.

The robust vertical well placement optimization under geological uncertainty is a blackbox optimization model which calls on the reservoir simulator at each function evaluation. Well placement plans were generated from reservoir models by using a subset of realizations from the

optimal realization reduction method and by using the superset of all the realizations. The well placement plan obtained from using a subset of realizations from the proposed method has mean and variance performance parameter values which are very close to the performance parameter values obtained from the well placement plan using all the realizations. In this study, well placement optimization under uncertainty considers to determine the optimal producer well location with fixed injector locations. In future, an extension to this study could be to obtain an optimal injector and producer well locations under geological uncertainty. As a result, a well placement plan with optimal injector and producer locations would be obtained.

The first stage of the DA arrangement optimization for SAGD wells uses a blackbox optimizer to generate an optimal compact arrangement for the set of all the DAs and the second stage uses a MILP optimization model to select a smaller number of DAs and SPs for development in the reservoir lease area. Selected realizations from the optimal realization reduction method are used to incorporate geological uncertainty to the first stage of the DA arrangement optimization model. A compact DA and SP plan with higher available bitumen content is obtained from the SAGD arrangement optimization method. In this study, geological uncertainty was incorporated to the first stage of the DA arrangement optimization method. In future, the study can be extended to incorporate geological uncertainty in the second stage of the SAGD DA arrangement optimization problem. This would lead to uncertainty being quantified in both stages of the SAGD DA arrangement problem. As a result, geological uncertainty would be included the selected DA and SP plan obtained from the second stage of the optimization method.

References

[1] Alberta Energy Regulator (AER), ST98-2014: Alberta's Energy Reserves 2013 and Supply/Demand Outlook 2014–2023, 2014

[2] Armstrong M, Ndiaye A, Razanatsimba R, Galli A (2013) Scenario reduction applied to geostatistical simulations. *Math Geosci* 45:165-182

[3] Audet C, Le Digabel S, Tribes C (2009). NOMAD user guide. Technical Report G-2009-37, Les cahiers du GERAD.

[4] Ballin PR, Journel AG, Aziz K (1992) Prediction of uncertainty in reservoir performance forecast. JCPT 31(4), 52-62

[5] Bangerth W, Klie H, Wheeler MF, Stoffa PL, Sen MK (2006). On optimization algorithms for the reservoir oil well placement problem. *Comput Geosci,* 10, 303-319.

[6] Beckner BL, Song X (1995). Field development planning using simulated annealing – optimal economic well scheduling and placement, SPE Annual Technical Conference and Exhibition Dallas, Texas.

[7] Bittencourt AC, Horne RN (1997). Reservoir development and design optimization, SPE Annual Technical Conference and Exhibition San Antonio, Texas.

[8] Christie MA, Blunt MJ (2001) Tenth SPE comparative solution project: A comparison of upscaling techniques. *SPE Journal*, 4(4):308-317

[9] Deutsch CV, Srinivasan S (1996) Improved reservoir management through ranking stochastic reservoir models. In: SPE/DOE Improved Oil Recovery Symposium, 21-24 April 1996, Tulsa, USA, doi: 10.2118/35411-MS

[10] Deutsch CV (1998) Fortran programs for calculating connectivity of three-dimensional numerical models and for ranking multiple realizations. *Comput Geosci* 24:69-76

[11] Deutsch CV (1999) Reservoir modeling with publicly available software. *Comput Geosci* 25:355-363

[12] Deutsch CV, Begg SH (2001) The use of ranking to reduce the required number of realizations. Centre for Computational Geostatistics (CCG) Annual Report 3, Edmonton

[13] Dupacova J, Growe-Kuska N, Romisch W (2003) Scenario reduction in stochastic programming an approach using probability metrics. *Math Program* 95:493–511

[14] Fenik DR, Nouri A, Deutsch CV (2009) Criteria for ranking realizations in the investigation of SAGD reservoir performance. In: Proceedings of Canadian International Petroleum Conference, 16-18 June 2009, Calgary, Canada. doi: 10.2118/2009-191

[15] Gilman JR, Meng H-Z, Uland MJ, Dzurman PJ, Cosic S (2002) Statistical ranking of stochastic geomodels using streamline simulation: A field application. In: SPE Annual Technical Conference and Exhibition, 29 September – 2 October 2002, San Antonio, USA. doi: 10.2118/77374-MS

[16] IBM (2009) User's Manual for CPLEX V12.1. ftp://public.dhe.ibm.com/

[17] Kantorovich LV (1942) On the transfer of masses. Dokl.Akad.Nauk 37:227-229

[18] Kumar A (2011) Optimal drainage area and surface pad positioning for SAGD development. MSc Thesis. University of Alberta, Canada

[19] Li SH, Deutsch CV, Si JH (2012) Ranking geostatistical reservoir models with modified connected hydrocarbon volume. In: Ninth International Geostatistics Congress, 11-15 June 2012, Oslo, Norway

[20] Li Z, Floudas CA (2014) Optimal scenario reduction framework based on distance of uncertainty distribution and output performance: I. Single reduction via mixed integer linear optimization. *Computers and Chemical Engineering* 70:50-66

[21] Lie KA, Krogstad S, Ligaarden I, Natvig J, Nilsen H, Skaflestad B (2012) Open-source MATLAB implementation of consistent discretization on complex grids. *Comput Geosci* 16:297-322

[22] Manchuk JG, Deutsch CV (2013) Optimization of Drainage-Area Configuarations to maximize recovery from SAGD Operations.

[23] MATLAB and Statistics Toolbox Release 2012b, The MathWorks, Inc., Natick, Massachusetts, United States.

[24] McLennan JA, Deutsch CV (2005) Selecting geostatistical realizations by measures of discounted connected bitumen. In: SPE International Thermal Operations and Heavy Oil Symposium, 1-3 November 2005, Calgary, Canada. doi: 10.2118/98168-MS

[25] McLennan JA, Deutsch CV (2004) SAGD reservoir characterization using geostatistics: applications to the Athabasca Oil Sands, Alberta, Canada. In: Press, Canadian Heavy Oil Association Handbook

[26] Monge G (1781) Mémoire sur la théorie des déblais et des remblais: Histoire de 1'AcademieRoyale des Sciences

[27] Nasrabadi H, Morales A, Zhu D (2012). Well placement optimization: A survey with special focus on application for gas/gas-condensate reservoirs. *Natural Gas Science and Engineering,* 5, 6-16.

[28] Onwunalu JE, Durlofsky LJ (2010). Application of a particle swarm optimization algorithm for determining optimum well location and type. *Comput Geosci,* 14, 183-198.

[29] Park K, Caers J (2011) Metrel: Petrel plug-in for modelling uncertainty in metric space. Department of Energy Resource Engineering, Stanford University

[30] Rahim S, Li Z, Trivedi J (2015). Reservoir Geological Uncertainty Reduction: an Optimization Based Method using Multiple Static Measures. *Math Geosci* doi:10.1007/s11004-014-9575-5

[31] Rosenwald GW, Green DW (1974). A method for determining the optimum location of wells in a reservoir using mixed-integer programming. *SPE Journal*, 14, 44-54.

[32] Scheidt C, Caers J (2009) Representing spatial uncertainty using distances and kernels. *Math Geosci* 41:397-419

[33] Scheidt C, Caers J (2010) Bootstrap confidence intervals for reservoir model selection techniques. *Comput Geosci* 14:369-382

[34] Singh AP, Maucec M, Carvajal GA, Mirzadeh S, Knabe SP, Al-Jasmi AK, El Din IH, (2014) Uncertainty quantification of forecasted oil recovery using dynamic model ranking with application to a ME carbonate reservoir. In: International Petroleum Technology Conference, 20-22 January 2014, Doha, Qatar. doi: IPTC 17476-MS

[35] Shi J, Malik J (2000) Normalized-cut and image segmentation. IEEE Trans Pattern Anal *Mach Intell* 22(8):888-905

[36] Wang H, Echeverria-Ciaurri D, Durlofsky LJ, Cominelli A (2012). Optimal well placement under uncertainty using a retrospective optimization framework. *SPE Journal*, 17 (1), 112-121.

[37] Yang C, Card C, Nghiem L, Fedutenko E (2011). Robust optimization of SAGD operations under geological uncertainties. SPE Reservoir Simulation Symposium, Woodlands, Texas.

[38] Yasari E, Pishvaie MR, Khorasheh F, Salahshoor K (2013). Application of multi criterion robust optimization in water-flooding of oil reservoir. *Petroleum Science and Engineering,* 109, 1-11.

[39] Yeten B, Durlofsky LJ, Aziz K (2003). Optimization of nonconventional well type, location and trajectory. *SPE Journal,* 8, 200-210.

Appendix A: Result of the traditional ranking method using single static measure

Table A.1 Results for selected realizations using static measure based traditional ranking method for case 1

Rank K_{net}	ID	32	22	62	15	2	36	21	25	92	85
	Measure	0.118297	0.125131	0.1305	0.133025	0.135416	0.138668	0.141106	0.145798	0.150113	0.177038
	NPV	854068	933089	948612	899776	1011890	1001050	952121	994556	1023790	1115370
	COP	1455.42	1525.08	1622.5	1538.54	1739.37	1658.81	1613.37	1691.51	1751.29	1860.24
Rank ϕ_{net}	ID	32	54	72	67	45	64	47	40	92	85
	Measure	0.316289	.0321223	0.323595	0.326025	0.326926	0.32911	0.329989	0.332874	0.335263	0.349669
	NPV	854068	962562	837264	1001950	886049	999070	1010080	978815	1023790	1115370
	COP	1455.42	1604.15	1428.54	1667.5	1486.46	1698.21	1723.39	1680.78	1751.29	1860.24
Rank $S_{iw,net}$	ID	32	54	34	44	59	68	100	25	92	85
	Measure	0.695634	0.698441	0.700001	0.701189	0.701692	0.702779	0.703499	0.704671	0.706054	0.713086
	NPV	854068	962562	852699	955461	969853	961850	1019180	994556	1023790	1115370
	COP	1455.42	1604.15	1466.04	1579.68	1638.93	1658.15	1689.56	1691.51	1751.29	1860.24
Rank F_{net}	ID	20	55	49	19	18	56	1	47	92	85
	Measure	0.0793651	0.188209	0.263039	0.369615	.433107	0.498866	0.571429	0.641723	0.712018	0.936508
	NPV	902143	906049	931274	954019	958356	968877	1007970	1010080	1023790	1115370
	COP	1501.79	1562.1	1541.44	1606.42	1625.59	1626.98	1678.65	1723.39	1751.29	1860.24
Rank F_{LC}	ID	1	14	25	41	55	71	89	93	58	87
	Measure	0	0	0	0	0	0	0	0.0566893	0.328798	0.834467
	NPV	1007970	896462	994556	962370	906049	976329	894100	953642	994775	1044260
	COP	1678.65	1510.83	1691.51	1655.95	1562.1	1617.49	1494.76	1606.59	1698.46	1760.18
Rank PV_{net}	ID	86	55	49	19	18	66	40	47	92	85
	Measure	11.5151	26.8169	38.1039	52.4137	62.0978	72.4813	83.5513	93.3868	105.273	144.413
	NPV	866981	906049	931274	954019	958356	979883	978815	1010080	1023790	1115370
	COP	1472.47	1562.1	1541.44	1606.42	1625.59	1712.41	1680.78	1723.39	1751.29	1860.24
Rank $OOIP$	ID	72	15	26	94	19	68	64	65	61	85
	Measure	40.0763	40.8896	41.1899	41.5216	41.6606	41.8843	42.1673	42.3819	42.6353	43.9658
	NPV	837264	899776	923974	946938	954019	961850	999070	100420	1021670	1115370
	COP	1428354	1538.54	1578.38	1604.91	1606.42	1658.15	1698.21	1718.53	1765.73	1860.24
Rank $OOIP_{net}$	ID	20	55	49	19	18	66	40	47	92	85
	Measure	3.42056	8.04557	11.3162	15.7602	18.5499	21.428	24.6179	27.6564	30.8813	41.3692
	NPV	902143	906049	931274	954019	958356	979883	978815	1010080	102790	1115370
	COP	1501.79	1562.1	1541.44	1606.42	1625.59	1712.41	1680.78	1723.39	1751.29	1860.24
Rank CHV_{local}	ID	1	14	25	41	55	71	89	93	58	87
	Measure	0	0	0	0	0	0	0	2.46114	14.2243	36.2371
	NPV	1007970	896462	994556	962370	976329	894100	953642	994775	994775	1044260
	COP	1678.65	1510.83	1691.51	1655.95	1562.1	1617.49	1494.76	1606.59	1698.46	1780.18

Table A.2 Results for selected realizations using static measure based traditional ranking method for case 2

Rank K_{net}	ID	63	29	39	26	34	99	36	74	49	5
	Measure	0.112065	0.119433	0.122698	.0124107	0.126492	.130122	0.133209	0.136253	0.141383	0.148686
	NPV	1198080	1278920	1994910	1246030	1271830	1280910	1298540	1212020	1332790	134440
	COP	4731.85	5091.02	4765.09	4734.71	4978.48	5053.3	5233.12	5046.22	5155.1	5454.71
Rank ϕ_{net}	ID	63	71	39	42	19	81	90	100	49	5
	Measure	0.312485	.317619	0.319721	0.32057	0.321962	0.324233	0.326194	0.327711	0.33056	0.334495
	NPV	1198080	1221240	1994910	1277770	1302830	1286270	1321750	1342290	1332790	134440
	COP	4731.85	4764.65	4765.09	4960.83	5131.82	5147.38	4977.19	5341.66	5155.1	5454.71
Rank $S_{iw,net}$	ID	63	57	59	77	24	13	90	74	58	5
	Measure	0.693443	0.696663	0.697792	0.698426	0.699165	0.700495	0.7015	0.702288	0.703849	0.705668
	NPV	1198080	1284730	1150250	1256880	1249910	1310660	1321750	1242020	132280	134440
	COP	4731.85	5073.8	4544.89	4953.51	4879.66	5261.48	4977.19	5046.22	5302.19	5454.71
Rank F_{net}	ID	55	60	16	24	29	62	91	70	61	25
	Measure	0.04125	0.1625	0.238125	0.30875	0.366875	0.455	0.53125	0.58875	0.62375	0.88625
	NPV	1169440	129330	1245360	1249910	1278920	1275780	1292750	1336350	1351660	147390
	COP	4557.34	4799.58	4907.44	4879.66	5091.02	5057.55	5174.18	5189.61	5485.42	5608.21
Rank F_{LC}	ID	1	15	31	44	60	73	86	100	52	25
	Measure	0	0	0	0	0	0	0	0	0.21125	0.88625
	NPV	1230740	1364860	1333880	1393770	1239330	1342980	121360	1342290	130410	1427390
	COP	4950.47	5233.38	5195.49	5499.21	4799.58	5269.27	4675.31	5341.66	5113.22	5608.21
Rank PV_{net}	ID	55	60	16	24	3	62	17	93	5	25
	Measure	20.8152	82.5262	121.575	159.291	188.319	232.765	275.319	307.78	349.882	470.754
	NPV	1169440	129330	1245360	1249910	1276140	1275780	1395770	1363120	134440	1427390
	COP	4557.34	4799.58	4907.44	4879.66	5091.15	5057.55	5259.06	5269.66	5454.71	5608.21
Rank $OOIP$	ID	59	26	84	88	94	22	6	35	23	76
	Measure	145.802	148.334	149.285	150.215	150.91	151.625	152.399	152.79	153.7	156.112
	NPV	1150250	1246030	1273790	1267960	1296690	1267970	1294440	1362770	1338830	1457430
	COP	4544.89	4734.71	5045.54	4950.76	5044.21	5050.09	5234.43	5295.53	5278.34	5640.14
Rank $OOIP_{net}$	ID	55	60	16	24	29	62	91	70	5	25
	Measure	6.33867	25.0174	36.7284	47.8371	56.4977	69.2924	82.499	91.7249	102.771	138.793
	NPV	1169440	129330	1245360	1249910	1278920	1275780	1292750	1336350	134440	1427390
	COP	4557.34	4799.58	4907.44	4879.66	5091.02	5057.55	5174.18	5189.61	5454.71	5608.21
Rank CHV_{local}	ID	1	15	31	44	60	73	86	100	52	25
	Measure	0	0	0	0	0	0	0	0	32.7893	138.793
	NPV	1230740	1364860	1333880	1393770	1239330	1342980	1212360	1342290	1302410	55497500
	COP	4950.47	5233.29	5195.49	5499.21	4799.58	5269.21	4675.31	5431.66	5113.22	5608.21

Table A.3 Results for selected realizations using static measure based traditional ranking method for case 3

Rank K_{net}	ID	80	24	43	83	65	19	50	51	93	64
	Measure	0.110095	0.113903	0.114924	0.11577	0.116863	0.118037	0.119597	0.120212	0.122409	0.131013
	NPV	43664800	47640100	49763600	47196900	47191500	49887900	50219700	50191100	50699500	55497500
	COP	115143	120888	123958	120248	120240	124137	124617	124575	125310	132245
Rank ϕ_{net}	ID	80	24	43	85	65	19	50	51	93	64
	Measure	0.311739	0.314379	0.315108	0.315591	0.316291	0.317081	0.318101	0.318519	0.319887	0.325338
	NPV	43664800	47640100	49763600	49291000	47191500	49887900	50219700	50191100	50699500	55497500
	COP	115143	120888	123958	123274	120240	124137	124617	124575	125310	132245
Rank $S_{iw,net}$	ID	80	24	43	72	96	19	87	51	93	64
	Measure	0.69326	0.694931	0.695405	0.695669	0.696057	0.696555	0.697178	0.697428	0.69821	0.701384
	NPV	43664800	47640100	49763600	49652100	47135900	49887900	51628000	50191100	50699500	55497500
	COP	115143	120888	123958	123796	120160	124137	126652	124575	125310	132245
Rank F_{net}	ID	80	68	56	62	45	54	77	31	39	64
	Measure	0.035909	0.222848	0.268985	0.335848	0.392773	0.440894	0.502288	0.543212	0.608697	0.878879
	NPV	43664800	45863600	47688000	48427800	48545900	48458600	50192000	50381300	51238200	55497500
	COP	115143	118321	120958	122027	122195	122071	124577	124850	126089	132245
Rank F_{LC}	ID	1	17	33	44	61	74	90	5	57	64
	Measure	0	0	0	0	0	0	0	0.307818	0.535045	0.878833
	NPV	52264700	48021100	50265300	49679300	52327100	50131200	44909400	47378400	50267000	55497500
	COP	127572	121439	124683	123836	127663	124489	116941	120510	124685	132245
Rank PV_{net}	ID	80	68	56	94	67	54	77	31	39	64
	Measure	738.822	4641.51	5580.93	7031.45	8198.67	9263.33	10601.7	11416.1	12870.2	18871.5
	NPV	43664800	45863600	47688000	48411600	48086500	48458600	50192000	50381300	51238200	55497500
	COP	115143	118321	120958	122003	121534	122071	124577	124850	126089	132245
Rank $OOIP$	ID	80	69	38	15	67	54	77	30	98	64
	Measure	6095.97	6185.46	6200.06	6218.59	6235.06	6248.6	6266.79	6275.41	6291.19	6382.59
	NPV	43664800	47095300	46945900	49003700	48086500	48458600	50192000	50347000	53302800	55497500
	COP	115143	120101	119885	122859	121534	122071	124577	124801	129073	132245
Rank $OOIP_{net}$	ID	80	68	56	62	67	54	77	31	39	64
	Measure	226.545	1411.89	1701.82	2133.68	2491.19	2802.07	3197.65	3452.49	3877.44	5630.32
	NPV	43664800	45863600	47688000	48427800	48086500	48458600	50192000	50381300	51238200	55497500
	COP	115143	118321	120958	122027	121534	122071	124577	124850	126089	132245
Rank CHV_{local}	ID	1	17	33	44	61	74	90	5	57	64
	Measure	0	0	0	0	0	0	0	1948.46	3399.02	5630.03
	NPV	52264700	48021100	50265300	49679300	52327100	50131200	44909400	47378400	50267000	55497500
	COP	127572	121439	124683	123836	127663	124489	116941	120510	124685	132245

Appendix B: Supporting study for case 3

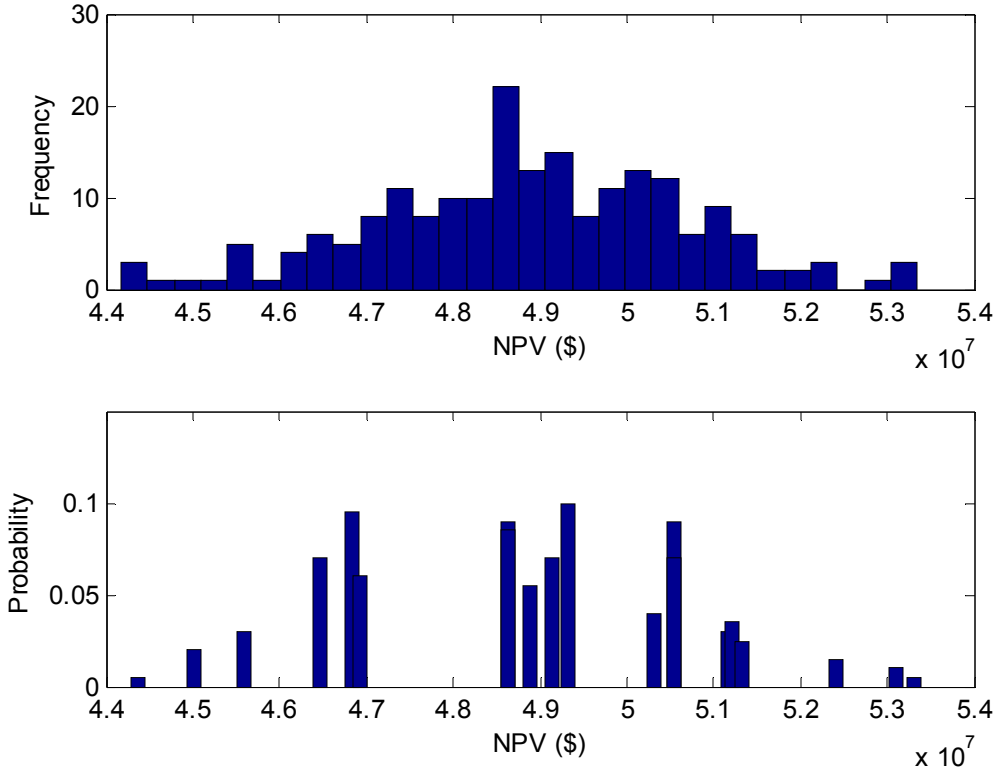

Figure B.1 Histogram using NPV for superset of 200 realizations (top), 10 selected realizations using proposed method (bottom)

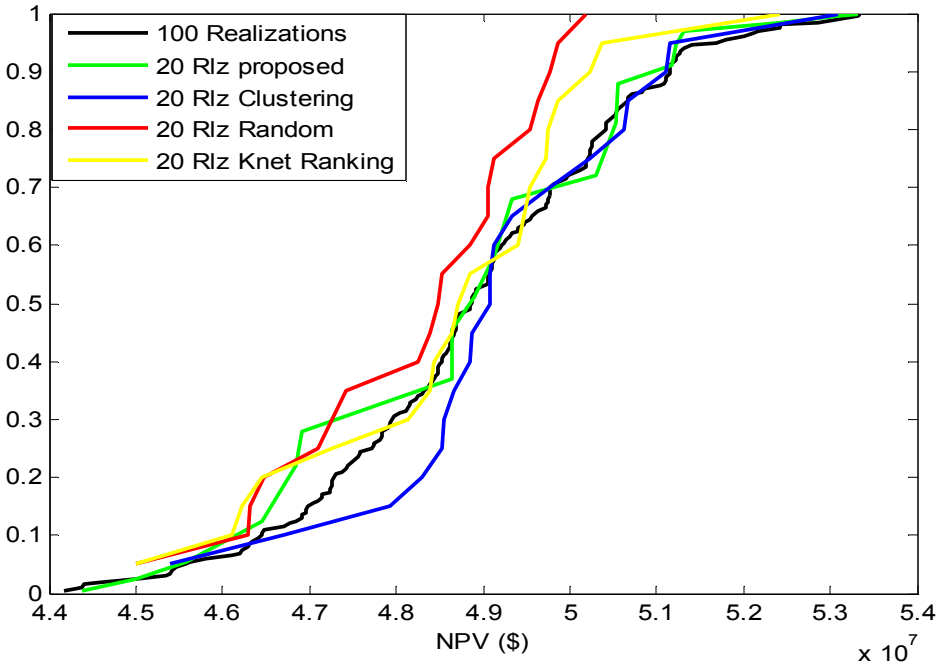

Figure B.2 CDF plot comparison using NPV between the superset of realization and selected set of realization using; (i) proposed method, (ii) Kernel k-means clustering, (iii) Knet ranking, (iv) random selection

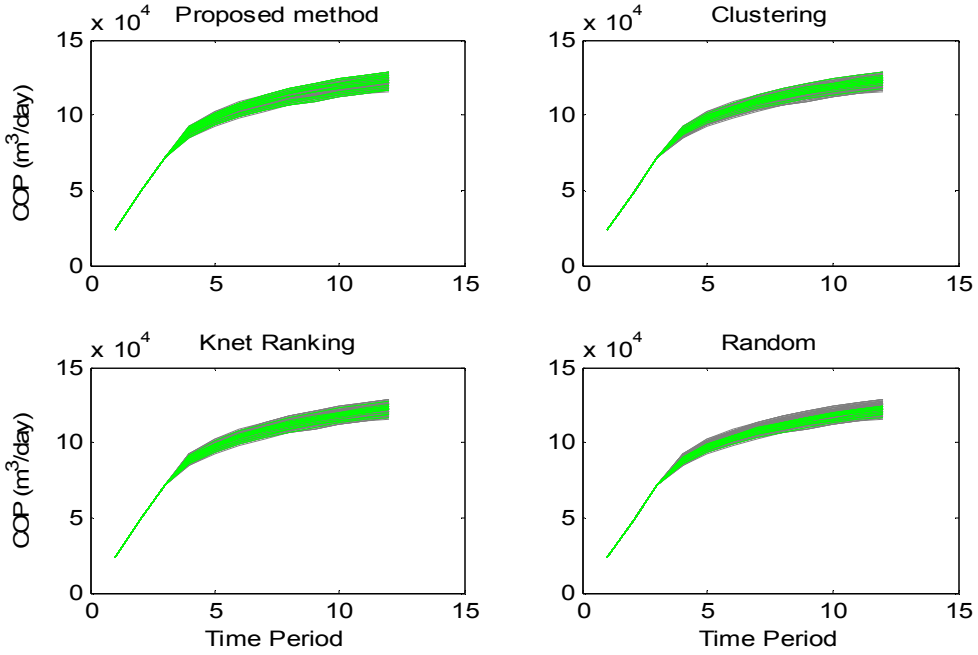

Figure B.3 COP versus time plot for 10 realizations selected from the (clockwise); (i) proposed method, (ii) Kernel k-means clustering, (iii) random selection, (iv) Knet ranking

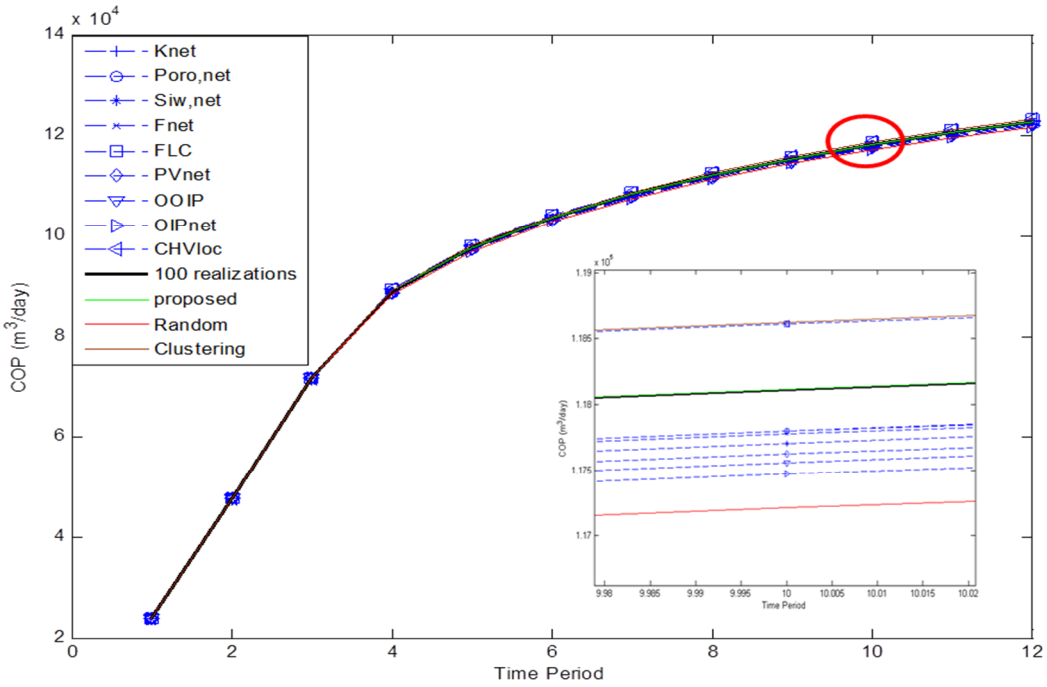

Figure B.4 Expected COP plots of the different realization reduction methods

Table B.1 Reservoir simulation results of all 200 realizations and 20 selected realizations

	$NPV_{\max}$ $(\times 10^7)$	$NPV_{\min}$ $(\times 10^7)$	$NPV_{\exp}$ $(\times 10^7)$	$COP_{\max}$ $(\times 10^5)$	$COP_{\min}$ $(\times 10^5)$	$COP_{\exp}$ $(\times 10^5)$
All realizations	5.335	4.418	4.887	1.291	1.159	1.2267
Proposed method	5.332	4.438	4.887	1.291	1.162	1.2267
Ranking						
K_{net}	5.242	4.501	4.865	1.278	1.171	1.2235
ϕ_{net}	5.168	4.501	4.865	1.267	1.171	1.2235
$S_{iw,net}$	5.168	4.501	4.858	1.267	1.171	1.2225
F_{net}	5.217	4.438	4.863	1.274	1.162	1.2232
F_{LC}	5.335	4.458	4.923	1.291	1.165	1.2319
PV_{net}	5.117	4.438	4.852	1.263	1.162	1.2216
$OOIP$	5.117	4.418	4.848	1.260	1.159	1.2210
OIP_{net}	5.140	4.438	4.842	1.263	1.162	1.2201
CHV_{local}	5.335	4.458	4.923	1.291	1.165	1.2319
Clustering	5.310	4.540	4.925	1.288	1.177	1.2322
Random	5.018	4.501	4.823	1.246	1.171	1.2174

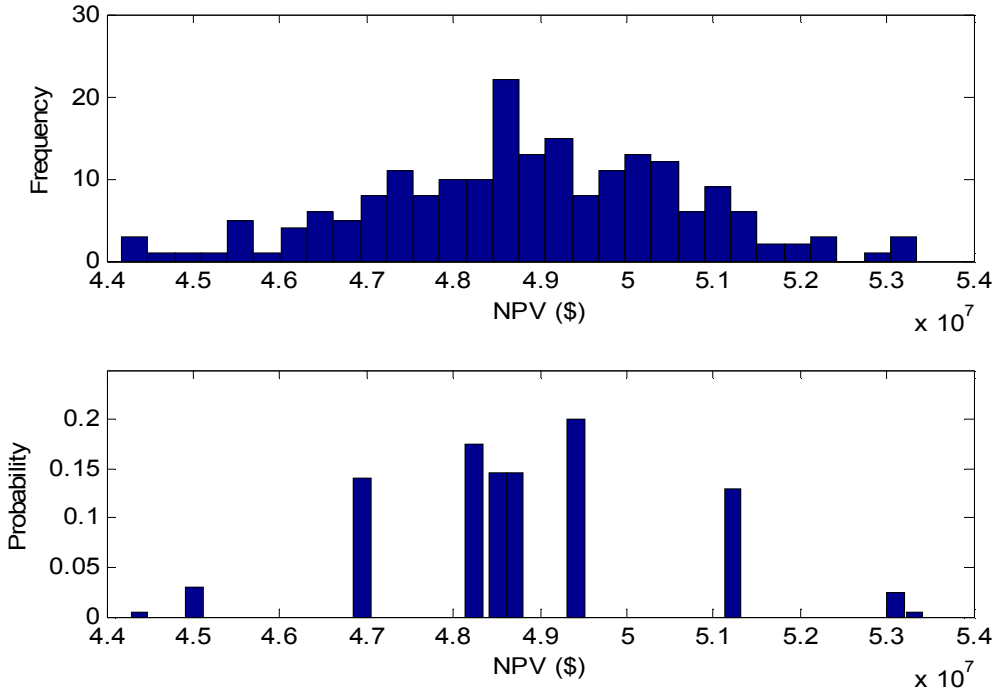

Figure B.5 Histogram using NPV for superset of 200 realizations (top), 10 selected realizations using proposed method (bottom)

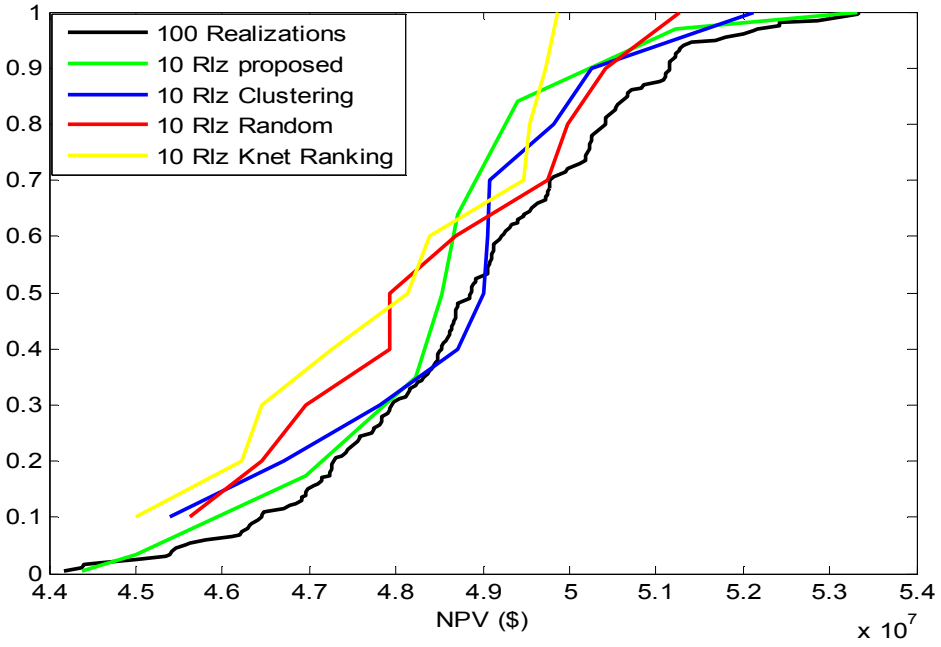

Figure B.6 CDF plot comparison using NPV between the superset of realization and selected set of realization using; (i) proposed method, (ii) Kernel k-means clustering, (iii) Knet ranking, (iv) random selection

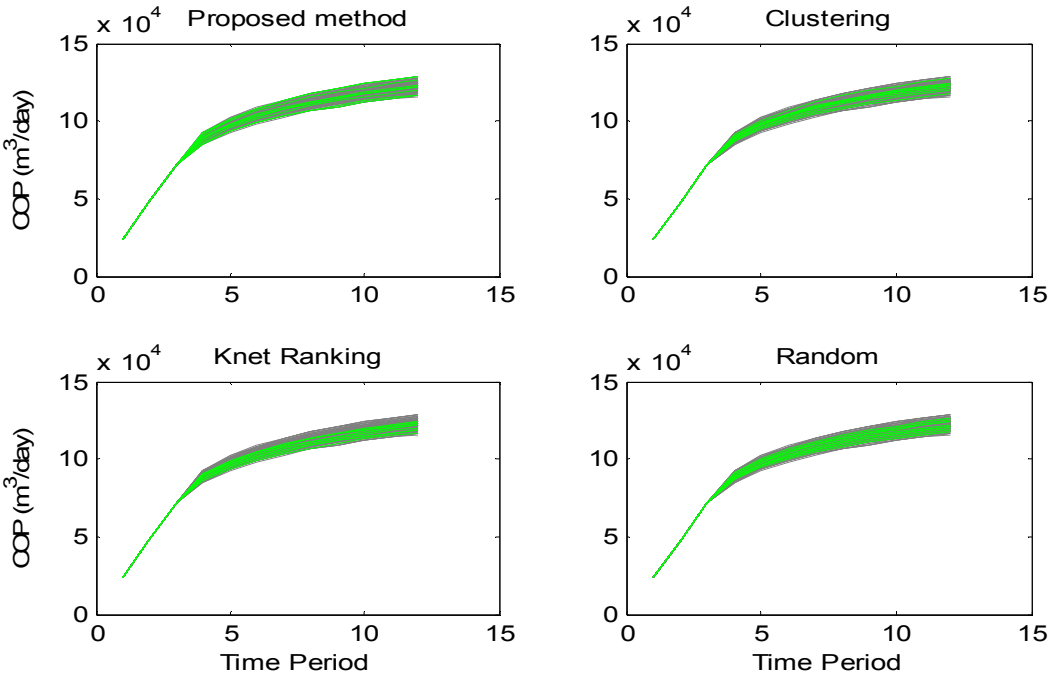

Figure B.7 COP versus time plot for 10 realizations selected from the (clockwise); (i) proposed method, (ii) Kernel k-means clustering, (iii) random selection, (iv) Knet ranking

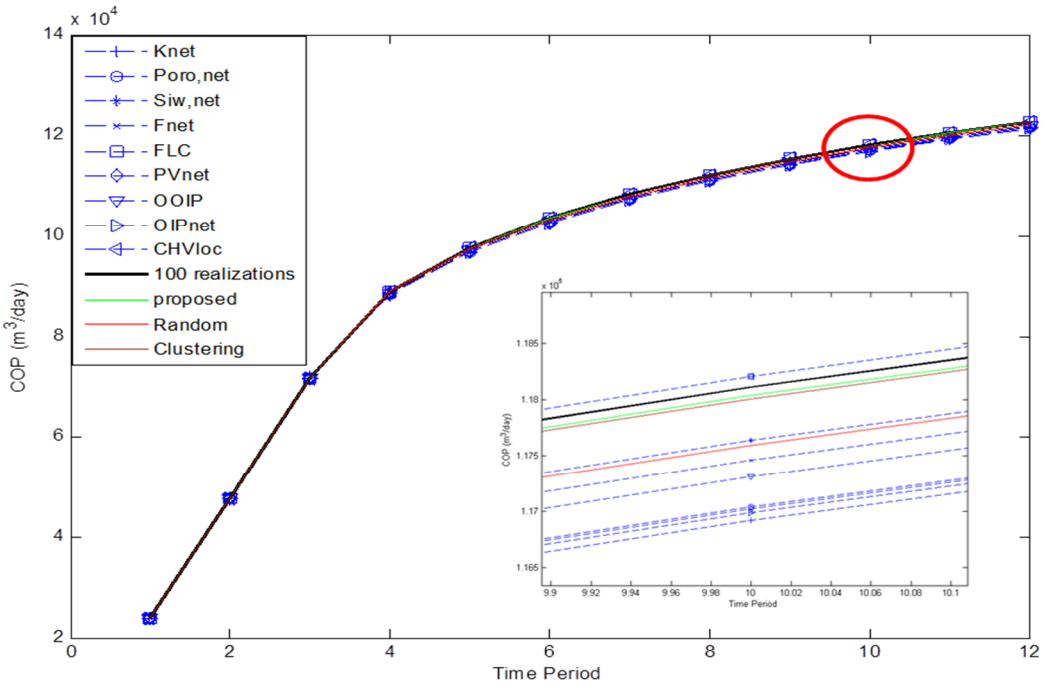

Figure B.8 Expected COP plots of the different realization reduction methods

Table B.2 Reservoir simulation results of all 200 realizations and 10 selected realizations

	$NPV_{\max}$ $(\times 10^7)$	$NPV_{\min}$ $(\times 10^7)$	$NPV_{\exp}$ $(\times 10^7)$	$COP_{\max}$ $(\times 10^5)$	$COP_{\min}$ $(\times 10^5)$	$COP_{\exp}$ $(\times 10^5)$
All realizations	5.335	4.418	4.887	1.291	1.159	1.2267
Proposed method	5.332	4.438	4.882	1.291	1.162	1.2260
Ranking						
K_{net}	5.217	4.501	4.879	1.274	1.171	1.2256
ϕ_{net}	5.211	4.501	4.876	1.274	1.171	1.2250
$S_{iw,net}$	5.211	4.501	4.874	1.274	1.171	1.2248
F_{net}	5.116	4.438	4.868	1.260	1.162	1.2238
F_{LC}	5.115	4.630	4.877	1.260	1.189	1.2253
PV_{net}	5.116	4.438	4.860	1.260	1.162	1.2227
$OOIP$	5.168	4.418	4.850	1.267	1.159	1.2213
OIP_{net}	5.116	4.438	4.874	1.260	1.162	1.2248
CHV_{local}	5.115	4.630	4.877	1.260	1.189	1.2253
Clustering	5.211	4.540	4.880	1.274	1.177	1.2257
Random	5.128	4.563	4.850	1.261	1.180	1.2213